

INTERNATIONAL DOCTORAL
SCHOOL OF THE USC

Marinela
Couselo Seijas

PhD Thesis

IDENTIFICATION AND REGULATION OF EPICARDIAL ADIPOSE TISSUE BIOMARKERS IN ATRIAL FIBRILLATION

Santiago de Compostela, 2022

Doctoral Programme in Molecular Medicine

DOCTORAL THESIS

IDENTIFICATION AND REGULATION OF EPICARDIAL ADIPOSE TISSUE BIOMARKERS IN ATRIAL FIBRILLATION

Marinela Couselo Seijas

ESCUELA DE DOCTORADO INTERNACIONAL DE LA UNIVERSIDAD DE SANTIAGO DE COMPOSTELA

PROGRAMA DE DOCTORADO EN MEDICINA MOLECULAR

SANTIAGO DE COMPOSTELA

2022

USC
UNIVERSIDADE
DE SANTIAGO
DE COMPOSTELA

DECLARACIÓN DE LA AUTORA DE LA TESIS

Identification and regulation of epicardial adipose tissue biomarkers in atrial fibrillation

Dª. Marinela Couselo Seijas

Presento mi tesis, siguiendo el procedimiento adecuado al Reglamento, y declaro que:

1) *La tesis abarca los resultados de la elaboración de mi trabajo.*
2) *En su caso, en la tesis se hace referencia a las colaboraciones que tuvo este trabajo.*
3) *La tesis es la versión definitiva presentada para su defensa y coincide con la versión enviada en formato electrónico.*
4) *Confirmo que la tesis no incurre en ningún tipo de plagio de otros autores ni de trabajos presentados por mí para la obtención de otros títulos.*

En Santiago de Compostela, a 10 de mayo de 2022

Fdo:

USC
UNIVERSIDADE
DE SANTIAGO
DE COMPOSTELA

AUTORIZACIÓN DE LOS DIRECTORES DE LA TESIS

Identification and regulation of epicardial adipose tissue biomarkers in atrial fibrillation

Dª. Sonia Eiras Penas
D. Moisés Rodríguez Mañero
D. José Ramón González Juanatey

INFORMAN:

Que la presente tesis, se corresponde con el trabajo realizado por Dª. Marinela Couselo Seijas, bajo nuestra dirección, y autorizamos su presentación, considerando que reúne los requisitos exigidos en el Reglamento de Estudios de Doctorado de la USC, y que como directores de esta no incurre en las causas de abstención establecidas en la Ley 40/2015.

De acuerdo con lo indicado en el Reglamento de Estudios de Doctorado, declaramos también que la presente tesis doctoral es idónea para ser defendida en base a la modalidad de COMPENDIO DE PUBLICACIONES, en los que la participación de la doctoranda fue decisiva para su elaboración y las publicaciones se ajustan al Plan de Investigación.

En Santiago de Compostela, a 10 de mayo de 2022

Fdo:

USC
UNIVERSIDADE DE SANTIAGO DE COMPOSTELA

USC
UNIVERSIDADE
DE SANTIAGO
DE COMPOSTELA

This doctoral thesis has received financial support from the following funding sources:

Fondo de Investigaciones Sanitarias* (PI16/01282 y PI19/01330) *del Plan Estatal de* I+D+I 2016-2020, *cofinanciación por el* ISCIII-*Subdirección General de Evaluación y Fomento de la investigación



***Fondo Europeo de Desarrollo Regional* (FEDER)**



***Consellería de Cultura, Educación e Ordenación Universitaria da Xunta de Galicia (Axudas para a consolidación e estructuración de unidades de investigación competitivas (*ED431B 2016/2022)**



***Instituto de Investigación Sanitaria de Santiago de Compostela* (IDIS) (*Axudas predoutorais* 2018)**



Programa* IACOBUS, *de cooperación cultural, científica e pedagóxica entre as Universidades e os Centros de Ensino Superior da Eurorrexión Galicia – Norte de Portugal



European Molecular Biology Organization Scientific Exchange Grant



USC
UNIVERSIDADE DE SANTIAGO DE COMPOSTELA

USC
UNIVERSIDADE
DE SANTIAGO
DE COMPOSTELA

CONFLICT OF INTEREST STATEMENT

The doctoral student states that she has no conflict of interest in relation to the doctoral thesis.

USC
UNIVERSIDADE DE SANTIAGO DE COMPOSTELA

USC
UNIVERSIDADE
DE SANTIAGO
DE COMPOSTELA

A mis padres

USC
UNIVERSIDADE DE SANTIAGO DE COMPOSTELA

USC
UNIVERSIDADE
DE SANTIAGO
DE COMPOSTELA

AGRADECIMIENTOS

Me gustaría empezar agradeciendo a mis directores, el Dr. Moisés Rodríguez Mañero, Dr. José Ramón González Juanatey y a la Dra. Sonia Eiras Penas. A Moisés por ser tan positivo siempre y por haberme enseñado el procedimiento de ablación. A Juanatey por la inspiración y su implicación, fundamental, en la investigación científica; y especialmente a Sonia, por compartir codo con codo mi evolución durante este período. Por haberme dado libertad para experimentar, para investigar y para realizar estancias en otros laboratorios. A los tres, muchas gracias por transmitirme la tenacidad y la voluntad de seguir trabajando en ciencia, y por haberme dado la posibilidad de luchar por seguir investigando con el respaldo y la base que me habéis ayudado a construir. Quiero agradecer también el apoyo y la ayuda prestada siempre por el Dr. Anxo Vidal, mi tutor de tesis.

A los Dres. Martínez Cereijo, Durán Muñoz, y especialmente al Dr. Fernández por su constancia a la hora de ofrecernos las muestras, a Ana y María y a todo el equipo de Cardiología. Gracias a todos los pacientes que participaron en el proyecto, y que han permitido que nuestro trabajo sea posible.

A la Dra. María Gómez Lázaro por acogerme durante mi estancia en Porto, por su amabilidad e implicación, por enseñarme lo que sé sobre Raman y por permitirme colaborar con el Dr. Paulo Aguiar, al que agradezco junto al Dr. Miguel Aroso haberme dado la oportunidad de analizar mis cardiomiocitos con los MEAs, por compartir mi ilusión al verlos contraerse y ayudarme a analizar los datos.

A la Dra. Laetitia Pereira por darme la oportunidad de realizar una estancia predoctoral en Francia en su laboratorio, integrarme desde el primer día en el grupo y por enseñarme a aislar los cardiomiocitos de ratón junto a la Dra. Florence. A la Dra. Ana María Gómez por hacerme siempre que se lo pedí un hueco para enseñarme los scripts del IDL. A la Dra. Pascale Gerbaud, por permitirme trabajar con ella con las hiPSC, y por explicarme todo lo que hacía y resolver mis dudas, entendiéndome

USC
UNIVERSIDADE DE SANTIAGO DE COMPOSTELA

a pesar de mi nivel de francés. Quiero agradecer especialmente durante mi estancia en Francia a la Dra. Almudena Val, por su infinita amabilidad, dedicación y paciencia. Eres de esas personas por las que uno se siente afortunado a la hora de trabajar en equipo.

A Adriana, porque no me parece fácil y hay que tener suerte para coincidir en el trabajo con alguien como tú. Los siguientes años de tesis no han sido lo mismo desde que te fuiste. A Ezequiel, por la tranquilidad y la paciencia para explicarme y debatir lo que fuera siempre que lo necesité. A Esther, Noemí, Nerea, Iñaki, Cristina, Xiaoran, David, Cibrán, Stephany y a todos los compañeros de laboratorio con los que coincidí durante la tesis, y que han sido de gran ayuda y apoyo durante todo el proceso.

Al Dr. Manuel Campos por ayudarme con mis primeros experimentos con el Fluo-4 y el confocal. A Lucía Alvariño por ayudarme con el *time-lapse* en los experimentos de *wound healing*. A la Dra. Susana Bravo, por ayudarme a entender la proteómica. Al Dr. Juan Viñuela, por ayudarme con la inmunología y el citómetro de flujo. A Marta y a José Luis, por responder a las incontables llamadas, la ayuda indispensable con la gestión y los diferentes equipos todos estos años. A Adrián, Vanesa, Marta, Ana, Eloy, Nerea, Rosa, Walma, Dalila, Andrea, Tamara, Rima, Maya, Juan, Laura, Sara, Alberto, Uxía, Ana Rita, Alana, Romain… y a todos los compañeros de otros laboratorios, del IDIS, CIMUS, i3S, INSERM… que siempre que lo necesité me ayudaron, por amenizar también los días en el laboratorio y compartir vivencias y experiencias, porque entre todos avanzamos mejor.

A Rita, Anael, Aitana y Quique, por todos los cafés, las comidas y los debates científicos…y porque hay vida más allá del laboratorio. Es muy satisfactorio poder tener amigas y amigos que entiendan la jerga y con quien poder hablar de ciencia; pero no menos importante es poder desconectar, vivir y hablar de muchas otras cosas más. Por eso también quiero agradecer a Maki, Katia, Nuria, Lucía y Alba, mis amigas de toda y para toda la vida.

A mamá y papá, a mis hermanos, Julio y Carlota, y a mis tíos, María y Adelino, por el apoyo incondicional y por sentir tanta o más

USC
UNIVERSIDADE DE SANTIAGO DE COMPOSTELA

alegría que yo misma al ir consiguiendo cosas y avanzando en mi carrera, y en mi vida en general. A Óscar, por compartir conmigo esta etapa, y las que vengan. Por interesarte por lo que hago, y sorprenderme acordándote después, aunque no sepa explicártelo bien. Por entender lo que este oficio pueda implicarnos, y por apoyarme siempre. Infinitas gracias a toda mi familia.

En último lugar en los agradecimientos de esta etapa de mi carrera profesional solo podías estar tú, María. Porque yo no habría bajado corriendo a matricularme en la carrera de biología ese año, el último día de plazo, si tú no llegas a llamarme para preguntarme si lo había hecho. No habría empezado a trabajar en un laboratorio después de acabar la carrera, cuando ya me había puesto a trabajar en otra cosa, si tú no hubieras insistido en que lo hiciese, que probase. Y así pude compartir contigo esos primeros años. Trabajar en un laboratorio con una de mis mejores amigas: la complicidad, el saber ver lo que a la otra se le está escapando…ojalá algún día otra vez. Y después de esos años, del máster, tampoco habría empezado la tesis con Sonia si (cómo no) tú no me hubieras avisado de que estaba buscando a alguien y que le escribiese. Porque no sé cómo voy a agradecértelo. Sobre todo, no sé dónde estaría ahora si tú no hubieras estado a mi lado todo el camino, y no quiero saberlo.

Para todo lo que vaya a venir en adelante, me siento preparada y es gracias a todos vosotros.

USC
UNIVERSIDADE DE SANTIAGO DE COMPOSTELA

USC
UNIVERSIDADE
DE SANTIAGO
DE COMPOSTELA

INDEX

ABBREVIATIONS 19
RESUMO 23
ABSTRACT 33
FIGURE INDEX 37
TABLE INDEX 39
1 INTRODUCTION 41
1.1 Nomenclature 41
1.2 Cardiovascular diseases 41
1.3 Atrial fibrillation 42
1.3.1 Definition and classification 42
1.3.2 AF incidence and prevalence 46
1.3.3 Associated risk factors 46
1.4 Epicardial adipose tissue 50
1.4.1 Definition 50
1.4.2 Composition 51
1.4.3 Characterization 52
1.4.4 Physiological functions 53
1.4.5 Article 1 | Pathophysiological mechanisms of EAT in AF 56
1.5 Autonomic nervous system 57
1.6 Heart impulse at the cellular level 58
1.6.1 Cardiac action potential 58
1.6.2 Intracellular Calcium mobilization 59
2 HYPOTHESIS AND GENERAL OBJECTIVES 61
3 MATERIALS AND METHODS 63
3.1 Patient samples 63
3.2 Cell cultures 63
3.2.1 hiPSC-derived atrial cardiomyocytes 63
3.3 Biochemical assays 65
3.3.1 Intracellular composition by confocal Raman microspectroscopy 65
3.4 Functional assays 66

USC
UNIVERSIDADE DE SANTIAGO DE COMPOSTELA

3.4.1 Intracellular calcium mobilization..... 66

3.5 Statistical analysis..... 67

4 RESULTS..... 69

4.1 Article 2 | Cholinergic activity regulates the secretome of epicardial adipose tissue: Association with atrial fibrillation..... 69

4.2 Article 3 | Inflammatory and lipid regulation by cholinergic activity in epicardial stromal cells from patients who underwent open-heart surgery..... 70

4.3 FABP4 effect on hiPSC-derived atrial CMs..... 71

4.3.1 Characterization of hiPSC-derived atrial CMs by confocal Raman microspectroscopy..... 72

4.3.2 FABP4 modified the nuclear composition of hiPSC-derived atrial CMs..... 94

4.3.3 FABP4 effect on the cytoplasmic composition of hiPSC-derived atrial CMs98

4.4 Effect of FABP4 on the differentiation of hiPSC into atrial CMs..... 101

4.4.1 Spontaneous [Ca^{2+}] transient interval from hiPSC-derived atrial CMs treated with FABP4 during its differentiation..... 103

4.4.2 $[Ca^{2+}]_i$ transient characteristics of hiPSC-derived atrial CMs submitted to FABP4 treatment during their differentiation..... 104

4.4.3 FABP4 treatment during the differentiation process could modulate diastolic Ca^{2+} content from SR in hiPSC-derived atrial CMs..... 105

4.5 Article 4 | Higher ACE2 expression levels in epicardial cells than in subcutaneous stromal cells from patients with cardiovascular disease: Diabetes and obesity as possible enhancers..... 106

5 DISCUSSION..... 107

6 CONCLUSIONS..... 123

7 REFERENCES..... 125

8 ANNEXES..... 155

8.1 Annex I. Doctoral student publications..... 155

8.2 Annex II. Declarations: Published content..... 159

8.3 Annex III. Supplementary table 1..... 163

USC
UNIVERSIDADE DE SANTIAGO DE COMPOSTELA

ABBREVIATIONS

$[Ca^{2+}]_i$	Intracellular calcium
ACE2	Angiotensin-converting enzyme 2
ACh	Acetylcholine
ADAM17	A disintegrin and metalloprotease 17
ADSC	Adipose-derived stem cells
aEAT	Atrial epicardial adipose tissue
AF	Atrial fibrillation
ANOVA	Analysis of variance
ANS	Autonomic nervous system
AP	Action potential
APD	Action potential duration
AT	Adipose tissue
ATP	Adenosine triphosphate
AV	Atrioventricular
BAT	Brown adipose tissue
BMI	Body mass index
Ca^{2+}	Calcium
CABG	Coronary artery bypass grafting
CAD	Coronary artery disease
CaMKII	Calcium/calmodulin-dependent protein kinase type II
cDNA	Complementary desoxyribonucleic acid
CMs	Cardiomyocytes
CMR	Cardiac magnetic resonance
CT	Computerized tomography
CVD	Cardiovascular disease
Cx40	Connexin 40
Cx43	Connexin 43
DADs	Delayed after-depolarizations
DAPI	4′,6-diamidino-2-phenylindole
DMSO	Dimethyl sulfoxide

USC UNIVERSIDADE DE SANTIAGO DE COMPOSTELA

EAT	Epicardial adipose tissue
ECC	Excitation-contraction coupling
ECG	Electrocardiogram
EDTA	Ethylene diamine tetra acetic acid
ELISA	Enzyme-linked immunosorbent assay
ESC	European society of cardiology
FABP4	Fatty acid-binding protein 4
FBS	Foetal bovine serum
FC	Fold change
FFA	Free fatty acids
GPCRs	G protein-coupled receptors
hiPSC	Human induced pluripotent stem cells
HEPES	4-(2-hydroxyethyl)-1-piperazineethanesulfonic acid
HF	Heart failure
HNP	Human neutrophil peptide
HUGO	Human genome organization
HSL	Hormone-sensitive lipase
I_{CaL}	Type L voltage-dependent Ca^{2+} current
IDIS	*Instituto de investigación sanitaria*
IL-6	Interleukin 6
INE	*Instituto nacional de estadística*
IQR	Interquartile range
ITPR3	Inositol 1,4,5-Trisphosphate Receptor Type 3
KCl	Potassium chloride
LA	Left atria
LAAT	Left atrial adipose tissue
LCFA	Long chain fatty acids
mAChR	Muscarinic acetylcholine receptor
MCP1	Monocyte chemoattractant protein 1
MESA	Multi-ethnic study of atherosclerosis
MPO	Myeloperoxidase
mRNA	Messenger ribonucleic acid

USC UNIVERSIDADE DE SANTIAGO DE COMPOSTELA

MYL2	Myosin regulatory light chain 2
Na^+	Sodium
NCX	Na^+/Ca^{2+} exchanger
NOVA	Study of neurotoxin (botulinum toxin type A) for the prevention of post-operative AF
OCT	Optical coherence tomography
OPLS-DA	Orthogonal Partial Least Squares-Discriminant Analysis
OSA	Obstructive sleep apnoea
PAT	Pericardial adipose tissue
PBMC	Peripheral blood mononuclear cells
PBS	Phosphate-buffered solution
PGC-1α	Peroxisome proliferator-activated receptor gamma coactivator-1 alpha
PLN	Phospholamban
PMNs	Polymorphonuclear cells
PPARγ	Peroxisome proliferator-activated receptor gamma
PRDM16	PR-domain-missing 16
RA	Right atrium
RFU	Relative fluorescence units
ROS	Reactive oxygen species
r.t.	Room temperature
RyRs	Ryanodine receptors
SA	Sinoatrial
SAT	Subcutaneous adipose tissue
SD	Standard deviation
SEM	Standard error medium
SERCA	Sarcoplasmic/endoplasmic reticulum Ca^{2+} ATPase
SPRINT	Systolic blood PRessure INtervention Trial
SR	Sarcoplasmic reticulum
SVF	Stromal vascular fraction

USC UNIVERSIDADE DE SANTIAGO DE COMPOSTELA

T2DM	Type 2 diabetes mellitus
TNFα	Tumour necrosis factor Alpha
UCP-1	Uncoupling protein 1
vEAT	Ventricular EAT
VIP	Variable Importance Parameter
PV	Pulmonary veins

USC
UNIVERSIDADE DE SANTIAGO DE COMPOSTELA

RESUMO

A fibrilación auricular (FA) é a taquicardia máis frecuente na práctica clínica. É un ritmo irregular debido a unha descarga repetitiva, rápida e caótica de múltiples circuítos de re-entrada auricular. Debido a que non hai unha contracción auricular efectiva, existe unha maior tendencia á formación de trombos por éxtase sanguíneo que poden provocar unha embolia sistémica. A súa prevalencia aumenta co envellecemento da poboación e a obesidade, cunha estimación de 18 millóns de enfermos en Europa en 2060. Esta arritmia desencadea unha importante disfunción hemodinámica e eventos tromboembólicos que repercuten nun risco elevado de morbilidade, especialmente ictus e insuficiencia cardíaca, e de mortalidade. Como consecuencia, constitúe a causa cardiovascular máis común de hospitalización, xerando un importante gasto sanitario. Estase a dedicar un gran esforzo en coñecer os seus mecanismos fisiopatolóxicos, os biomarcadores e os posibles obxectivos terapéuticos para a súa xestión eficiente. Con todo, a evolución dos factores de risco debido á súa interacción con factores ambientais provoca unha clara necesidade de coñecer novos indicadores que se adapten á poboación en todo momento e que melloren a previsión, a estratificación e as intervencións, xestionado esta patoloxía de forma eficiente.

Os mecanismos fisiopatolóxicos máis descritos céntranse en comprender a remodelación eléctrica (redución do potencial de acción, acurtamento do período refractario auricular, formación de circuítos de reentrada e bloqueos da condución), estrutural (acumulación de tecido adiposo e tecido fibroso) e contráctil (modificación das proteínas contráctiles e alteración da homeostase do calcio (Ca^{2+})). Para que se estableza esta arritmia, necesítase un evento promotor e un substrato favorable para perpetuala. Un dos eventos promotores da FA é a alteración no ton autonómico e un dos substratos de apoio é a inflamación. Así, aínda que a contribución total do sistema adrenérxico ou colinérxico é descoñecida, sábese que hai unha innervación auricular alterada. Mentres que o neurotransmisor do sistema parasimpático, a acetilcolina (ACh), participa na hiperpolarización e

USC
UNIVERSIDADE DE SANTIAGO DE COMPOSTELA

o acurtamento da duración do potencial de acción, o neurotransmisor do sistema nervioso simpático, a noradrenalina, mantén o efecto arritmoxénico a través do aumento de Ca^{2+} transitorio. Ademais, os mediadores inflamatorios poden conferir un estado protrombótico, en parte mediado pola lesión endotelial, a produción de factor tisular de monocitos e activación de plaquetas, que promoven a fibrose e contribúen á remodelación estrutural. Un dos tecidos adxacentes ao miocardio que segrega mediadores inflamatorios e presenta innervacións simpáticas e parasimpáticas é o tecido adiposo epicárdico (TAE).

Debido ao aumento dos avances e á dispoñibilidade de técnicas de imaxe non invasivas, tales como a tomografía computerizada (TC) e a resonancia magnética cardíaca (RMC), actualmente existen máis evidencias do risco de enfermidade asociado aos diferentes depósitos de tecido adiposo. O TAE é particularmente relevante cando falamos de enfermidades cardiometabólicas. Este tecido está situado sobre o miocardio, especialmente en ramas atrioventriculares, e baixo condicións fisiolóxicas protexe do exceso de ácidos graxos en circulación e da hipotermia, debido á súa elevada capacidade de incorporar ácidos graxos e á presenza da proteína de desacoplamento-1 (UCP- 1), respectivamente. Con todo, en condicións patolóxicas este tecido segrega adipocitoquinas que inducen a fibrose como a activina A, e inflamación, ou reduce a expresión e secreción de outras que regulan á arritmoxénese ou procesos ateroxénicos e inflamatorios. Así, o aumento do seu grosor ou volume, medido por técnicas de imaxe como as previamente mencionadas, relacionouse con parámetros de síndrome metabólica e enfermidades cardiovasculares, como a enfermidade cardíaca isquémica, insuficiencia cardíaca e FA.

Nos últimos anos, demostrouse que a inxección de toxina botulínica na graxa epicárdica de pacientes sometidos a cirurxía cardíaca, co obxectivo de inhibir a liberación de ACh dos plexos ganglionares, reduciu a taxa de recurrencia da FA a curto e longo prazo. Estas probas confirmaron a estreita relación entre o sistema nervioso autónomo (SNA), a graxa epicárdica e a FA. Así, o obxectivo

USC UNIVERSIDADE DE SANTIAGO DE COMPOSTELA

deste traballo foi estudar os mecanismos do neurotransmisor ACh no TAE e a súa relación coa FA.

Dados os antecedentes e o coñecemento actual sobre a asociación entre o TAE e a FA, o noso grupo de investigación partiu das seguintes hipóteses:

a) A FA é a arritmia máis frecuente na actualidade, unha prevalencia que está relacionada mecánicamente coa obesidade, o envellecemento e a insuficiencia cardíaca. Estes factores están asociados co TAE e, á súa vez, con marcadores locais e sistémicos.

b) Os pacientes cun TAE máis disfuncional (maior secreción de certos factores inflamatorios derivados da graxa epicárdica) teñen maior recorrencia de FA postoperatoria e postablación.

c) A disfunción do SNA (parasimpático) participa no desenvolvemento e mantemento da FA en parte mediante a súa mediación coa graxa epicárdica.

Con base nos datos previos, o noso grupo considera que existe unha rede entre o TAE, a disfunción do sistema autónomo e a inflamación que promove o desenvolvemento da FA. Deste xeito, o TAE segrega unha ou máis proteínas, reguladas polo SNA, que actúan como promotores de FA. Ademais, dado que o TAE é un órgano endocrino, estas proteínas poden ser detectadas a nivel sistémico como indicadores de pronóstico e/ou diagnóstico de FA.

Para probar estas hipóteses, realizáronse probas en mostras de TAE e plasma de pacientes sometidos a cirurxía cardíaca, e modelos celulares preclínicos de células estromais de TAE, neutrófilos e cardiomiocitos auriculares derivados de células nai pluripotentes inducidas humanas (hiPSC) para:

a) Estudar por proteómica, adipocitoquinas diferencialmente segregadas por explantes de TAE, con/sen tratamento de ACh.

b) Avaliar o efecto de proteínas reguladas por tratamento colinérxico na activación de monocitos, e na funcionalidade e composición de cardiomiocitos (CMs) auriculares derivados de hiPSC.

USC
UNIVERSIDADE DE SANTIAGO DE COMPOSTELA

c) Analizar o valor que engaden as adipocitoquinas locais cuxos niveis periféricos se asociaron como indicadores de FA postoperatoria e FA persistente de longa duración.

d) Estudar o efecto das adipocitoquinas do TAE relacionadas coa FA na diferenciación e composición intracelular de CMs auriculares derivados de hiPSC.

Para levar a cabo este proxecto de tese, establecemos un plan de traballo no que a estratexia experimental constou das seguintes tarefas:

a) Ensaios "ex vivo". Estudo do secretoma (proteínas segregadas) dos explantes de TAE de pacientes sometidos a cirurxía cardíaca tratados ou non con ACh. Análise diferencial proteómico do secretoma de dous depósitos de TAE (auricular (TAEa) e ventricular (TAEv)) con e sen tratamento con ACh. Validación mediante arrays de anticorpos específicos e outros inmunoensayos necesarios, como multiplex, ELISA e Western Blot para as adipocitoquinas diferenciais. A súa correlación coa expresión xénica analizouse por PCR en tempo real. Isto permitiunos identificar as proteínas locais do TAE diferencialmente segregadas en pacientes de de cirurxía cardíaca con FA.

b) Probas observacionais. Xa que o 20-50% dos pacientes desenvolven FA na primeira semana despois da cirurxía, comprobouse a través dun estudo retrospectivo o valor que engaden as proteínas diferencialmente segregadas polo TAE como un indicador ou pronóstico de FA, comparando a súa asociación cos niveis periféricos. Para iso, recolléronse mostras de sangue periférica de pacientes de cirurxía cardíaca. Analizáronse as adipocitoquinas previamente seleccionadas e por un estudo prospectivo lonxitudinal avaliouse o seu valor como indicador de recorrencia de FA.

c) Ensaios "in vitro". Avaliación dos niveis de expresión dos receptores muscarínicos nas biopsias e nas células estromais do TAE mediante PCR en tempo real e Western Blot. Selección das proteínas, adipocitoquinas, diferencialmente segregadas polo tratamento

USC
UNIVERSIDADE DE SANTIAGO DE COMPOSTELA

colinérxico con efecto sobre as células estromais vasculares do TAE de pacientes sometidos a cirurxía cardíaca.

d) Trala identificación das adipocitoquinas do TAE relacionadas coa FA, estudouse o seu efecto sobre a funcionalidade e composición das hiPSC diferenciadas ou durante a súa diferenciación a CMs auriculares. Para iso, analizouse a mobilización de Ca^{2+} mediante ensaios de microscopía confocal de fluorescencia e a composición química mediante a espectroscopía Raman, respectivamente.

Os resultados do estudo comparativo da actividade secretora do TAEv e do TAEa mostraron unha alta porcentaxe de semellanza entre ambos tecidos. Ambos segregaron proteínas ao medio extracelular, principalmente relacionadas co metabolismo, o crecemento celular, o transporte e a resposta inmune. A maioría das proteínas segregadas eran comúns a ambos tecidos. Independentemente da súa localización, o comportamento do TAE foi moi similar a nivel de secreción de proteínas, e viuse modificado despois do tratamento con ACh. Por estes motivos, xunto á menor complexidade de obtención, o noso grupo decidiu seguir utilizando o TAEv como modelo preclínico para estudar a implicación do SNA na FA, a través do TAE.

O noso grupo demostrou a presenza de receptores muscarínicos (receptores de acetilcolina muscarínicos, mAChR) no TAE. Dentro dos diferentes subtipos de mAChR, o mAChR 2 foi o subtipo máis expresado, do mesmo xeito que no miocardio, e como tamén fora descrito no tecido adiposo. Non obstante, o subtipo 3 mostrou os resultados máis interesantes xa que a súa expresión foi regulada positivamente despois da indución da diferenciación adipoxénica.

As células estromais do TAE mostraron unha maior resposta colinérxica (inducida por ACh) que as células estromais do tecido adiposo subcutáneo (TAS) que foi empregado como control, no que respecta ao manexo de Ca^{2+}. Así, observamos un aumento da concentración de calcio intracelular ($[Ca^{2+}]_i$) nas células estromais do TAE en resposta á ACh. Este efecto podería deberse á presenza de

USC
UNIVERSIDADE DE SANTIAGO DE COMPOSTELA

mAChR no tecido xa que mAChR 2 e mAChR 3 mostraron unha maior expresión no TAE en comparación coas células estromais do TAS. O aumento da expresión de mAChR 3 despois da diferenciación adipoxénica podería indicar unha maior resposta á actividade colinérxica en pacientes con maior volume de TAE. Ademais, o aumento de $[Ca^{2+}]_i$ causado por este receptor, é importante para a regulación de varias respostas celulares, incluíndo a activación enzimática ou as modificacións transcricionais.

Os distintos tipos de FA poderían ter compoñentes diferenciais, de tal xeito que a FA postoperatoria ou paroxística podería estar máis relacionada coa inflamación e a actividade eléctrica dos CMs; mentres que a FA persistente de longa duración ou permanente estaría máis asociada a cambios estruturais, fibrose, infiltración de adipocitos e actividade celular metabólica.

Os nosos resultados mostraron niveis máis altos de citoquinas inflamatorias e quimioquinas na fracción estromal do TAE en comparación co TAS. Despois de comparar os tecidos de graxa epicárdica auricular e ventricular, observamos que ambas mostraron unha actividade endocrina similar despois do tratamento con ACh. Algunhas destas proteínas estaban implicadas na inflamación, a desintoxicación e a composición estrutural. Curiosamente, observamos unha menor secreción de interleucina 6 (IL-6) e α-defensina 3 (DEFA3) despois do tratamento con ACh. A actividade colinérxica aguda aumentou os niveis de expresión do ARNm da quimioquina atraente de monocitos (MCP-1) nas células estromais do TAE. Este xene, xunto co da IL- 6, mostrou unha maior expresión no TAE en comparación co TAS, o que indica un perfil máis proinflamatorio desta graxa local. Os resultados suxiren que a modulación da actividade colinérxica no TAE de pacientes sometidos a cirurxía cardíaca podería previr a resposta inflamatoria aguda e o recrutamento de células inmunitarias causadas por MCP1. En relación coa FA, atopamos que os niveis plasmáticos de DEFA3 foron menores en pacientes de cirurxía cardíaca que desenvolveron FA postoperatoria. En contraste coa maior concentración de DEFA3, que foi interpretada como un marcador na progresión de insuficiencia cardiaca ou enfermidade coronaria, unha

USC UNIVERSIDADE DE SANTIAGO DE COMPOSTELA

diminución desta molécula tamén pode implicar unha protección reducida contra axentes externos. Así, os fenómenos agudos pro-inflamatorios aumentan a probabilidade de desenvolver FA postoperatoria.

Por outra banda, nos tratamentos de ACh a longo prazo, o efecto nas células estromais do TAE atopouse máis asociado coa acumulación de lípidos. Un dos marcadores lipídicos no estroma epicárdico asociado á FA persistente de longa duración foi a proteína 4 de unión a ácidos graxos (FABP4) dos adipocitos. As FABP son unha familia de proteínas de 14-15 kDa, coñecidas como chaperonas lipídicas intracelulares, que regulan o tráfico e a resposta de lípidos nas células. Ademais da súa función principal de transporte intracelular de ácidos graxos, a FABP4 foi descrita recentemente con funcións hormonais, polo que esta chaperona podería desempeñar un papel no mantemento da homeostase e na desregulación metabólica. Así, o noso grupo descubriu que os niveis plasmáticos periféricos e locais de FABP4 distinguían o volume de TAEa en pacientes con FA permanente do dos pacientes con FA paroxística. Ademais, dentro dos pacientes con FA permanente, a FABP4 estivo asociada con aqueles con maior risco de recorrencia despois do procedemento de illamento das veas pulmonares mediante ablación.

Nesta liña, os nosos resultados mostraron un aumento da expresión xénica de FABP4 en células estromais do TAE de pacientes con FA persistente de longa duración. Ademais, demostramos a súa regulación parasimpática a longo prazo mediante un modelo de rata vagotomizada, no que observamos que despois da denervación do nervio vago, os niveis plasmáticos de FABP4 reducíronse de forma independente do peso corporal.

Para comprender o efecto que FABP4 podería estar a exercer na función do miocardio, o noso grupo iniciou unha serie de procedementos en CMs auriculares derivados de hiPSC. Estas células convertéronse nunha poderosa ferramenta para estudar os mecanismos das enfermidades específicas auriculares ou para probar a eficacia de fármacos selectivos auriculares. Así, pódense usar para desvelar os mecanismos, a fisiopatoloxía e as opcións de tratamento da FA. Por

USC UNIVERSIDADE DE SANTIAGO DE COMPOSTELA

estes motivos, seleccionamos hiPSC e CMs auriculares derivados de hiPSC.

Para saber se o efecto de FABP4 se produce durante o proceso de diferenciación, realizamos experimentos incluíndo FABP4 no medio de cultivo celular das hiPSC durante a súa diferenciación, e analizamos o comportamento das correntes de Ca^{2+} intracelulares, comparando células diferenciadas sometidas ou non a tratamento con FABP4 a 10 e 100 ng/mL durante as primeiras fases do proceso. O Ca^{2+} regula a contracción a través do acomplamento da excitación coa contracción (ECC) en CMs. Para cada latido cardíaco, as canles tipo L de Ca^{2+} da membrana plasmática ábrense durante o potencial de acción, o que leva á entrada de Ca^{2+} na célula, que o mesmo tempo activa a liberación de Ca^{2+} do retículo sarcoplásmico (RS) a través dos receptores de rianodina (RyR). Esta liberación de Ca^{2+} polos RyR (visualizada como un transitorio $[Ca^{2+}]i$) activa as miofibrillas contráctiles para xerar a contracción do CM. Despois da contracción, o Ca^{2+} é recaptado no RS pola bomba ATPasa de Ca^{2+} do (retículo sarco(endo)plasmático (SERCA) e extruído fóra do CM principalmente polo intercambiador Na^{+}/Ca^{2+} (NCX), o que resulta na relaxación dos cardiomiocitos. Hai varios mecanismos dependentes de Ca^{2+} implicados no control da duración do potencial de acción. Nesta liña, demostrouse que na miocardiopatía diabética, a disfunción cardíaca está asociada ao mal manexo do Ca^{2+}.

Os nosos resultados indicaron que FABP4 a baixa concentración aumentou o intervalo de tempo entre as correntes espontáneas de $[Ca^{2+}]i$ dos CMs auriculares derivados de hiPSC. FABP4 a 100 ng/mL aumentou a amplitude e o tempo ata o pico dos transitorios $[Ca^{2+}]i$ evocados eléctricamente nos CMs auriculares derivados de hiPSC, en comparación co control. O aumento da amplitude da liberación de $[Ca^{2+}]i$ podería indicar unha modulación dos RyRs, xa que previamente se demostrou que FABP4 non modifica a actividade das correntes de Ca^{2+} tipo L, o principal responsable da súa internalización celular. FABP4 a 100 ng/mL durante a diferenciación diminuíu a constante de desintegración do $[Ca^{2+}]i$ transitorio nos CMs auriculares, o que podería indicar unha mellora

USC
UNIVERSIDADE DE SANTIAGO DE COMPOSTELA

na activación ou funcionamento da SERCA2. A carga total de Ca^{2+} do RS, que se suxire pola amplitude do transitorio de $[Ca^{2+}]i$ evocado pola cafeína, mostrou unha tendencia á regulación positiva despois do tratamento con FABP4. Estes resultados foron en consonancia co aumento da amplitude do transitorio $[Ca^{2+}]i$ evocado eléctricamente, xa que unha maior concentración de Ca^{2+} no RS permitiría un aumento da súa liberación no citosol por RyR, e a súa recaptación no RS por SERCA2.

Durante a relaxación, a liberación de Ca^{2+} no citosol non se produce en condicións normais, xa que os RyR están pechados. Non obstante, hai fugas de Ca^{2+}, coñecidas como sparks, que son liberacións de Ca^{2+} do RS, mediadas pola activación espontánea dun número variable de RyRs. A análise da modulación destas fugas de Ca^{2+} despois do tratamento con FABP4, podería revelar a súa implicación na aparición destes eventos pro-arritmoxénicos, relacionando a actividade de FABP4 coa FA.

Entre os diferentes efectos exóxenos FABP4 descritos, xa se describiu que FABP4 exerce un efecto cardiodepresivo nos CMs ventriculares maduros de rata, reducindo o acurtamento celular e o pico de fluorescencia de $[Ca^{2+}]i$. Polo tanto, quixemos probar o efecto de FABP4 nos CMs auriculares xa diferenciados derivados de hiPSC. Realizamos microespectroscopía confocal de Raman para estudar as modificacións intracelulares resultantes do tratamento con FABP4 neste tipo celular. Empregamos un modelo matemático usando espectros Raman de CMs auriculares tratados ou non con FABP4. O modelo mostrou diferenzas substanciais na comparación entre as condicións, sendo o máis distinguible entre control e FABP4 a 10 ng/mL dentro dos núcleos das células. Os primeiros resultados indicaron que as diferencias químicas que observamos nos CMs en resposta á FABP4 poderían estar debidas a cambios na composición lipídica das células. Serán necesarios outros enfoques de análise en colaboración con especialistas en estatística para atopar modelos que permitan discernir mellor as células relativas ao tratamento con FABP4 e garantir e validar a caracterización dos picos Raman responsables destes cambios.

USC
UNIVERSIDADE DE SANTIAGO DE COMPOSTELA

En conclusión, os resultados deste traballo dilucidan o papel do sistema colinérxico na actividade secretora e inflamatoria do TAE como posible mecanismo asociado á FA postoperatoria. Ademais, o desequilibrio colinérxico na FA persistente de longa duración podería explicar a maior acumulación de ácidos graxos e, en consecuencia, a maior presenza de FABP4 no estroma epicárdico, cun efecto sobre a actividade paracrina na estrutura e fisioloxía dos CMs auriculares. O coñecemento de promotores da FA, en base a graxa epicárdica, e a súa regulación pola actividade física ou farmacolóxica mellorarán a saúde e benestar social, e atraerán o interese de empresas especializadas no desenvolvemento de test prognóstico ou para o diagnóstico eficaz da FA. En consecuencia, a continuación desta liña de investigación terá un gran impacto clínico, social e empresarial para o noso grupo de investigación.

Por último, durante o período de pandemia quixemos destacar a relación do TAE co receptor SARS-CoV-2. Os niveis de expresión deste receptor, a enzima convertidora de angiotensina 2 (ACE2), foron máis elevados en comparación co TAS, aumentándose en presenza de obesidade e diabetes en pacientes con enfermidades cardiovasculares. Ambos poderían indicar a maior susceptibilidade deste grupo de pacientes para a infección por SARS-CoV-2 e o aumento da severidade da enfermidade.

USC
UNIVERSIDADE DE SANTIAGO DE COMPOSTELA

ABSTRACT

Atrial fibrillation (AF) is defined as the most common arrhythmia in the clinical practice. It is a multifactorial disease aggravated by a myriad of pathophysiological mechanisms. This arrhythmia takes a high percentage of the health system budget, derived from hospitalization and preventive treatments of its associated comorbidities. A great effort has been devoted to understanding its pathophysiological mechanisms, biomarkers, and potential therapeutic targets to improve the diagnosis and management efficiency. However, the evolution of its risk factors, due to their interaction with environmental factors, leads to a clear need to know new indicators adapted to the population. This would improve AF prediction, stratification, and treatment to maximize the patient outcome success and to mitigate this pathology.

Given its multifactorial nature, this arrhythmia has a great number of associated risk factors, among which hypertension, heart failure or obesity are the main ones. The latter is associated with an increase in subcutaneous and visceral adiposity. The local adipose depot most associated with AF is epicardial adipose tissue (EAT), located under the pericardial fascia and therefore in direct contact with the myocardium, sharing the same blood circulation. These characteristics allow it to exert an influence on the behaviour of the cardiomyocytes (CMs). The vicinity with CMs allows EAT cells to infiltrate between them causing a physical disruption. Besides, as a very metabolically active tissue, EAT-secreted molecules can influence the myocardium in a vasocrine and paracrine manner. This is due to the fact that the coronary arteries are embedded in EAT. Similarly, the ganglionated plexus of the autonomic nervous system (ANS) that innervate the myocardium to control the heart rate are also embedded in this fat pad.

One of the promoter events of AF is the alteration in the autonomic tone and one of the favouring substrates of this phenomenon is inflammation. Thus, although the total contribution of the adrenergic (sympathetic) or cholinergic (parasympathetic) systems is unclear, it is

USC
UNIVERSIDADE DE SANTIAGO DE COMPOSTELA

known that there is an altered atrial innervation. While the neurotransmitter of the parasympathetic system, acetylcholine (ACh), participates in the hyperpolarization and shortening of the duration of the action potential; the neurotransmitter of the sympathetic system, norepinephrine, maintains the arrhythmogenic effect through increasing calcium (Ca^{2+}) transients.

In recent years, it has been shown that the injection of botulinum toxin into the epicardial fat of patients undergoing cardiac surgery, with the aim of inhibiting ACh release from the ganglionated plexus, reduced short and long-term AF recurrence. These results confirmed the close relationship between ANS, epicardial fat, and AF. Thus, the objective of this work was to study the mechanisms of ACh in EAT and its relationship with AF. To this end, EAT and blood samples from patients undergoing cardiac surgery, and preclinical cellular models of neutrophils and atrial CMs derived from human induced pluripotent stem cells (hiPSC) have been used.

The methodology included common molecular and biochemical techniques such as RT-qPCR, Western Blot; or proteomic analysis; and confocal microscopy for Ca^{2+} mobilization analysis or Raman confocal microspectroscopy for intracellular molecular composition. Ventricular EAT was used as a preclinical model after demonstrating a similar protein secretion profile in comparison with atrial EAT. We showed the expression of muscarinic receptors in the stromal cells of this tissue, and its regulation during adipogenesis. After that, we observed that cholinergic activity modified the secretory, inflammatory and lipid profile of EAT, in comparison with subcutaneous adipose tissue (SAT). These results suggest a local effect of ACh, due to the differential expression of muscarinic receptors, being higher in EAT.

One of the lipid markers in the epicardial stroma associated with long-standing persistent AF was adipocyte fatty acid-binding protein 4 (FABP4). It can be secreted by adipose tissue and through its paracrine activity it exerts a direct effect on contractility and CM differentiation. Our results showed that this protein induces in hiPSC-derived atrial cardiomyocytes a) changes in the mobilization of intracellular Ca^{2+}, the main ion responsible for contraction, and b) an increase in the

USC UNIVERSIDADE DE SANTIAGO DE COMPOSTELA

concentration of Ca^{2+} in the sarcoplasmic reticulum (SR), increasing its release to the cytosol via ryanodine receptors (RyR). The preliminary results from the study of the changes in the chemical composition due to FABP4 require future experiments to find the molecules responsible for the effect of this lipid chaperone and its intracellular location.

In conclusion, the results of this work elucidate the role of the cholinergic system in the secretory and inflammatory activity of EAT and a possible mechanism associated with postoperative AF. In addition, chronic cholinergic imbalance in long-term persistent AF could explain the greater accumulation of fatty acids. Consequently, FABP4 increases in the epicardial stroma, with an effect on paracrine activity in the structure and physiology of atrial cardiomyocytes.

Finally, during the pandemic period we studied the relationship of EAT with SARS-CoV-2 receptor. The expression levels of this receptor, angiotensin converting enzyme 2 (ACE2), were higher in this fat pad compared to SAT; being increased in the presence of obesity and diabetes in cardiovascular disease (CVD) patients. Both could be risk factors for SARS-CoV-2 infection susceptibility.

USC
UNIVERSIDADE DE SANTIAGO DE COMPOSTELA

USC
UNIVERSIDADE
DE SANTIAGO
DE COMPOSTELA

FIGURE INDEX

Figure 1. Causes of death in Spain in 2019 and 2020. 42
Figure 2. Electrical conduction system of the heart 43
Figure 3. Atrial fibrillation: Graphical description 44
Figure 4. Main AF associated risk factors 47
Figure 5. Example of some adipose tissue (AT) depots according to their location. 49
Figure 6. Scientific literature on epicardial adipose tissue (EAT). 50
Figure 7. Epicardial adipose tissue (EAT) location compared to pericardial adipose tissue (PAT). 51
Figure 8. Epicardial adipose tissue cellular composition 52
Figure 9. Physiological functions of epicardial adipose tissue 53
Figure 10. Simplified graphic description of cardiac innervation by the autonomic nervous system (ANS) 57
Figure 11. Graphic scheme of the action potential and the main ionic currents involved 58
Figure 12. Main pumps and channels involved in the cardiac excitation-contraction coupling mechanism. 59
Figure 13. Atrial cardiomyocyte (CM) differentiation protocol from hiPSC 64
Figure 14. Raman spectra from the cytoplasm (blue) and the nucleus (black) of a single hiPSC-derived atrial cardiomyocyte. 72
Figure 15. Median Raman spectra from the nuclei (a) and the cytoplasm (b) of hiPSC-derived atrial cardiomyocytes (n= 118 cells) in black. 72
Figure 16. Average Raman spectra of the hiPSC-derived atrial CM control clusters74
Figure 17. Average Raman spectra of the hiPSC-derived atrial CM clusters treated with FABP4 at 10 ng/mL (F10) 75
Figure 18. Average Raman spectra of the hiPSC-derived atrial CM clusters treated with FABP4 at 100 ng/mL (F100) 76
Figure 19. Multivariate analysis of the spectral regions from 400 to 1800 cm^{-1} and from 2650 to 3100 $cm^{-1}$of the Raman spectra obtained from unlabelled hiPSC-derived atrial CM nuclei. 94
Figure 20. Differential Raman peaks found within CM nucleus attending FABP4. . 97
Figure 21. Multivariate analysis of the spectral regions from 400 to 1800 cm^{-1} and from 2650 to 3100 $cm^{-1}$of the Raman spectra obtained from unlabelled hiPSC-derived atrial CM cytoplasm. 99
Figure 22. Quality control of hiPSC differentiation 102
Figure 23. Spontaneous $[Ca^{2+}]$ transient interval from hiPSC-derived atrial CMs treated with FABP4 during its differentiation 103
Figure 24. Characteristics of $[Ca^{2+}]_i$ transients from hiPSC-derived atrial CMs 104
Figure 25. Amplitude of $[Ca^{2+}]_i$ stored in the sarcoplasmic reticulum 105

USC
UNIVERSIDADE DE SANTIAGO DE COMPOSTELA

USC
UNIVERSIDADE
DE SANTIAGO
DE COMPOSTELA

TABLE INDEX

Table 1. Atrial fibrillation classification 45
Table 2. Major regulatory molecules secreted by epicardial adipose tissue (EAT). 55
Table 3. Raman peaks detected in the average spectra of the atrial CMs. 77
Table 4. OPLS-DA results obtained for the different comparisons from the nuclei spectra of hiPSC-derived atrial CMs between conditions. 95
Table 5. OPLS-DA results obtained for the different comparisons from the cytoplasm spectra of hiPSC-derived atrial CMs between conditions. 99
Table 6. Statistical analysis of the different comparisons from the Raman peaks typically assigned in the literature as lipids found in our unlabelled samples. 100

USC
UNIVERSIDADE DE SANTIAGO DE COMPOSTELA

USC
UNIVERSIDADE
DE SANTIAGO
DE COMPOSTELA

1 INTRODUCTION

1.1 NOMENCLATURE

The names of genes and proteins presented in this doctoral thesis follow the guidelines of the gene nomenclature Committee of the HUman Genome Organization (HUGO).

The initials or acronyms maintain the original nomenclature corresponding to the English designation in the case of genes, proteins, molecules, cell types, organizations, clinical studies, statistical terms, and laboratory techniques, due to their standardized use in the scientific community.

1.2 CARDIOVASCULAR DISEASES

Cardiovascular diseases (CVD) continue to be the leading cause of death worldwide. In 2017, there were 108.7 million people living with CVD in the 54 member countries of the European Society of Cardiology (ESC). The incidence that year was 19.9 million cases[1].

The latest data from the Spanish national institute of statistics (*Instituto Nacional de Estadística*, INE) show that in 2020 24.3% of deaths were due to diseases of the circulatory system and 22.8% to tumours. Infectious diseases, including identified COVID-19 virus and suspected COVID-19, were the third leading cause of death (16.4% of the total). In this sense, although it is true that in 2019 ischemic heart diseases topped the list of the 15 most frequent causes of death in Spain; in 2020 they were vastly outnumbered by the COVID-19 virus (Figure 1)[2].

USC
UNIVERSIDADE DE SANTIAGO DE COMPOSTELA

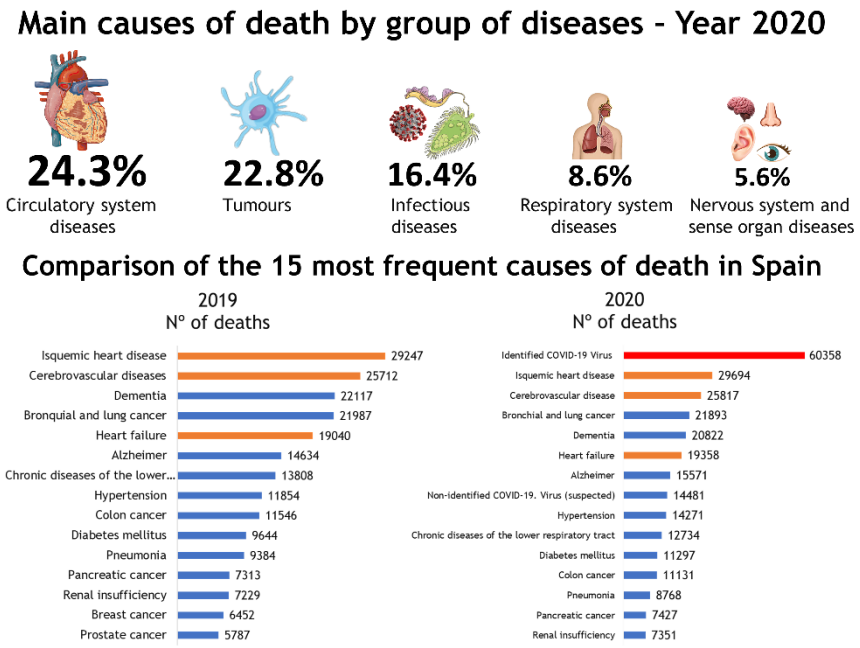


Figure 1. Causes of death in Spain in 2019 and 2020.

Figure designed from data extracted from the National Institute of Statistics (INE)[2], and made from images modified from Servier Medical Art (https://smart.servier.com) licensed under the Creative Commons Attribution 3.0 Unported License

1.3 ATRIAL FIBRILLATION

Within CVD, atrial fibrillation (AF) is the most common tachycardia in the clinical practice.

1.3.1 Definition and classification

AF is an irregular rhythm due to repetitive, rapid, and chaotic discharges from multiple atrial re-entry circuits. This disease has been defined by S. Bellet *et al*. as a supraventricular tachyarrhythmia, which consists of an uncoordinated atrial activation leading to a deterioration of the mechanical function[3].

Under physiological conditions, cardiac impulse arises in the sinoatrial (SA) node, located in the posterior wall of the right atrium

USC UNIVERSIDADE DE SANTIAGO DE COMPOSTELA

(RA) near the entrance of the superior vena cava. When generated, impulse spreads to several conduction pathways: the anterior internodal tract of Bachman, the middle internodal tract of Wenkebach, and the posterior internodal tract of Thorel, which carry the impulse to the atrioventricular (AV) node. The AV node is in the RA near the opening of the coronary sinus. It fulfils two very important functions: it delays the cardiac impulse to allow ventricular filling, and it controls the number of impulses that reach the ventricles. Cardiac impulse then travels from the AV node to the bundle of His and divides into the right and left bundle branches. Each branch ends in a network of fibres called the Purkinje system, which stimulates ventricular contraction (Figure 2)[4].

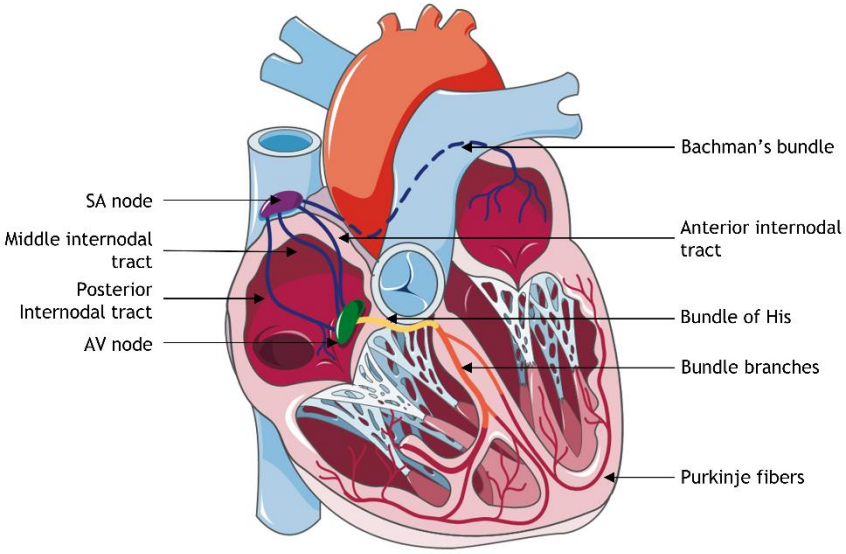


Figure 2. Electrical conduction system of the heart

SA: Sinoatrial; AV: Atrioventricular

Figure created from a modified image of Servier Medical Art (https://smart.servier.com) licensed under Creative Commons Attribution 3.0 Unported License

USC UNIVERSIDADE DE SANTIAGO DE COMPOSTELA

Heart rate is influenced by many factors (exercise, age, blood pressure, hormones, temperature...). Among them, autonomic nervous system (ANS) influences heart rate through the sympathetic and parasympathetic branches (see 1.5).

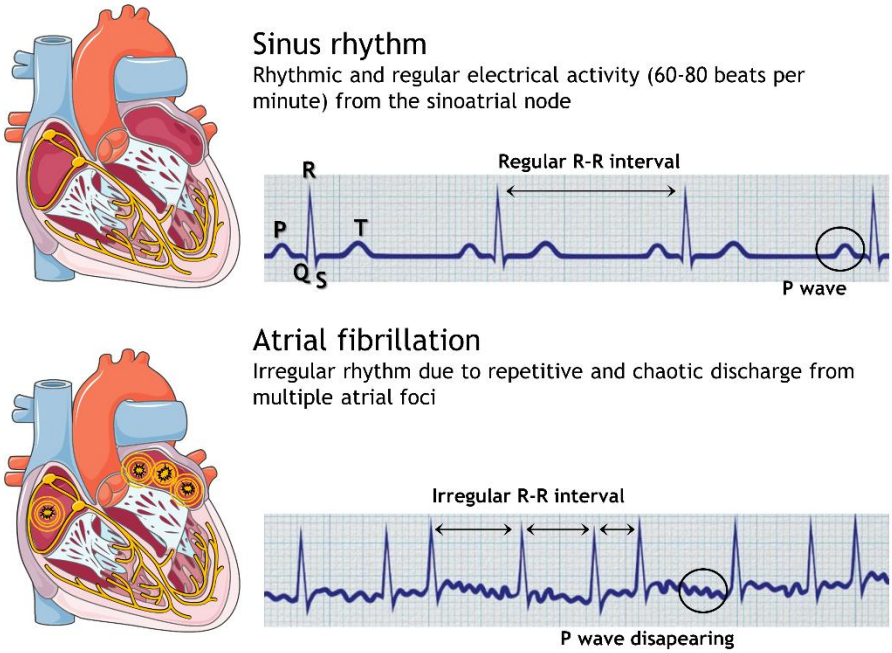


Figure 3. Atrial fibrillation: Graphical description

Figure created from modified images of Servier Medical Art (https://smart.servier.com) licensed under Creative Commons Attribution 3.0 Unported License

In a normal electrocardiogram (ECG), P wave reflects atrial depolarization, which triggers atrial contraction. QRS wave represents ventricular depolarization, which will initiate ventricle contraction. Finally, T wave reflects repolarization and the consequent ventricular relaxation[5]. AF has been described as a change from normal P waves to rapid oscillations that vary in size, shape, and duration. They are associated with an irregular ventricular response when AV conduction is intact[3] (Figure 3).

USC UNIVERSIDADE DE SANTIAGO DE COMPOSTELA

Due to the absence of an effective atrial contraction, there is a greater tendency to form blood clots that could lead to stroke.

This arrhythmia triggers significant hemodynamic dysfunction and thromboembolic events that carry a high risk of morbidity, specifically the aforementioned stroke[6], heart failure (HF)[7], and mortality[8]. Consequently, AF is a common cardiovascular cause of hospitalization, generating significant healthcare costs. The latest clinical practice guidelines for the management of AF by the ESC have not changed the previous classification (new-onset, paroxysmal, persistent, long-standing persistent, and permanent) based on the presentation, duration, and spontaneous termination of AF episodes (Table 1).

Table 1. Atrial fibrillation classification

AF type	*Definition*
New onset	Previously undiagnosed AF, regardless of its duration or the presence/severity of its associated symptoms
Paroxysmal	AF ending spontaneously or after surgery within 7 days
Persistent	Continuously sustained AF for more than 7 days, including episodes terminated after that period by cardioversion (pharmacologic or electrical)
Long-standing persistent	Continuous AF of more than 12 months for which it has been decided to adopt a rhythm control strategy.
Permanent	AF accepted by the patient and the physician, in which no further attempts to restore/maintain sinus rhythm will be made. Permanent AF represents a therapeutic approach rather than an inherent pathophysiologic attribute of AF, and the term should not be used in the context of a rhythm control strategy with antiarrhythmic drug therapy or AF ablation. If a rhythm control strategy were adopted, the arrhythmia would be reclassified as "long-standing persistent AF."

Added to this classification, it should also be highlighted the so-called postoperative AF, which is diagnosed when the episodes appear two to four days after a surgical procedure. Episodes are usually short and self-terminated. Even so, this type of AF appears between 20% and 40% after cardiac surgical procedures and 10% to 20% after non-cardiac thoracic operations, increasing the risk of events, hospitalization times, and its associated costs[9].

USC UNIVERSIDADE DE SANTIAGO DE COMPOSTELA

As a novelty, the last ESC guidelines have encouraged a structured characterization of AF according to stroke risk, symptom severity, burden, and underlying substrate[10]. Adjusting AF classification according to the presence of biomarkers related to its associated risk factors can help to delineate more specific strategies for the prevention, diagnosis, and treatment of patients affected by AF.

1.3.2 AF incidence and prevalence

According to ESC data, the prevalence and incidence of this disease in Europe in 2017 was 25.8 million people and 750.000 new cases, respectively[11]. The incidence of this arrhythmia varies globally among different ethnic groups[12]. Based on results from the Multi-Ethnic Study of Atherosclerosis (MESA), which included participants from six regions of the United States, the incidence of AF was higher in non-Hispanic white Americans than in Hispanic Americans , African-Americans, and Asians[13].

However, this incidence may not be accurate due to the disparity in the detection methods or the duration of arrhythmia monitoring, among other factors[14]. Blum *et al*. highlighted in a meta-analysis that the incidence of AF is lower as the follow-up period increases[15].

Despite the global differences that exist in the prevalence and incidence of this disease, it is undeniable that AF has a significant epidemiological impact. In Europe, one out of three individuals over fifty-five years old will suffer from AF at some point in their life[10].

1.3.3 Associated risk factors

AF is a multifactorial disease that is mainly accompanied by other comorbidities. In fact, the use of the so-called “lone AF” category is currently discouraged.[10].

AF associated risk factors (Figure 4) include smoking[16], alcohol consumption[17], lifestyle[18] and genetic predisposition[19,20], recognized as important players in the susceptibility, maintenance and recurrence of AF. Among them, the most attributable risk factors to this arrhythmia

USC UNIVERSIDADE DE SANTIAGO DE COMPOSTELA

are detailed below, including the latest discoveries that relate each one with the disease.

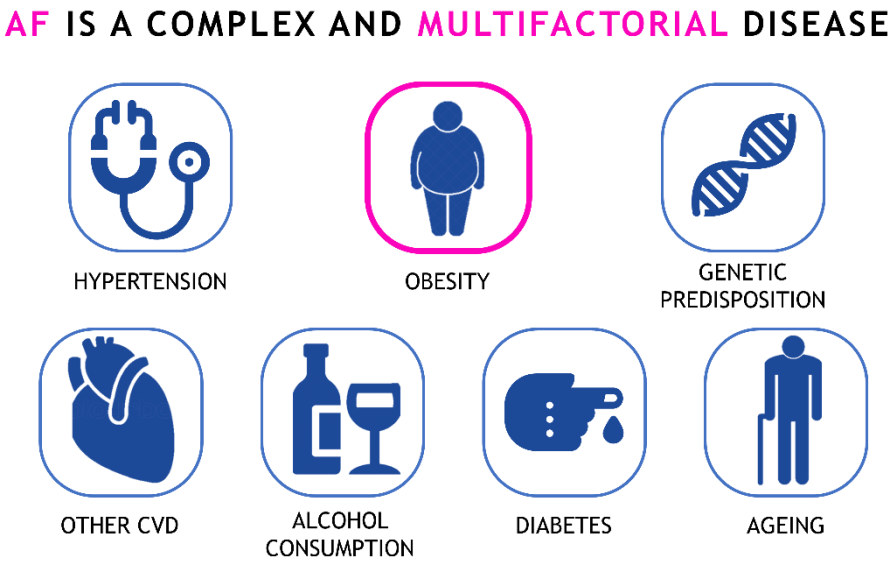


Figure 4. Main AF associated risk factors

AF: Atrial fibrillation, CVD: Cardiovascular diseases

Figure made from modified images of Servier Medical Art (https://smart.servier.com) licensed under Creative Commons Attribution 3.0 Unported License

a) Hypertension

Hypertension is the most attributable risk factor for AF[21,22]. In a recent manuscript reviewing the Systolic blood PRessure INtervention Trial (SPRINT), intensive blood pressure control (<120 mm Hg) showed a statistically significant decrease in AF rates, although a longer-term study remains to be done to know if this implies an inhibition or if it is an actual AF risk delay[23].

It has recently been reported that, as in the case of weight change, long-term blood pressure monitoring may be more indicative of AF risk

USC UNIVERSIDADE DE SANTIAGO DE COMPOSTELA

than a single measurement. Two people with the same blood pressure at the same time had a different risk of AF incidence depending on whether they maintained or changed their levels over time. This study concluded that the risk of AF associated with hypertension differs with gender, being higher in women than in men[24].

b) Ageing

The association of AF with age has been very well reviewed in recent publications[25,26]. Given the increase in life expectancy thanks to medical advances, it is important to focus our attention on improving the quality of life of our elderly population. It has been seen that, despite the absence of significant differences in the first year after catheter ablation with respect to age, older patients showed higher rates of recurrence of atrial flutter/AF after 5 years. The authors encouraged to take this into account in order to consider anticipating the procedure when possible[27].

c) Diabetes

Type 2 diabetes mellitus (T2DM) is another well-known established AF risk factor[28]. Recently, a large number of patients was evaluated to study the implication of diabetes in new-onset AF and its relationship with body mass index (BMI). The results showed that not only the presence, but also the stage of T2DM and its association with BMI, were an independent risk factor for developing AF, with obese diabetic patients being at the highest risk[29].

d) Obstructive sleep apnoea (OSA)

The relationship between OSA and AF, with respect to common risk factors, ablation outcomes, and biological mechanisms, has been nicely reviewed in the past year by Shantha G. *et al.*[30]. It has been hypothesized that the relationship between OSA and AF can be explained by RA volume remodeling[31]. Through a rat model of OSA, the main dysregulated proteins between severe, moderate and control subjects were described. They were related to mitochondrial function and the glycolysis pathway (as citrate synthase) and downregulated in apnoea-affected relative to control subjects. In contrast, proteins

USC UNIVERSIDADE DE SANTIAGO DE COMPOSTELA

involved in apoptosis, structural features, or lipid metabolism showed lower expression in control subjects compared to subjects with severe or moderate apnoea[32]. These results may pave the way to the identification of the mechanistic involvement of OSA in AF in humans.

e) Obesity

Obesity has been recognized as one of the most important AF risk factors, only behind hypertension[33]. A recent large population-based study highlighted the increased incidence of AF with weight change and long-term obesity, even adjusting for recent BMI[34].

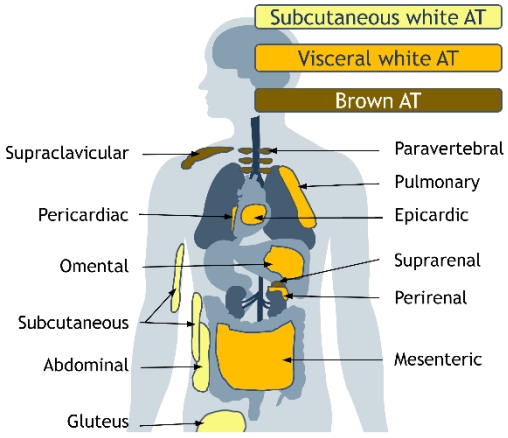


Figure 5. Example of some adipose tissue (AT) depots according to their location.

Figure created from a modified image of Servier Medical Art (https://smart.servier.com) licensed under Creative Commons Attribution 3.0 Unported License

Advances in science and imaging techniques allowed to discern and classify different body fat depots. Depending on their location, a wide variety of local fat depots with particular characteristics can be distinguished (Figure 5)[35].

Thus, epicardial adipose tissue (EAT) is more related to CVD, and to AF, than classical measures of general adiposity and other local adipose tissue (AT) depots.

The current unsuccessful results of the generalized clinical approaches to AF treatment alert us to the need to develop therapies targeting each patient's comorbidities and risk factors.

USC UNIVERSIDADE DE SANTIAGO DE COMPOSTELA

1.4 EPICARDIAL ADIPOSE TISSUE

Since 1898, year in which the first article mentioning epicardial fat was published in PubMed[36], EAT had gone practically unnoticed by the scientific community, being considered as an anecdotic fat depot. In the early 2000s, G.L. Iacobellis *et al.*[37–42] described, by ECG, its association with cardiac dysfunction. Since then, there has been a very pronounced exponential growth in the number of scientific publications about this cardiac fat pad (Figure 6).

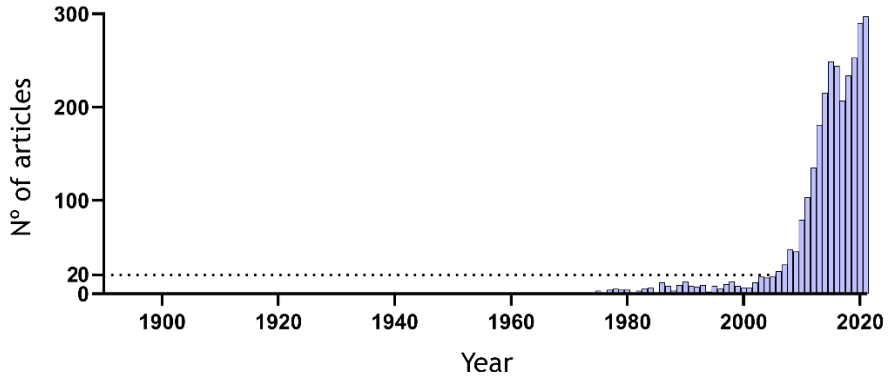


Figure 6. Scientific literature on epicardial adipose tissue (EAT).

Articles collected in PubMed referring to "epicardial adipose tissue" or "epicardial fat" since its first appearance, in 1898.

EAT is no longer considered a simple store of fatty acids (FA), to become the AT with the greatest influence on myocardial behaviour and functionality.

1.4.1 Definition

EAT constitutes, together with the pericardial adipose tissue (PAT), the visceral fat pad of the heart. Both are found surrounding this organ, but there are some differences that have made it imperative to discern them. EAT is in direct contact with the myocardium, below the visceral layer of the pericardium. PAT, on the other hand, is located above it (Figure 7)[43]. They also differ in their embryonic origin (the splanchnopleuric layer of the mesoderm in the case of EAT *versus* the primitive thoracic mesenchyme, which forms the parietal pericardium

USC UNIVERSIDADE DE SANTIAGO DE COMPOSTELA

and the external thoracic wall, and gives rise to PAT) [39]. In addition, unlike PAT, irrigated by the pericardiophrenic branches of the internal mammary artery, EAT shares the same microvasculature with the myocardium, since the coronary arteries are embedded in it[44].

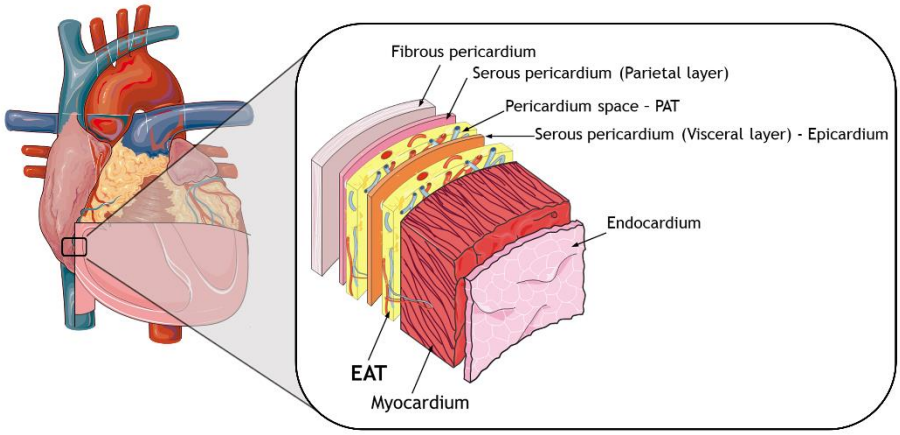


Figure 7. Epicardial adipose tissue (EAT) location compared to pericardial adipose tissue (PAT).

Figure created from modified images of Servier Medical Art (https://smart.servier.com) licensed under Creative Commons Attribution 3.0 Unported License

All these characteristics give EAT the particularity of influencing the myocardium, either directly through cellular infiltration and cell to cell contact, or in an endocrine and/or vasocrine way, as it is a very metabolically active tissue.

1.4.2 Composition

EAT, apart from mature adipocytes, includes many other cell types, constituting its stromal vascular fraction (SVF). EAT SVF is mainly composed of fibroblasts, mesenchymal cells, adipose-derived stem cells (ADSC), pericytes, vascular cells and immune system (myeloid and lymphoid) cells (Figure 8).

USC UNIVERSIDADE DE SANTIAGO DE COMPOSTELA

Crosstalk between different cell types plays an important role in EAT functioning and differentiation[45]. The disorder of this communication may involve structural and molecular changes that will promote and/or help to sustain different CVD.

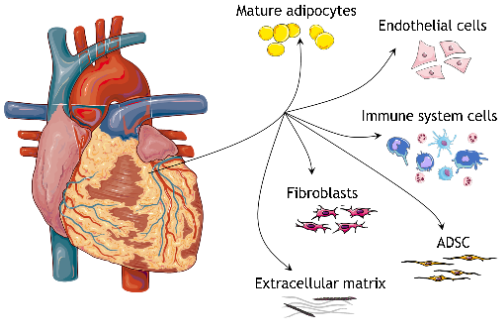


Figure 8. Epicardial adipose tissue cellular composition

ADSC: Adipose-derived stem cells

Figure created from modified images of Servier Medical Art (https://smart.servier.com) licensed under Creative Commons Attribution 3.0 Unported License

1.4.3 Characterization

Imaging techniques evolution allowed the scientific community to an improvement in the characterization of EAT. ECG, being the cheapest and most accessible technique, allows to measure EAT thickness[37,46]. It is seen as a space without echo or if it is massive, hyperechoic. EAT is usually measured in the free wall of the right ventricle. However, ECG has some disadvantages, such as the chance of misclassification with the pericardial space[47], or the lack of accuracy (its distribution is three-dimensional and variable, and this imaging technique is two-dimensional)[48]. Other techniques that allow to a more precise designation of EAT include computed tomography (CT), characterized by high spatial resolution and a real coverage of heart volume as a whole[49]; or cardiac magnetic resonance (CMR) imaging, which evaluates the entire heart in consecutive layers and, therefore, it is not limited by the position and orientation of the image planes[50]. However, both techniques have a higher cost, and they require specialization. Besides, unlike ECG, they are not used routinely in clinical practice.

Regardless of the technique used, it is important to distinguish between EAT and PAT, due to the afore-mentioned reasons. In addition, within the techniques that allow to an optimal characterization

USC UNIVERSIDADE DE SANTIAGO DE COMPOSTELA

of EAT, those able to identify not only the quantity (volume/thickness), but also the quality (composition) of EAT, would be more useful.

1.4.4 Physiological functions

EAT is characterized by being a metabolically active tissue, which under physiological conditions can cover up to 80% of the myocardium and weigh 20% of the total mass corresponding to the heart[51]. In these circumstances, EAT fulfils certain functions that contribute to the correct functioning of the myocardium, summarized in the following figure:

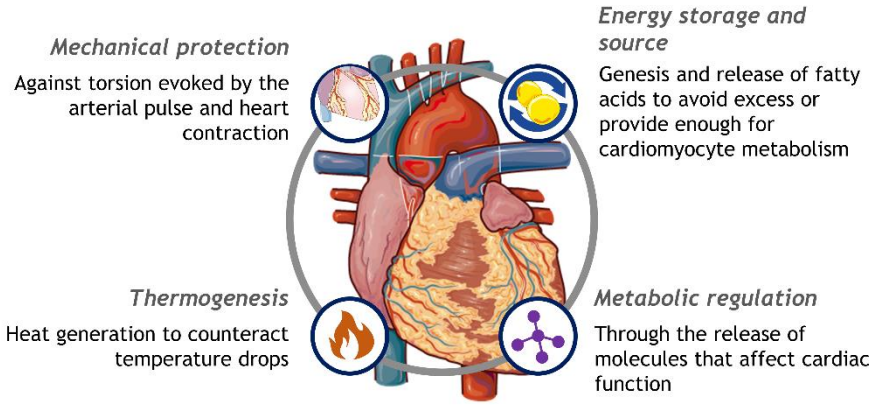


Figure 9. Physiological functions of epicardial adipose tissue

Figure made from modified images of Servier Medical Art (https://smart.servier.com) licensed under Creative Commons Attribution 3.0 Unported License

a) Mechanical protection

EAT surrounds the main branches of the coronary arteries and is also found in the AV and interventricular grooves. In addition, the ganglionated plexuses that regulate heart rate through the ANS are also embedded in this tissue. Its compressibility and elasticity allow this pad to mechanically protect all these components against an excessive distortion caused by the arterial pulse and myocardial contraction[52].

USC UNIVERSIDADE DE SANTIAGO DE COMPOSTELA

b) Energy source and storage

Human heart has the ability to use any type of energy substrate, varying between lipids, carbohydrates, amino acids and ketone bodies[53]. In healthy individuals, cardiac metabolism is mainly based on glucose and free fatty acids (FFA) catabolism. Under fasting conditions, the preferred substrate is FFA[54] whose oxidation is responsible for between 50% and 70% of myocardial energy production[39]. EAT has been shown to be more metabolically active than other fat depots[44,55]. It shows greater FFA release and uptake ability, for disposal by cardiomyocytes (CMs), or to avoid possible damage from an excess of circulating FFA, respectively[56].

c) Thermogenesis

Brown adipose tissue (BAT) is characterized by its unique ability to generate heat in a process known as thermogenesis, whereby uncoupling protein 1 (UCP1) dissociates mitochondrial oxidative phosphorylation leading to the rapid conversion of electrochemical energy into heat instead of adenosine tri-phosphate (ATP)[57]. This process is carried out in mammals to avoid hypothermia or to manage energy excess. In humans, BAT is considerably reduced after birth to small mediastinal depots (cervical, supraclavicular and superior)[58].

Recently, the presence of the BAT specific marker UCP1 has been described in EAT, as well as BAT differentiation transcription factors, such as PR-domain-missing 16 (PRDM16) and peroxisome proliferator-activated receptor gamma (PPARγ) coactivator-1 alpha (PGC-1α). The expression of these genes is higher in this tissue compared to the rest of the AT depots, and practically negligible in the subcutaneous adipose tissue (SAT)[59,60].

Although further studies are needed to confirm this hypothesis, EAT could be acting as BAT, protecting the myocardium against hypothermia and energy excess.

d) Metabolic regulation of the myocardium

USC UNIVERSIDADE DE SANTIAGO DE COMPOSTELA

EAT has been widely recognized for its high metabolic activity[44,55,61]. Given its cellular variability, this tissue secretes many molecules with cardioprotective functions, some of which are included in the following table:

Table 2. Major regulatory molecules secreted by epicardial adipose tissue (EAT)

Molecule	*Main functions*	*References*
Adiponectin	*Vasodilation, anti-inflammation, suppression of cytokine production, and lipid accumulation in macrophages*	62–64
Adrenomedullin	*Vasodilation, anti-oxidation, angiogenesis, anti-inflammation, and anti-apoptosis*	65,66
FABP4	*Glucose and lipid homeostasis*	67
Leptin	*Vasodilation, anti-inflammation*	64,68
Omentin	*Vasodilation, anti-inflammation, improvement of insulin sensitivity*	69,70
Visfatin	*Stimulation of glycaemic metabolism*	69,71

FABP4: Fatty acid binding protein 4

On the other hand, EAT disfunction can modify adipokine expression and secretion, counteracting their beneficial effects, as in the case of leptin, whose increased expression has been associated with coronary artery disease (CAD)[72]. Under pathological conditions, this tissue secretes adipokines that induce fibrosis, such as activin A[73,74], or inflammation, such as interleukin 6 (IL-6), monocyte chemoattractant protein 1 (MCP-1) and tumour necrosis factor alpha (TNFα)[61].

Fibrosis and inflammation, together with arrhythmogenesis, are processes closely related to AF. Thus, EAT activity may be involved in the pathological mechanisms that trigger and maintain this arrhythmia, as we will see in the next section.

USC UNIVERSIDADE DE SANTIAGO DE COMPOSTELA

1.4.5 Article 1 | Pathophysiological mechanisms of EAT in AF

The content from this chapter has already been published as Marinela Couselo-Seijas[1,2], Moisés Rodríguez-Mañero[1,3,4], José Ramón González-Juanatey[2,3,4,5], Sonia Eiras[1,3] Updates on epicardial adipose tissue mechanisms on atrial fibrillation. Obes Rev. 2021 Sep;22(9):e13277.

DOI: 10.1111/obr.13277., PMID: 34002458., ISSN: 1467-7881

Affiliations: [1]Grupo de Cardiología Traslacional, IDIS, Santiago de Compostela, España; [2]Universidad de Santiago de Compostela, Santiago de Compostela, España; [3]CIBERCV, Madrid, España; [4]Área Cardiovascular, Hospital Clínico Universitario, Santiago de Compostela, España; [5]Grupo de Cardiología, IDIS, Santiago de Compostela, España

Link: https://onlinelibrary.wiley.com/doi/10.1111/obr.13277

1.5 AUTONOMIC NERVOUS SYSTEM

EAT involves the anatomical location of the intrinsic cardiac ANS (Figure 10), which includes the ganglionated plexuses and interconnecting nerves that, in the case of the left atrium (LA), are located mainly in the posterior wall around the pulmonary veins (PV) .

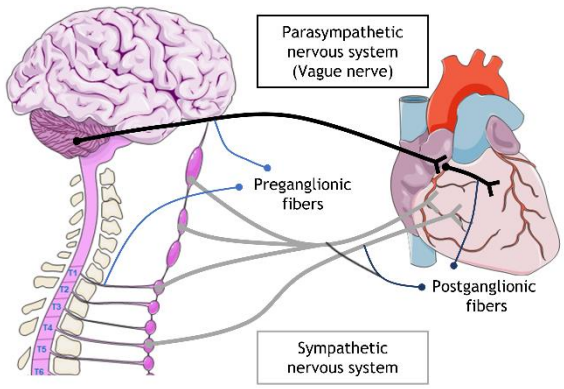


Figure 10. Simplified graphic description of cardiac innervation by the autonomic nervous system (ANS)

Figure made from a modified image of Servier Medical Art (https://smart.servier.com) licensed under Creative Commons Attribution 3.0 Unported License

Cardiac **sympathetic innervation** originates in the vertebral column and reaches the stellate ganglion located near the first rib below the subclavian artery. At synapses in this ganglion, preganglionic neurons release acetylcholine (ACh), which activates nicotinic ACh receptors on postganglionic cells. In response to sympathetic stimulation, postganglionic neurons release norepinephrine, activating β-adrenergic receptors. CM response to these receptors is mediated by stimulatory G proteins (Gs), whose activation causes the stimulation of adenylyl cyclase and consequently the protein kinase A (PKA)-mediated phosphorylation of voltage dependent Ca^{2+} channels[75].

Cardiac **parasympathetic nervous system** originates in the medulla, from which the efferent vague nerve extends and connects with the postganglionic nerves that innervate the atrium. At the cellular level, type 2 muscarinic acetylcholine receptors (mAChRs) are the main mediators of the parasympathetic control of cardiac function. mAChR 2 effects are opposite to β-adrenergic receptors. Its stimulation inhibits adenylyl cyclase and cAMP via inhibitory G proteins (Gi), which inhibit L-type voltage-dependent Ca^{2+} current (I_{CaL}) and the funny

USC UNIVERSIDADE DE SANTIAGO DE COMPOSTELA

current (I_f) activated by hyperpolarization. Gi proteins activated by mAChR 2 can directly activate acetylcholine-dependent potassium (K^+) current (I_{KACh}), causing the shortening of the effective refractory period of the atrium. The effect of vagal stimulation in this refractory period is heterogeneous due to the spatial distribution of parasympathetic endings and mAChR 2[75].

1.6 HEART IMPULSE AT THE CELLULAR LEVEL

1.6.1 Cardiac action potential

The shape of the cardiac action potential (AP) is a response to specific ionic currents, which can be depolarizing or repolarizing (Figure 11).

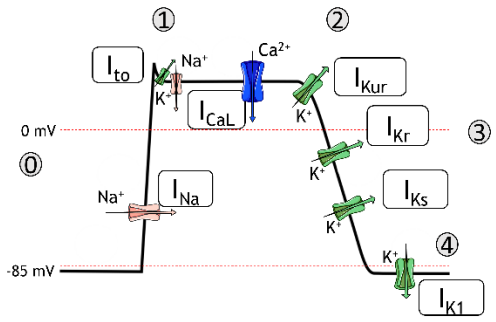


Figure 11. Graphic scheme of the action potential and the main ionic currents involved

Figure made from modified images of Servier Medical Art (https://smart.servier.com) licensed under Creative Commons Attribution 3.0 Unported License

Depolarizing ionic currents are basically composed by Na^+ currents (I_{Na}) and I_{CaL}. K^+ channels trigger the AP repolarization phase. There are three types of K^+ currents, the voltage dependent ones (I_{to}, I_{Kur}, I_{Kr}, and I_{Ks}), the rectifying input currents (I_{K1}, I_{KACh}, and I_{KATP}), and the background K^+ currents (TASK-1 and TWIK -1/2)[76].

An I_{K1} gradient has been described in paroxysmal AF, with higher expression in LA, which allows to higher depolarization frequencies compared to RA. Greater AF-induced remodelling leads to an increase in I_{K1}, I_{KACh}, and K2P3.1 channels together with a decrease in I_{CaL}; changes that could explain the reduction in APD in persistent and permanent AF, leading to re-entries stabilization[77–80]. Changes in I_{K1} have also been described in the progression from paroxysmal to persistent AF, increasing its expression in both atria. However,

USC UNIVERSIDADE DE SANTIAGO DE COMPOSTELA

electrical remodelling is not uniform in persistent AF, which was associated with an increase in I_{Ks} in both atria and specific decreases in I_{to} and I_{Kur} in LA and RA, respectively[81]. These observations demonstrate the complexity of electrical remodelling caused by AF, depending on its chronicity and the type of tissue studied.

1.6.2 Intracellular Calcium mobilization

Ca^{2+} is the main ion responsible for muscle contraction, and its intracellular location is key in the excitation-contraction coupling (ECC) mechanism. ECC connects the electrical impulse derived from the ionic currents responsible for the AP with the mechanical contraction of the cells[82–84]. Precise control of the intracellular Ca^{2+} cycle depends on the interaction between various channels and pumps that act together (Figure 12).

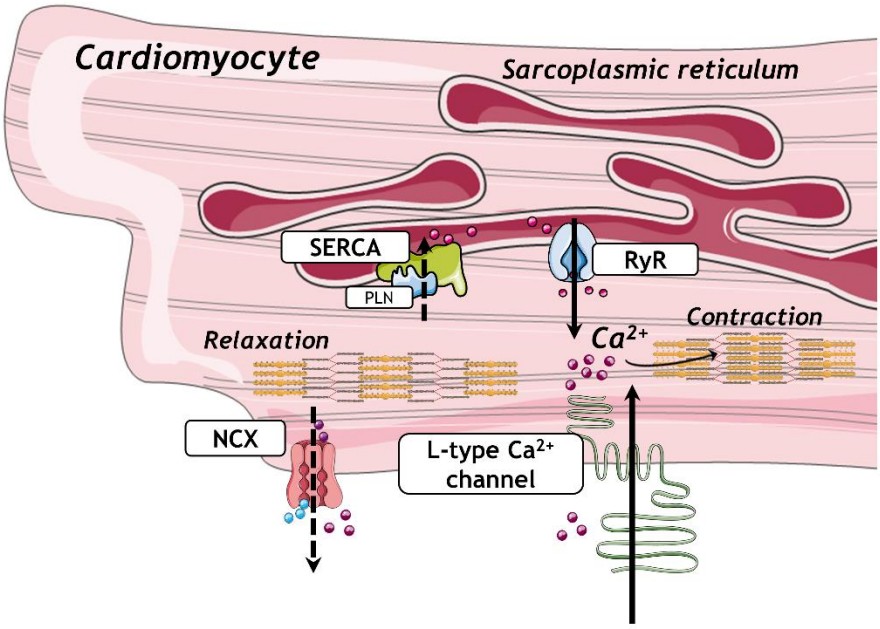


Figure 12. Main pumps and channels involved in the cardiac excitation-contraction coupling mechanism.

NCX: Sodium/calcium exchanger; SERCA: Sarco/endo plasmic reticulum calcium (Ca2+) ATPase cardiac isoform; RyR: Ryanodine receptor; PLN: Phospholamban

USC UNIVERSIDADE DE SANTIAGO DE COMPOSTELA

Figure created from modified images of Servier Medical Art (https://smart.servier.com) licensed under Creative Commons Attribution 3.0 Unported License

Alterations in Ca^{2+} handling have been described, generally explained by RyR_2[85] dysfunction, which predispose atrial CMs to delayed after-depolarizations (DADs) due to increased Ca^{2+} leaks from the sarcoplasmic reticulum (SR)[86]. Similarly, in persistent AF, hyperphosphorylation of RyR_2 due to increased activity of Ca^{2+}/calmodulin-dependent protein (CaMKII) leads to increased Ca^{2+} leaks coupled with increased activity of the Na^{+}/Ca^{2+} exchanger (NCX) current (I_{NCX})[87].

Alterations in the ANS associated with abnormal PV activity have also been described. These alterations correlate sympathetic activity with DADs, while parasympathetic dysfunction can increase the heterogeneity of the effective refractory period of CMs, generating a substrate for reentry[88].

USC UNIVERSIDADE DE SANTIAGO DE COMPOSTELA

2 HYPOTHESIS AND GENERAL OBJECTIVES

Observational studies that quantify the amount of EAT have shown its close association with AF risk. This should be considered after cardiac surgery, where 30-50% of the patients develop AF within the following forty-eight hours. A recent clinical trial demonstrated a reduction in AF recurrence in cardiac surgery patients after injection of botulinum toxin into the ganglionated plexus located within EAT pads. Knowing that this toxin decreases ACh release, we hypothesized a relationship between this neurotransmitter, EAT and AF. Thus, cholinergic activity could regulate EAT metabolic, inflammatory, and endocrine activity.

Based on previous data, our group believes that there is a crosstalk between ANS dysfunction, EAT and inflammation. In this way, EAT could secrete one or more proteins, regulated by the ANS, that would act as AF promoters. Furthermore, since EAT is an endocrine organ, these proteins could be detected systemically as prognostic and/or diagnostic AF biomarkers. Besides, the regulation of the expression or activity of these proteins could be the objective of new therapies, and the measurement of their levels could be used as indicators of treatment efficiency.

To demonstrate the hypotheses of the thesis project, the objectives of this work consisted of:

1. To study the cholinergic effect on EAT activity. To achieve this, the following procedures were carried out:

    a) Analysis of the differential expression of ACh cholinergic receptors and identification of the released proteins after cholinergic activity in atrial and ventricular EAT (aEAT, vEAT).

    b) Identification of the proteins released by EAT after ACh treatment

    c) Validation of the identified proteins in plasma from patients undergoing cardiac surgery and their association with AF.

USC
UNIVERSIDADE DE SANTIAGO DE COMPOSTELA

2. To study the cholinergic effect on inflammatory and adipogenic activity of EAT cells. To achieve this objective, it was required:

a) To analyse the inflammatory markers in EAT SVF cells after cholinergic treatment.

b) To test EAT genesis and its markers after cholinergic treatment.

c) To study the association between these markers and AF.

3. To test the effect of EAT markers associated with AF on atrial CMs derived from human induced pluripotent stem cells (hiPSC).

USC
UNIVERSIDADE DE SANTIAGO DE COMPOSTELA

3 MATERIALS AND METHODS

3.1 PATIENT SAMPLES

To carry out the experimental procedures performed during this doctoral thesis, tissue and blood samples have been obtained from patients undergoing cardiac surgery. The study was approved by the Galician Research Ethics Committee (Registration Code 2016/262 and 2019/439). The studies were performed in full compliance with the Declaration of Helsinki. This work has been developed within the project "*Indicadores de fibrilación auricular en el tejido adiposo epicárdico y su regulación por la actividad física*" (PI16/011282) and its continuation project (PI19/01330). Prior to the extraction of the samples, each participant signed a written informed consent in which the main objectives of the study were detailed

Apart from the material and methods already specified in the articles (see 4.1, 4.2 and 4.5), the following procedures were performed:

3.2 CELL CULTURES

3.2.1 hiPSC-derived atrial cardiomyocytes

During the development of this doctoral thesis, two lines of hiPSC-derived atrial CMs were cultured:

1. **Differentiated** hiPSC-derived atrial CMs (AxolBio) were cultured following the manufacturer's protocol. Cells were maintained for eight days, starting FABP4 (Cloud Clone Corp.) treatment at concentrations of 10 and 100 ng/mL from the fourth to the eighth day, with medium replacement every 24 h, under standard culture conditions (37º C and 5% CO_2). Cells were maintained on sterile CaF_2 coverslips (Crystran Ltd.) placed in 24-well plates, to acquire Raman spectra with no contribution from cell growth support (see 3.3). After treatment, cells were washed once with phosphate-buffered solution (PBS) 0.01 M containing (in mM): 0.5 ethylene diamine tetra acetic acid

USC UNIVERSIDADE DE SANTIAGO DE COMPOSTELA

(EDTA), 5 potassium chloride (KCl), 10 (4-(2-hydroxyethyl)-1-piperazineethanesulfonic acid (HEPES), 2 magnesium chloride ($MgCl_2$), 10 sodium bicarbonate ($NaHCO_3$), 0.5 potassium dihydrogen phosphate (KH_2PO_4), 0.5 sodium dihydrogen phosphate (NaH_2PO_4), 10 glucose, 110 sodium chloride (NaCl) and 0,16 calcium chloride ($CaCl_2$) (pH 7.4). Subsequently, plates were washed with distilled water. Then, they were left to dry at room temperature (r.t.) for 12 hours.

2. **Undifferentiated** hiPSC obtained after dedifferentiation from peripheral blood mononuclear cells (PBMC) according to the laboratory procedure[89]. Cells were plated at the density of 200 000 cells/cm² in 12-well plates coated with hESC-Qualified Matrigel® (Corning). Maintenance medium was changed the next day and 2 days after plating (considered as day 0). Cells were then subjected to atrial CM differentiation using the commercial STEMdiff™ Atrial Cardiomyocyte Differentiation Kit (StemCell Technologies) (Figure 13).

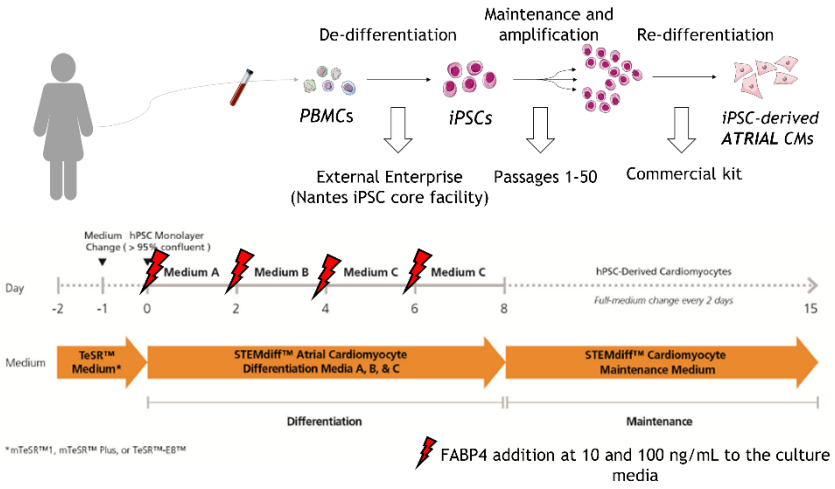


Figure 13. Atrial cardiomyocyte (CM) differentiation protocol from hiPSC

PBMC: Peripheral blood mononuclear cells; hiPSC: human induced pluripotent stem cells

USC UNIVERSIDADE DE SANTIAGO DE COMPOSTELA

Figure made from modified images of Servier Medical Art (https://smart.servier.com) licensed under Creative Commons Attribution 3.0 Unported License

Manufacturer's protocol was followed, with the only modification being the addition of FABP4 at 10 or 100 ng/ mL to the culture medium on days 0, 2, 4 and 6 of the differentiation process. At day 19 of differentiation, atrial CMs were gently detached using TrypLE^{TM} Express and 70 000 hiPSC- derived atrial CMs were plated in a 2 well culture insert (Ibidi) placed at the centre of a 35 mm µ-Dish (Ibidi) coated with Matrigel®. The differentiation medium was changed every two days and cells were analysed between day 27 and 30.

3.3 BIOCHEMICAL ASSAYS

3.3.1 Intracellular composition by confocal Raman microspectroscopy

Vibrational spectroscopy techniques have been shown to be powerful tools to determine the chemical fingerprint of tissues and cells under specific conditions, with little or no prior sample preparation steps. Furthermore, they only require a small amount of sample.

Raman scattering is a phenomenon of inelastic light scattering. When monochromatic light reaches a sample it scatters, both elastically and inelastically. Elastically scattered light (also known as the Rayleigh effect) is emitted with the same energy as the incident light, while inelastically scattered light (Raman effect) is emitted with a different wavelength. This difference is due to an energy change called the Raman shift, which provides specific molecule fingerprints[90].

Raman spectra were obtained using a LabRAM HR 800 Raman system (Horiba-Jobin Yvon) and a fully integrated Olympus BX41 confocal microscope (Olympus) using a 514 nm laser as the excitation source. Spectra were collected in the region between 400 and 3100 cm^{-1}. Samples were focused using a 100× objective (Type LWD, LMPlanFL N NA 0.50, Olympus) and an aperture of 100 µm. Nuclei and cytoplasm atrial CM spectra were acquired in different areas of the culture plates and averaged for each condition, with an integration time

USC UNIVERSIDADE DE SANTIAGO DE COMPOSTELA

of 120 seconds and 2 accumulations using the Labspec5 software (Horiba Jobin Yvon, version 5.25.15). Light was scattered using a 1800 lines/mm grating with a spectral resolution of 0.45 cm^{-1}. Prior to spectra acquisition, the instrument was calibrated daily using a reference silicon sample (peak at 520.7 cm^{-1}).

Spectra were analysed using R software (version 3.4.3). Briefly, error spectra were revised and removed. Then, spectra were corrected and normalized to the baseline. Orthogonal Partial Least Squares-Discriminant Analysis (OPLS-DA) was used to decipher differential Raman features. Peaks relevant to changes, determined by Variable Importance Parameter (VIP) values > 1, were further analysed using GraphPad Prism v7 software (GraphPad Software), using two-way Analysis Of Variance (ANOVA) or Welch's ANOVA followed by a post hoc test (Šídák's multiple comparisons test).

3.4 FUNCTIONAL ASSAYS

During this doctoral thesis, the following procedures were carried out to evaluate a specific functionality:

3.4.1 Intracellular calcium mobilization

Atrial CMs were loaded with Calbryte™ 520 AM fluorescent Ca^{2+} indicator (5 mmol/L) for 1 h under standard culture conditions. Culture plates were placed in the fluorescence microscope, where they were kept at a constant temperature of 37º C in a thermostatic stage. Cells were perfused until complete replacement of the maintenance medium by the colourless AP solution with the following components: 140 mM NaCl, 4 mM KCl, 10 mM HEPES, 1.1 mM $MgCl_2$, 1.8 mM $CaCl_2$ and 20 mM glucose (pH=7.4). To record spontaneous transients of intracellular calcium concentration ($[Ca^{2+}]i$), cells loaded with Calbryte™ 520 AM were maintained without stimulation, in order to acquire measurements of their spontaneous activity (contraction rate). Subsequently, cells were stimulated with two platinum electrodes at 1 Hz, to study the different kinetic characteristics of the $[Ca^{2+}]i$ transients. Fluorescence (F) values were normalized to baseline fluorescence (F0) after background subtraction to obtain

USC UNIVERSIDADE DE SANTIAGO DE COMPOSTELA

fluorescence amplitude (F:F0). Decay time constant of Ca^{2+} transients, τ, was obtained by fitting the decay trace.

Caffeine was applied rapidly to deplete SR Ca^{2+} stores, which gives an estimation of the SR Ca^{2+} load; for this, CMs were perfused with 10 mmol/L of caffeine immediately after field stimulation. The amplitude of caffeine-induced Ca^{2+} transients (F:F0) was used to assess the global Ca^{2+} load in the SR.

Recording protocols, carried out with Leica Application Suite (LAS X) software on a Leica SP5 confocal microscope (Leica Microsystems), were as follows:

1. Video (xyt) at 1000 Hz, 2.5 zoom, 60 frames
2. Arrhythmias (xt) at 400 Hz, 2.5 zoom, 1500 lines
3. Transients (xt) at 700 Hz, 2.5 zoom, 2000 lines
4. Caffeine (xt) at 400 Hz, 2.5 zoom, 15000 lines

All the analysis of the Ca^{2+} images obtained were performed using scripts designed by the group with the Interactive Data Language software, IDL (Research Systems) and ImageJ[91,92].

3.5 STATISTICAL ANALYSIS

All analyses were performed with SPSS version 22.0 (SPSS Software Inc). Data distribution was analysed using Shapiro-Wilk normality test to check its fit to a normal or Gaussian distribution.

Quantitative variables were presented as arithmetic mean ± standard error media (SEM) or median ± interquartile range (IQR), depending on whether they followed a normal distribution or not, respectively. Continuous clinical variables were presented as mean ± standard deviation (SD) and categorical variables as frequency and percentage.

Comparisons between different treatments or tissues were performed using t-test for paired samples and non-parametric Wilcoxon

USC UNIVERSIDADE DE SANTIAGO DE COMPOSTELA

signed-rank test according to the distribution of the data (normal or not, respectively). Comparisons between categorical clinical variables were performed using Pearson's χ^2 test. Differences between patients affected/non-affected by AF were defined using unpaired t-test (for data sets with a normal distribution) or nonparametric Mann-Whitney test (for data sets that do not fit a normal distribution).

Statistical significance was defined as *p*-value <0.05. For the representation of the statistical results in graphs, the GraphPad Prism v7 software (GraphPad Software) was used.

USC
UNIVERSIDADE DE SANTIAGO DE COMPOSTELA

4 RESULTS

4.1 ARTICLE 2 | CHOLINERGIC ACTIVITY REGULATES THE SECRETOME OF EPICARDIAL ADIPOSE TISSUE: ASSOCIATION WITH ATRIAL FIBRILLATION

The results from this chapter have already been published as Marinela Couselo-Seijas[1,6], José N. López-Canoa[1,2], Rosa M. Agra-Bermejo[1,2,3], Esther Díaz-Rodríguez[1], Ángel L Fernández[3,4], José M. Martínez-Cereijo[4], Darío Durán-Muñoz[3,4], Susana B. Bravo[5], Alba Velo[1], Laila Rodríguez-Melchor,[2] Xesús A. Fernández-López[2], José L. Martínez-Sande[1,2,3], Javier García-Seara[1,2,3], José Ramón González-Juanatey[1,2,3,6], Moisés Rodríguez-Mañero[1,2,3], Sonia Eiras[1,3] Cholinergic activity regulates the secretome of epicardial adipose tissue: Association with atrial fibrillation. J Cell Physiol. 2019 Jul;234(7):10512-10522.

The study was approved by the Galician Research Ethics Committee (Registration Code 2016/262).

DOI: 10.1002/jcp.27723., PMID: 30480808., ISSN: 0021-9541

Affiliations: [1]Grupo de Cardiología, IDIS, Santiago de Compostela, España Grupo de Cardiología Traslacional, IDIS, Santiago de Compostela, España;[2]Área Cardiovascular y Unidad Coronaria, Hospital Clínico Universitario, Santiago de Compostela, España; [3]CIBERCV, Madrid, España; [4]Departamento de Cirugía Cardíaca, Hospital Clínico Universitario, Santiago de Compostela, España; [5]Unidad de Proteómica, IDIS, Santiago de Compostela, España; [6]Universidad de Santiago de Compostela, Santiago de Compostela, España

Link: https://onlinelibrary.wiley.com/doi/10.1002/jcp.27723

USC UNIVERSIDADE DE SANTIAGO DE COMPOSTELA

4.2 ARTICLE 3 | INFLAMMATORY AND LIPID REGULATION BY CHOLINERGIC ACTIVITY IN EPICARDIAL STROMAL CELLS FROM PATIENTS WHO UNDERWENT OPEN-HEART SURGERY

The results from this chapter have already been published as Marinela Couselo-Seijas[1,2], José N. López-Canoa[1,3], Ángel L Fernández[2,4,6], Laila Rodríguez-Melchor[5,6], Luisa M. Seoane[7,8], Darío Durán-Muñoz[4,6], Susana B. Bravo[5], Adriana Rozados-Luis[1], José Ramón González-Juanatey[2,3,5,6], Moisés Rodríguez-Mañero[1,3,6*], Sonia Eiras[1,6*] Inflammatory and lipid regulation by cholinergic activity in epicardial stromal cells from patients who underwent open-heart surgery. J Cell Mol Med. 2020 Sep;24(18):10958-10969.

Institutional animal care and use committee statement: The approaches in the present manuscript were performed under the procedure 15005/2015/003 reviewed and approved by the Faculty Animal Committee at the University of Santiago de Compostela.

Patient's samples: The study was approved by the Galician Research Ethics Committee (Registration Code 2019/439).

DOI: 10.1111/jcmm.15727., PMID: 32767737., ISSN: 1582-1838

Affiliations: [1]Grupo de Cardiología Traslacional, IDIS, Santiago de Compostela, España [2]Universidad de Santiago de Compostela, Santiago de Compostela, España; [3]Área Cardiovascular y Unidad Coronaria, Hospital Clínico Universitario, Santiago de Compostela, España; [4]Departamento de Cirugía Cardíaca, Hospital Clínico Universitario, Santiago de Compostela, España; [5]Grupo de Cardiología, IDIS, Santiago de Compostela, España; [6]CIBERCV, Madrid, España; [7]Grupo de Fisiopatología Endocrina, IDIS, Santiago de Compostela, España; [8]CIBERobn, Madrid, España

Link: https://onlinelibrary.wiley.com/doi/10.1111/jcmm.15727

USC UNIVERSIDADE DE SANTIAGO DE COMPOSTELA

4.3 FABP4 EFFECT ON HIPSC-DERIVED ATRIAL CMS

The results shown in this subchapter were obtained in collaboration with Dr. María Lázaro (Head of the Bioimaging Scientific Platform), under her supervision, at the "*Instituto de Investigação e Inovação em Saúde, Universidade do Porto*" (i3S), in a 3-month internship during the predoctoral period.

The increased FABP4 mRNA expression levels in EAT SVF cells from long-persistent AF patients together with its secretion and circulating levels being good predictors of AF recurrence[93] lead us to focus on this protein in the subsequent experiments. It was already described a cardiodepressive effect of FABP4 in ventricular CMs from rats[94]. For this reason, we decided to study the effect of this adipokine in atrial CMs. In this chapter, we used confocal Raman microspectroscopy to investigate the molecular changes in hiPSC-derived atrial CMs treated with FABP4 protein at 10 and 100 ng/mL for 4 days, with medium replacement every 24 h.

USC UNIVERSIDADE DE SANTIAGO DE COMPOSTELA

4.3.1 Characterization of hiPSC-derived atrial CMs by confocal Raman microspectroscopy

The high spatial resolution of the Raman microspectrometer allows to collect the spectra from different positions within the cell. The spectral difference between the nucleus and the cytoplasm for an atrial CMs is illustrated in Figure 14.

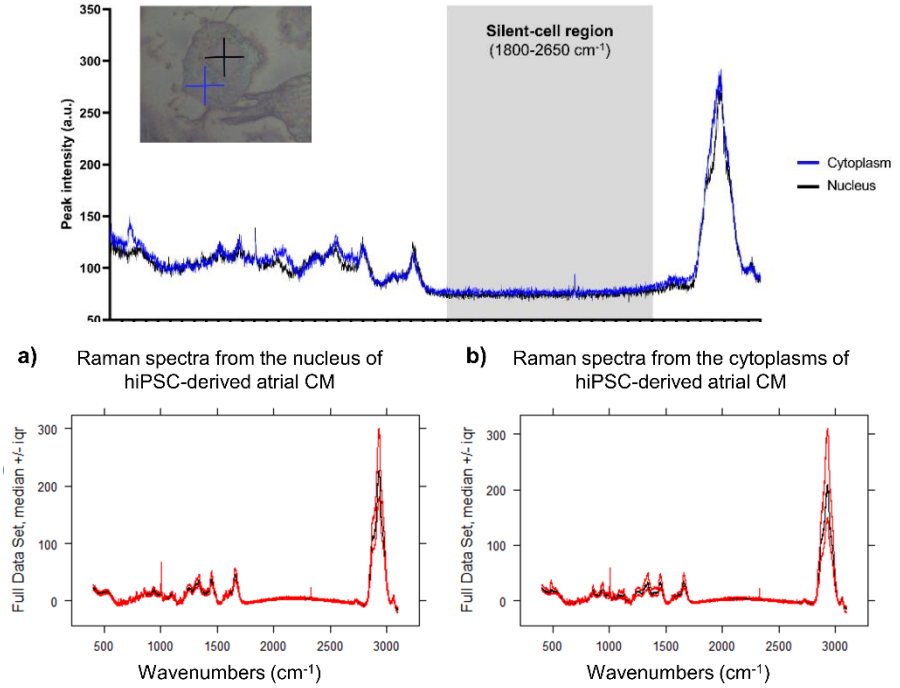


Figure 15. Median Raman spectra from the nuclei (a) and the cytoplasm (b) of hiPSC-derived atrial cardiomyocytes (n= 118 cells) in black.

In red the upper and lower hinges are shown.

To uncover if there are any spectral regions that might be uninformative, which only will contribute to our analysis as noise, we identified the informative regions of the spectra. To this end, a summary statistic was computed for all the intensities at every frequency in the total spectra region. In Figure 15, the median spectra are plotted together with the upper and lower hinge. From this plot we observed

USC UNIVERSIDADE DE SANTIAGO DE COMPOSTELA

three different wavenumber spectral regions with only two of them showing alterations between all the conditions.

The first region (from 400 to 1800 cm^{-1}) is considered the cell-fingerprint region, usually showing a higher number of detectable molecular groups. The second region (from 2650 to 3100 cm^{-1}) is a superposition of broad features dominated by the stretching of various lipid and protein CH_2 and CH_3 groups. There are also weak contributions from =CH stretching in lipids and from aromatic groups in both nucleic and amino acids. Lastly, the silent-cell region (from 1800 to 2650 cm^{-1} offers almost no contribution to the spectra[95,96]. For this reason, the silent-cell spectral region was discarded in the subsequent analysis.

Figures 16, 17 and 18 show the average Raman spectra after baseline correction and smoothing for hiPSC-derived atrial CMs from the control group (n= 40 cells, 79 total spectra), from the ones treated with the FABP4 protein at low concentration (10 ng/mL) (n= 40 cells, 79 total spectra), and from those treated at high concentration (100 ng/mL) (n= 41 cells, 81 total spectra), recorded in the region from 400

USC
UNIVERSIDADE DE SANTIAGO DE COMPOSTELA

to 3100 cm-1. Spectra were grouped by clustering the spectra from the nuclei or cytoplasm for each corresponding group.

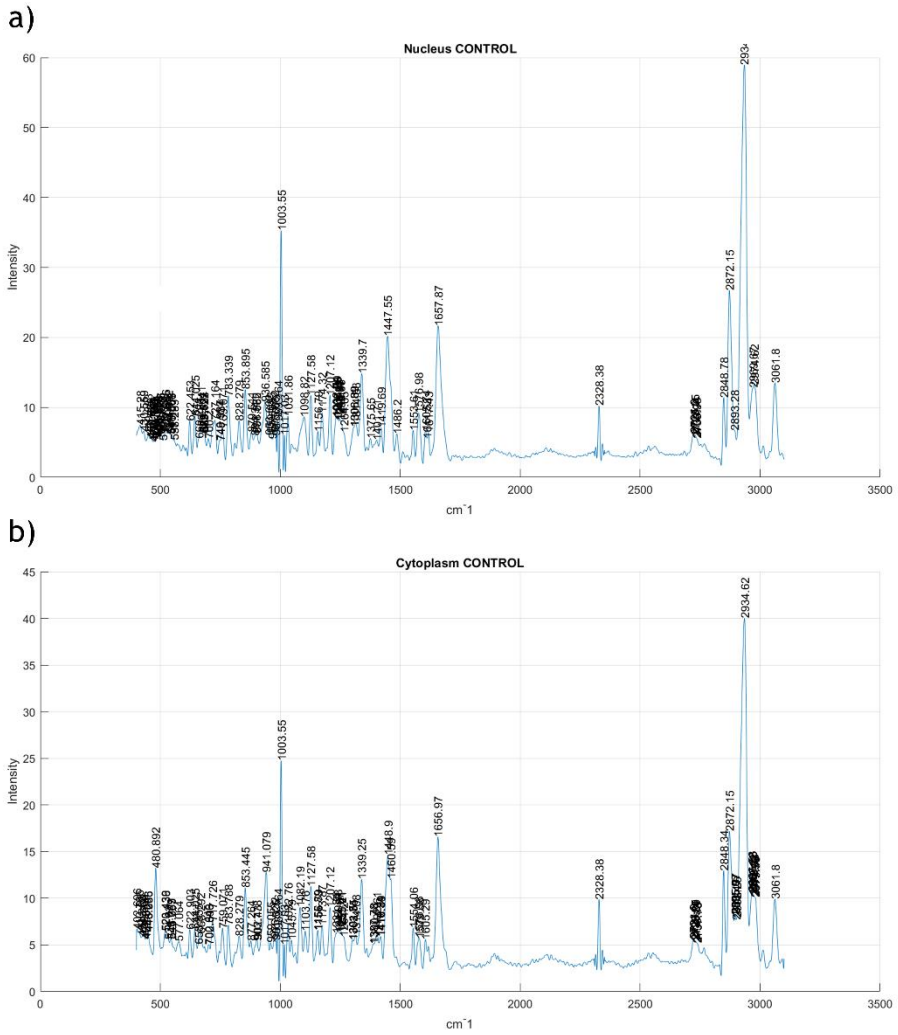


Figure 16. Average Raman spectra of the hiPSC-derived atrial CM control clusters

Grouped and averaged spectra of nuclei (a) and cytoplasm (b) from control cells (n= 40 cells, 79 total spectra). For rendering purposes, MATLAB Software (v 4.0.813654 (R2018a) (MathWorks Inc.), was used to obtain the average background-subtracted smoothed spectrum. Information on the assigned peaks can be found in Table 5

USC
UNIVERSIDADE DE SANTIAGO DE COMPOSTELA

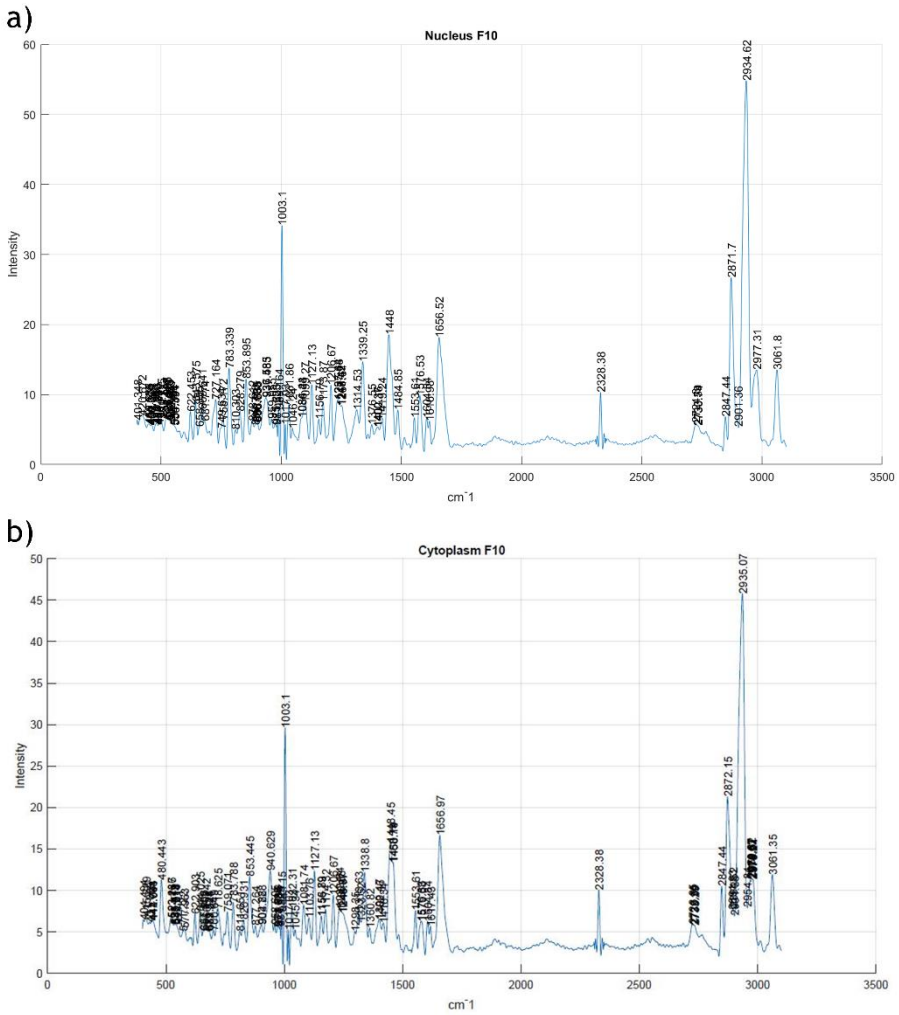


Figure 17. Average Raman spectra of the hiPSC-derived atrial CM clusters treated with FABP4 at 10 ng/mL (F10)

Grouped and averaged spectra of nuclei (a) and cytoplasm (b) from cells (n= 40 cells, 79 total spectra). For rendering purposes, MATLAB Software (v 4.0.813654 (R2018a) (MathWorks Inc.), was used to obtain the average background-subtracted smoothed spectrum. Information on the assigned peaks can be found in Table 5

USC
UNIVERSIDADE DE SANTIAGO DE COMPOSTELA

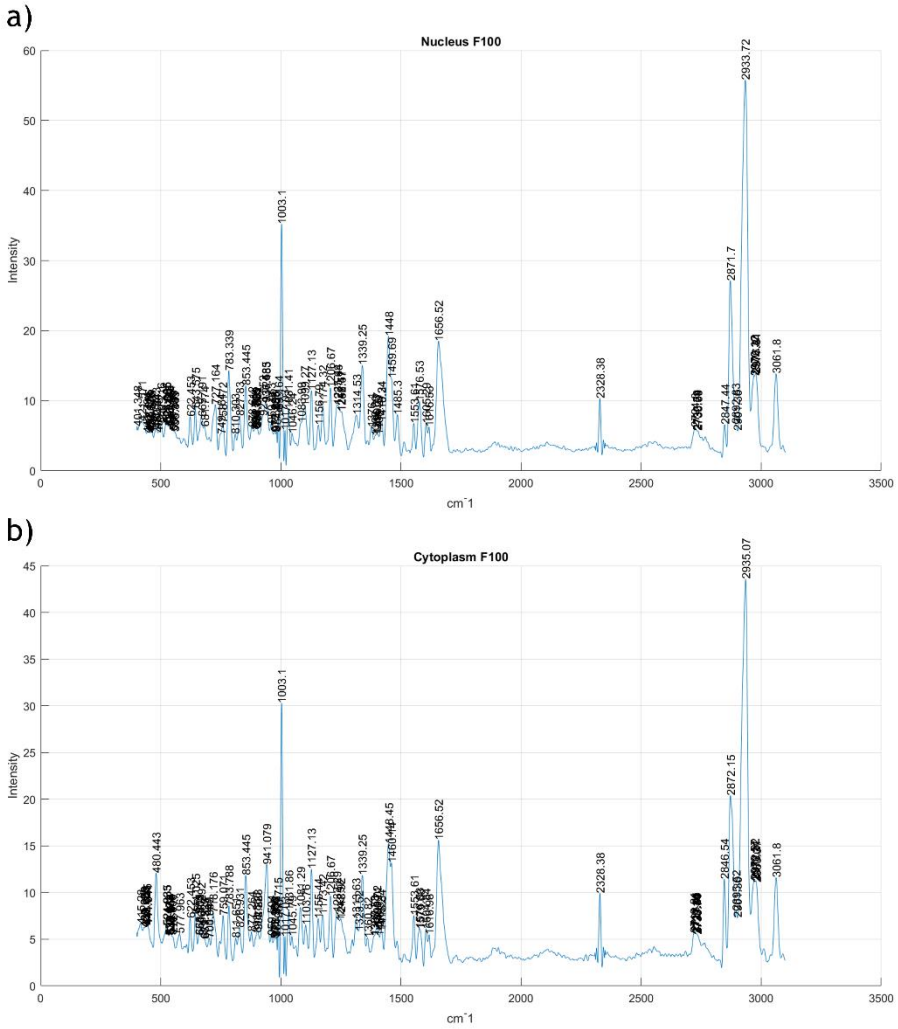


Figure 18. Average Raman spectra of the hiPSC-derived atrial CM clusters treated with FABP4 at 100 ng/mL (F100)

Grouped and averaged spectra of nuclei (a) and cytoplasm (b) from cells (n= 40 cells, 79 total spectra). For rendering purposes, MATLAB Software (v 4.0.813654 (R2018a) (MathWorks Inc.), was used to obtain the average background-subtracted smoothed spectrum. Information on the assigned peaks can be found in Table 5

USC
UNIVERSIDADE DE SANTIAGO DE COMPOSTELA

Table 3. Raman peaks detected in the average spectra of the atrial CMs.

Spectra were acquired in the spectral region from 400 to 3100 cm^{-1}. Known peaks of vibrational assignments are included (some with small changes)

Table 3 shows the peaks that appeared in the Raman spectra of these samples with their corresponding assignments.

Peak (cm^{-1})	Assignment	Localization	References
401.35	*(400 cm^{-1}) Skeletal modes of carbohydrates (401 cm^{-1}) Acetoacetate*	*N*	97,98
402.70	*(403 cm^{-1}) Deformation mode of the endocyclic CCO group in the fructosyl moiety (characteristic for the a-anomer of sucrose)*	*C*	99
404.49	*(404 cm^{-1}) L-Histidine*	*C*	98
410.79	*(410 cm^{-1}) D(+)Xylose*	*C*	98
415.28	*(415 cm^{-1}) Phosphatidyninositol*	*N, C*	97,100,101
415.73	*(414 cm^{-1}) CCO rock (417 cm^{-1}) B (COC); B(CCC); B(CCO); B (OCO)*	*C*	
420.67	*(420 cm^{-1}) D(-)Fructose and citric acid*	*N*	98
421.57	*(420 cm^{-1}) D(+)galactosamine*	*N*	98
424.27	*(424 cm^{-1}) CH_2 bending in ring in cholesterol (cholesterol and cholesterol ester)*	*C*	102
429.66	*(429 cm^{-1}) Cholesterol, cholesterol ester (430 cm^{-1}) V2 PO43- (429/30/31) B(CH2) in ring in cholesteryl oleate, cholesteryl linoleate, cholesteryl*	*C*	100,103
430.56		*N, C*	
431.01		*C*	
433.26	*(433 cm^{-1}) palmitic acid*	*C*	98
436.85	*(436 cm^{-1}) Thymidine (ring breathing modes of the DNA/RNA bases*	*C*	104
437.30	*(?)*	*C*	
438.65	*(?)*	*C*	
439.10	*(?)*	*C*	
441.35	*(441 cm^{-1}) (COC)in-plane bending in D(-)Ribose*	*C*	99
441.79		*N, C*	
442.69	*(442 cm^{-1}) (CCC)in-plane bending in amylopectin and amylose*	*C*	99
444.04		*C*	105

USC UNIVERSIDADE DE SANTIAGO DE COMPOSTELA

444.94	*(445 cm^{-1}) N-C-S stretch (one of three thiocyanate peaks, with 2095 and 735 cm^{-1})*	*C*	
446.29	*(446 cm^{-1}) (CCC) in-plane bending of glycogen*	*C*	99
448.09	*(447 cm^{-1}) Ring torsion of phenyl(2)*	*N, C*	106
448.54		*N*	
449.88		*N*	
450.33		*N*	
452.13		*N*	
454.38		*N*	
456.63	*(?)*	*N*	
457.52	*(?)*	*N*	
459.32	*(?)*	*N*	
459.77		*N*	
460.67	*(?)*	*N*	
461.57	*(?)*	*N*	
470.11	*(?)*	*N*	
473.70	*(?)*	*N*	
479.10	*(479 cm^{-1}) C-C-C deformation (carbohydrates)*	*N*	107
479.99		*N*	
480.44	*(480 cm^{-1}) v(C1-O-C4) Ring breathing (glycogen) (481 cm^{-1}) DNA*	*N, C*	90,97,100,108
480.89		*C*	
482.24	*(482 cm^{-1}) glycogen Raman band appearing in cardiomycocyte differentiated embryioid bodies*	*N*	109
484.04	*(484-490 cm^{-1}) Glycogen*	*N*	110,111
484.94		*N*	
486.29		*N*	
488.53		*N*	
489.88		*N*	
490.78		*N*	
493.03	*(?)*	*N*	
499.32	*(?)*	*N*	
500.22	*(?)*	*N*	
501.12	*(?)*	*N*	
501.56		*N*	
510.55	*(509 cm^{-1}) S-S disulfide stretching band of collagen v(S-S) gauche-gauche-gauche (amino acid cysteine)*	*N*	112,113
520.44	*(519 cm^{-1}) Phosphatidylinositol*	*C*	114
522.24	*(?)*	*N, C*	
522.69		*N*	
523.14	*(?)*	*N, C*	
523.59	*(?)*	*N*	

USC UNIVERSIDADE DE SANTIAGO DE COMPOSTELA

524.03	*(524 cm^{-1}) S-S disulfide stretching in proteins* *Phosphatidylserine* *v(S-S) gauche-gauche-trans (amino acid cysteine)*	*N, C*	110,111,113,114
524.93		*N, C*	
527.18	*(?)*	*N*	
527.63		*N*	
530.78	*(?)*	*N*	
531.23	*(?)*	*N*	
533.02	*(?)*	*N*	
533.47		*N, C*	
534.82	*(535 cm^{-1}) Cholesterol ester* *v(S-S) gauche-gauche-trans (amino acid cysteine)*	*N, C*	100
535.27		*C*	
535.72		*N, C*	
537.52		*C*	
538.41	*(538 cm^{-1}) CCC deformation in hyaluronan* *Cholesterol ester* *Disulfide bridges in cysteine (this peak seems to be the main factor for the FT-Raman determination of the boundaries between healthy and pathological tissue)*	*C*	114-116
538.87		*N*	
539.76	*(540 cm^{-1}) v(S-S) trans-gauche-trans (amino acid cysteine)* *Glucse-saccharide band (overlaps with acyl band)*	*C*	100,114
540.21		*C*	
541.56	*(?)*	*N*	
542.01	*(?)*	*N, C*	
543.36	*(?)*	*C*	
543.81		*N*	
544.71	*(544 cm^{-1}) PO deformation in aggrecan*	*C*	115
545.61	*(?)*	*C*	
546.05	*(548 cm^{-1}) B(CH_2) in ring in cholesterol (cholesterol and cholesterol ester)*	*C*	114
546.50		*N*	
550.55	*(?)*	*N*	
551.90	*(?)*	*N*	
554.14	*(?)*	*N*	
556.39	*(?)*	*N*	
556.84		*N*	
557.29	*(?)*	*N*	
558.19	*(?)*	*N*	
571.22	*(570 cm^{-1}) δ(C=O-C) in myristic acid (fatty acids)*	*C*	102
577.06	*(576 cm^{-1}) Phosphatidylinbositol* *(577 cm^{-1}) Raman band appearing in cardiomycocyte differentiated embryioid bodies*	*C*	100,114
577.96		*C*	

USC UNIVERSIDADE DE SANTIAGO DE COMPOSTELA

622.45	*(622 cm^{-1}) Protein peak Phenylalanine*	*N, C*	117
622.90	*C-C twisting mode of phenylalanine in tumours*	*C*	
643.58	*(644 cm^{-1}) Tyrosine (protein)*	*N*	100,118-120
644.02	*(645 cm^{-1}) C-C twisting mode of tyrosine Ring, cyclic deformation*	*N, C*	
657.96	*(?)*	*C*	
658.86	*(659 cm^{-1}) Ring deformation, cyclic rock*	*N, C*	119
660.20	*(661 cm^{-1}) δ(C=O-C) in myristic acid (fatty acids)*	*N, C*	102,110,112
661.10	*(662 cm^{-1}) C-S stretching mode of cysteine (collagen type I)*	*C*	
668.29	*(667/9 cm^{-1}) C-S stretching mode of cysteine (collagen type I) T,G (DNA/RNA) (669 cm^{-1}) C-S stretching mode of cytosine (669 cm^{-1}) v7(δ:porphyrin deformation), observed inn spectra of single human RBC*	*C*	110-112,121
668.74		*C*	
669.19		*N*	
669.64		*N*	
676.83	*(676 cm^{-1}) Ring deformation*	*N*	119
679.53	*(678 cm^{-1}) Ring breating modes in the DNA bases G (ring breathing modes in the DNA bases)/C-2'-endo-anti*	*N, C*	122
681.33	*(?)*	*C*	
681.77		*N*	
682.22	*(?)*	*C*	
683.12	*(?)*	*N*	
700.20	*(699 cm^{-1}) G, T (DNA)*	*N*	113,118
700.65	*(700-745 cm^{-1}) ν(C-S) trans (amino acid methionine)*	*C*	
702.00	*(702 cm^{-1}) cholesterol ring deformation in cholesteryl stearate and cholesteryl palmitate (cholesterol and cholesterol ester) (702-703 cm^{-1}) Ring, C-NR2, cyclic stretch with C-H rock*	*C*	114,119
702.90		*C*	
717.73	*(717 cm^{-1}) C-N (membrane phospholipids head)/adenine $CH_{5',2'}$ out-of-plane bend and ring puckering (718 cm^{-1}) Choline group C-N (membrane phospholipid head)/nucleotide peak symmetric choline stretcc, phospholipides, $(H_3C)N^+$ stretch band (719 cm^{-1}) C-N (membrane phospholipid head)/nucleotide peak*	*C*	106,110,111,114,119
718.18		*C*	
718.63		*C*	

USC UNIVERSIDADE DE SANTIAGO DE COMPOSTELA

	Symmetric stretch vibration of choline group $N^{+}(CH_3)3$, characteristic for phospholipids Phosphatidylcholien, sphingomyelin vsN+(CH3)3 in phosphatidylcholine (membrane lipids) (720 cm^{-1}) Phospholipid (choline) Ring breathing (adenine)		
727.16	*(727 cm^{-1}) Adenine (ring breathing modes of DNA/RNA bases) 727/8 cm−1 C-C stretching, proline (collagen assignment)*	*N*	104,123
746.94	*(746 cm^{-1}) T (ring breathing mode of DNA/RNA bases)*	*N*	122
749.18	*(749 cm^{-1}) Symmetric breathing of tryptophan (protein assignment)*	*N*	110,112
749.63	*(750 cm^{-1}) CH_2, 6 out-of-plane bending, observed in the spectra of single human RBC*	*N*	106
758.17	*(758 cm^{-1}) Symmetric ring breathing of tryptophan, vs(O-P-O)*	*N*	117
759.07	*(759 cm^{-1}) Tryptophan Ethanolamine group Phosphatidyletanolamine (760 cm^{-1}) ethanolamine in L-alpha-phosphatidylethanolamine (membrane lipids)*	*N, C*	100,113,114,118
783.34	*(782 cm^{-1}) U,C,T ring breathing (DNA/RNA)*	*N*	108,117,119
783.79	*(784 cm^{-1}) Phosphodiester; cytosine U,C,T ring breathing, DNA (785 sm^{-1}) Phosphodiester bonds of DNA*	*C*	117,122,124
810.30	*(810/2 cm^{-1}) Phosphodiester (Z-marker)*	*N*	124
811.65	*(811 cm^{-1}) O-P-O stretching RNA and lipids*	*C*	100,125
826.93	*(823/5/6 cm^{-1}) Phosphodiester (825 cm^{-1}) lactic acid*	*C*	124
827.83	*(827 cm^{-1}) Proline, hydroxyproline, tyrosine, v2PO2- stretch of nucleic acids*	*N*	112
828.28	*(828 cm^{-1}) Out-of-plane ring breathing, tyrosine/O-P-O stretch DNA Phosphodiester Ring breathing Tyrosine (proteins)*	*N, C*	110,111,118,124,125
853.45	*(853 cm^{-1}) Ring breathing mode of tyrosine and C-C stretch of proline ring Glycogen Sulfate vibrational modes of GAGs C-O-S in chondroting-4-sulfate*	*N, C*	108,110,111,126

USC UNIVERSIDADE DE SANTIAGO DE COMPOSTELA

	(853/4 cm^{-1}) Structural proteins like collagen *(853 cm^{-1}) CH in chondroitin-6-sulphate*		
853.89	*(854 cm^{-1}) CH2',6' out-of-plane bending (C-O-C) skeletal mode of alpha-anomers (polysaccharides, pectin)* *Protein peak* *Ring breathing of tyrosine and ν(C-C) hydroxyproline ring specific for collagen* *Ring breathing in tyrosine/C-C stretching in proline* *Hemiacetal stretches and methylene deformation (carbohydrates)*	*N*	106,113,117,118,120
877.26	*(876 cm^{-1}) ν(C-C), hydroxyproline (protein assignment)* *C-C stretching, hudroxyproline (collagen assignment)* *vasN+$(CH_3)_3$ in sphingomylenin and phosphatidylcholine (membrane lipids)*	*C*	102,123,127
878.61	*(879 cm^{-1}) Hydroxyproline, tryptophan*	*N*	112
879.51		*N*	
890.75	*(890 cm^{-1}) Protein bands* *Structural protein modes of tumours* *B-anomers* *Ring deformation and symmetric C-N-C stretch*	*N*	114,119,128,129
892.54	*(892 cm^{-1}) (C-O-O) skeletal mode in trilaurin (TAG)*	*N*	102
894.34	*(894 cm^{-1}) (C-O-O) skeletal modeiln palmitoleic acid (fatty acid)*	*N*	102
894.79		*N*	
895.69	*(893/5/6 cm^{-1}) Phosphodiester, deoxyribose (896 cm^{-1}) ν(C-C) protein backbone a-helix (proline/glycogen), collagen* *(896 cm^{-1}) (C-O-O) skeletal mode in stearic acid (Fatty acid)*	*N*	102,117,124
896.14		*N*	
898.84	*(898 cm^{-1}) Monosaccharides (B-glucose), (C-O-C) skeletal mode Disaccharide (maltose)* *(C-O-C) skeletal mode in palmitic acid and arachidic acid (fatty acids)* *(899 cm^{-1}) C1-H deformation of B-monomers in chondrotin-4-sulfate*	*N, C*	102,113,130
900.63	*(900 cm^{-1}) C-C skeletal stretching in protein*	*N*	100,102,120,131
901.08		*N*	
902.43		*C*	

USC UNIVERSIDADE DE SANTIAGO DE COMPOSTELA

902.88	*(900-950 cm^{-1}) Variations in the secondary structures of proteins (904 cm^{-1}) C-C skeletal stretching (904 cm^{-1}) (CH) bending in linoleic acid (fatty acid)*	*C*	
903.78		*C*	
904.23		*C*	
923.55	*(?)*	*N*	
936.59	*(936 cm^{-1}) Protein peak*	*N*	117
937.48	*937 cm^{-1} Proline (collagen type I) Amino acid side chain vibrations of proline and hydroxyproline, as well as a (C-C) vibration of the collagen backbone; C-C backbone (collagen assignment); Glycogen; v(C-C) residues (a-helix)*	*N*	108,112,119,123,132
940.63	*(940 cm^{-1}) CH_2 rocking mode*	*C*	133
941.08	*(941 cm^{-1}) Skeletal modes (polysaccharides, amylose) Sleletal modes (polysaccarides, amylopectin) C-O-C of polysaccharides*	*C*	113
953.66	*(?)*	*N*	
958.61	*(958 cm^{-1}) Hydroxyproline/collagen backbone CH=CH bending B(CH) in mirystic acid (fatty acids)*	*C*	102,130,134
959.05	*(959 cm^{-1}) CH_2 rock Ring, C-N-R2 stretch, cyclic C-C-C bend V1 PO43-*	*N, C*	119,135
959.95		*N*	
967.59	*(?)*	*N*	
971.19	*(971 cm^{-1}) v(C-C) wagging B(CH) in alpha-linoleic acid (fatty acids)*	*C*	100,132
971.64		*C*	
972.99	*(972 cm^{-1}) lipid collagen Proline*	*N, C*	102,123
973.88	*(972/3 cm^{-1}) C-C backbone (collagen assignment) (973 cm^{-1}) p(CH3), dleta(CCH) olefinic (protein assignment) B(CH) in linoleic acid (fatty acids)*	*C*	102,123,136
974.78	*(974 cm^{-1}) Ribose vibration, one of the distinct RNA modes (with 874 and 915 cm^{-1}) B(CH) in arachidonic acid (fatty acids)*	*C*	100,102,122
975.23	*(975 cm^{-1}) CH_2 rock C-C in lipids B(CH) in arachidonic acid and palmitoleic acid (fatty acids)*	*N, C*	101,102,118
975.68		*N*	
976.13	*(976 cm^{-1}) B(CH) in oleic acid (fatty acids)*	*C*	102
977.48	*(?)*	*N*	
981.08	*(980 cm^{-1}) C-C stretching B-sheet (proteins)*	*N*	100,102,125

USC UNIVERSIDADE DE SANTIAGO DE COMPOSTELA

	C=H bending in (lipids) *B(CH) in palmitic acid (fatty acids)*		
981.52	*(?)*	*N, C*	
988.72	*(989 cm^{-1}) B-sheets of protein*	*C*	119,137
989.16	*(990-1010 cm^{-1}) Ring stretch modes of benzene derivatives*	*N, C*	
1003.10	*(1003 cm^{-1}) Phenylalanine, C-C skeletal Phenylalanine residues*	*N, C*	112,117,122,127,138-141
1003.50	*(1004 cm^{-1}) Phenylalanine (of collagen)* *vs(C-C), symmetric ring breathing, phenylalanine (protein assignment)* *Phenyl breathing mode*	*N, C*	
1017.00	*(1018 cm^{-1}) stretching C-O ribose Phenylalanine*	*N, C*	90,100,142
1031.40	*(1030 cm^{-1}) C-H in-plane bend (Phenylalanine)*	*N, C*	97,100,112,125,136
1031.90	*(1031 cm^{-1}) δ(C-H), phenylalanine (protein assignment)* *C-H in-plane bending mode of phenylalanine* *Carbohydrate residues of collagen* *Phenylalanine, C-N stretching of proteins* *C-H in-plane bending mode of phenylalanine*	*N, C*	
1032.80	*(1032 cm^{-1}) CH_2CH_3 bending modes of collagen and phospholipids* *Phenylalanine of collagen* *Proline (collagen assignment)* *Proline* *(1033 cm^{-1}) Differences in collagen content* *Phenylalanine mode* *v(CO), v(CC), v(CCO) (polysaccharides, pectin)* *C-H in-plane phenylalanine (proteins)*	*C*	112,113,117,122,123,129,141,143
1045.30	*(?)*	*C*	
1045.80	*(1046 cm^{-1}) C-O stretching of charbohydrates*	*C*	117
1046.20		*N*	
1081.30	*(1081 cm^{-1}) v1CO32-,v3PO43-, v(C-C) skeletal of acyl backbone in lipid (gauche conformation)*	*C*	112
1081.70		*C*	
1082.20	*(1082 cm^{-1}) Carbohydrate residues of collagen Nucleic acids Carbohydrates (C-O, C-C stretching) Phospholipids O-P-O and C-C Lipids (skeletal C-C stretching (all-trans)* *Carbohydrate C-O-H bending (1080^{-1}158 cm^{-1}) Proteins (C-C, C-N str.), P=O symmetric vibration from*	*C*	110,111,129,135,144

USC UNIVERSIDADE DE SANTIAGO DE COMPOSTELA

	nucleic acids and phospholipids L-tryptophan (1083 cm^{-1}) Raman band appearing in cardiomycocyte differentiated embryioid bodies		
1084.00	*(1084 cm^{-1}) Phosphodiester groups in nucleic acids DNA (band due to PO2−vibrations) (1084 cm^{-1}) (C-C) stretching in oleic acid (fatty acid)*	*N*	102,129,145
1084.40		*N*	
1086.20	*(1086 cm^{-1}) ν(C-C) gauche (1086 cm^{-1}) (C-C) stretching in palmitoleic acid and a-linoleic acid (fatty acids)*	*N*	102,132
1098.80	*(1099 cm^{-1}) ν(C-N)*	*N*	112
1099.30		*N*	
1103.80	*(1104 cm^{-1}) Phenylalanine (proteins) (C-C) stretching in sphingomylein (membrane lipids)*	*C*	100,102,132
1127.10	*(1126 cm^{-1}) C-N stretching (proteins) Skeletal C-C stretching (gauche) in lipids C-O stretching in carbohydrates (1127 cm^{-1}) ν(C-N) (proteins) and C-C (lipids) ν(C-C) in trialurin and tripetroselinin (triacylglycerols) (1128/9 cm^{-1}) ν(C-C) skeletal of acyl backbone in lipid (trans conformation) (1128 cm^{-1}) C-N stretching (proteins) C-O stretching (carbohydrates) Ceramide*	*N, C*	112,113,117,122,129,132
1127.60		*N, C*	
1155.40	*(1555 cm^{-1}) C-C (and C-N) stretching of proteins (also carotenoids) Glycogen*	*C*	128,129
1155.90		*C*	
1156.80	*(1556 cm^{-1}) C-C, C-N stretching (protein) (1557 cm^{-1}) In-plane vibrations of the conjugated =C-C= Β-carotene accumulation (C=C stretch mode) carotenoids (1557/9 cm^{-1}) In-plane CH bend, ring, cyclic stretch C-C stretching*	*N, C*	119,122,141,146-148
1173.40	*(1173 cm^{-1}) Tyrosine (collagem type I) Cytosine, guanine*	*C*	112,124
1173.90		*N, C*	
1174.30	*(1174 cm^{-1}) Tyrosine, phenyalanine, C-H bend (protein) Protein peak (1175 cm^{-1}) Cytosine, guanine*	*N, C*	117,122,125,141

USC UNIVERSIDADE DE SANTIAGO DE COMPOSTELA

	Tyrosine (proteins) *Phenylalanine* *v(C-C) in mitystic acid (fatty acids)*		
1206.70	*(1206 cm^{-1}) Hydroxyproline,* *tyrosine (collagen assignment)* *Hydroxyproline, tyrosine* *(1208 cm^{-1}) C-C6H5 stretching in* *Phenylalanine and tryptophan* *Tyrosine*	*N, C*	111,112,122,123,127
1207.10		*N, C*	
1231.80	*(1230 cm^{-1}) assymetric phosphate stretching vibration*	*C*	129,144
1232.30	*(1232 cm^{-1}) SO3- asymmetric stretch deformation in chondroitin-4-sulfate*	*C*	100,130
1232.70		*N, C*	
1234.10	*(1234 cm^{-1}) A concerted ring mode*	*N*	105
1235.40	*(1235 cm^{-1}) Amide III In-phase ring, C-C, C-N-C stretch*	*N*	113,119
1237.20	*(1237 cm^{-1}) Amide III and CH_2 wagging vibrations from glycine backbone and proline side chains*	*N*	129
1237.70		*N*	
1238.60	*(1238 cm^{-1}) Phospholipid, O-P-O antisymmetric stretching, Amide III B-sheet*	*C*	100
1239.50	*(1239 cm^{-1}) Amide III* *(1240 cm^{-1}) One of the two most distinct peaks for RNA (with 813 cm^{-1})* *Differences in collagen content* *Asymmetric phosphate [PO_2- (assym.)] stretching modes* *(Phosphate stretching modes originate from the phosphodiester groups of nuclei acids and suggest an increase in the nucleic acids in the malignant tissues.)* *Antisymmetric stretching vibrations of the PO2- group*	*C*	110,122,129,143
1243.10	*(1243 cm^{-1}) C-O4 aromatic stretch* *Amide III of collagen (CH_2 wagging, C-N stretching) and pyrimidine bases (C,T)*	*N*	106,111,112,129
1244.00	*(1245 cm^{-1}) Amide III*	*C*	113
1244.90		*C*	
1245.80	*(1246 cm^{-1}) Amide III (of collagen)*	*N, C*	112
1247.10	*(1247 cm^{-1}) Amide III (collagen assginment)*	*N*	123
1248.50	*(1247/8 cm^{-1}) Guanine, cytosine (NH2)* *(1248 cm^{-1}) Found in collagen* *Amide III* *Sulfate vibrational modes of GAGs*	*N*	100,124,134
1248.90		*C*	

USC
UNIVERSIDADE DE SANTIAGO DE COMPOSTELA

	Nucleic acids (Try, Ala)/Proteins (amide III B-sheet or random coil), lipid, phospholipid =C-H bending		
1251.20	*(1250/2 cm^{-1}) Guanine, cytosine (NH2)* *C-O4 aromatic stretch* *(1250 cm^{-1}) Amide III (proteins)* *=CH bend in lipids T,A in DNA/RNA* *C=C stretching*	*N*	100,124,128
1251.60		*N, C*	
1252.10	*(1252 cm^{-1}) δ(CH) in tripetroselinin (triacylglycerols) C-O4 aromatic stretch*	*N*	102,106
1252.50		*N*	
1253.40	*(1254 cm^{-1}) C-N in-plane stretching δ(CH_2) in tri-11-eicosenoin (triacylglycerols)*	*C*	100,102,149
1255.20	*(1255 cm^{-1}) Lipids*	*C*	129
1264.20	*(1264 cm^{-1}) Triglycerides (fatty acids) Ring stretch* *Δ(=CH) of lipids* *(1265 cm^{-1}) Amide III of collagen; Amide III; ν(CN), δ(NH) amide III, alpha-helix, collagen (protein assignment); Phenylalanine stretching (C-C6H5) mode*	*C*	117,119,123,136,147
1264.70		*N*	
1298.30	*(1297 cm^{-1}) τ (CH_2) in trilaurin, trimyristin, tripalmitin, tristearin, tripetroselinin and cholesterol (triacylglycerols and cholesterol and cholesterol ester)* *(1298 cm^{-1}) Palmitic acid* *Acyl chains Fatty acids* *τ(CH_2) in arachidic acid and cholesteryl palmitate (fatty acids and cholesterol and cholesterol ester)* *(1299-1300 cm^{-1}) CH_2 deformation (lipid)* *(1299 cm^{-1}) τ(CH_2) in tricaprin (triacylglycerols)*	*C*	100,102,111,114,118
1301.50	*(1300 cm^{-1}) CH_2 twisting in palmitic acid, stearic acid, linoleic acid, alpha-linoleic acid, phosphatidylcholine and phosphatidylethanolamine (fatty acids and membrane lipids)* *(1301 cm^{-1}) Assign for Parker (lipid in normal tissue)* *Triglycerides (fatty acids)* *τ(CH_2) in cholesteryl strearate (cholesterol and cholesterol ester), lipids* *Indicates the concentration of lipids (in-phase CH_2 twist mode)*	*C*	100,102,132,147,150,151

USC UNIVERSIDADE DE SANTIAGO DE COMPOSTELA

1302.80	*(1302 cm^{-1}) δ(CH_2) twisting, wagging, collagen (protein assignment)* *δ (CH_2) twisting, wagging, phospholipids (lipid assignment)* *CH_3/CH_2 twisting of bending mode of lipid/collagen* *Amide III (protein)* *Methylene bending mode (a combination of proteins and phospholipids)* *(CH_2) twist, phospholipides and collagen* *CH_2 twisting in triolein (triacylglycerols)*	*C*	112,117,122,127
1303.70	*(1303 cm^{-1}) CH_2 twisting in elaidic acid (fatty acids)* *(1303/4 cm^{-1}) CH_3, CH_2 twisting (collagen assignment)* *(1304 cm^{-1}) CH_2 deformation (lipid), adenine, cytosine* *Unsaturated lipids* *phospholipids CH_2 twist, collagen, protein amide III, DNA* *CH_2 twisting in tripalmitolein (triacylglycerols)*	*C*	100,102,103,111,123,134
1306.90	*(1306 cm^{-1}) CH_2 twisting in oleic acid (fatty acid) and cholesteryl oleate and cholesteryl linoleate* *(1307 cm^{-1}) CH_3/CH_2 twisting or bending mode of lipid/collagen; CH_3/CH_2 twisting, wagging and/or bending mode of collagens and lipids*	*N*	102,112
1308.70	*(1308 cm^{-1}) C-N asymmetric stretching in asymmetric aromatic amines; C-N-C and cyclic C-C stretch; CH_2 deformation in lipids, adenine, guanine;* *(1309 cm^{-1}) CH_3/CH_2 twisting or bending mode of lipid/collagen; CH_3/CH_2 twisting, wagging and/or bending mode of collagens and lipids*	*N*	112,119,120,149
1313.60	*(1313 cm^{-1}) CH_3CH_2 twisting mode of collagen/lipid*	*C*	110,111
1314.10	*(1314 cm^{-1}) CH_3CH_2 twisting mode of collagen* *CH_2 twisting and wagging* *Amide III in chondroitin-4-sulfate*	*C*	141,152
1314.50		*N*	
1323.50	*(1323 cm^{-1}) Guanine (B, Z marker)* *(1324 cm^{-1}) CH_3CH_2 wagging mode present in collagen and purine bases of DNA*	*C*	110,124

USC UNIVERSIDADE DE SANTIAGO DE COMPOSTELA

1338.80	*(1338 cm^{-1}) Protein peak Amide III, hydrated alpha-helix δ(N-H) and ν(C-N), desmosine Isodesmosine (elastin) (A and G of DNA/RNA) in tumors*	*C*	117,125
1339.30	*(1339 cm^{-1}) CH_2/CH_3 wagging and twisting mode in collagen and lipids, nucleic acids and tryptophan C-C stretch of phenyl(1) and C_3-C_3 stretch and C5-O5 stretch CH alpha in-plane bend Trp, Ca-H def*	*N, C*	100,106,134,153
1339.70	*(1340 cm^{-1}) Nucleic acid mode; Differences in collagen content; Nucleic acid modes indicating the nucleic acid content in tissues; DNA; Nucleic acid vibrational mode; Polynulceotide chain (DNA bases); Molecular vibrations of GAGs; Amide III in chondroitin-6sulfate; Carbohydrate CH_2 deformation and C-O-H bending; CH deformation in proteins; Raman band appearing in cardiomycocyte differentiated embryioid bodies*	*N*	104,129,131,146
1360.80	*(1360 cm^{-1}) Tryptophan (1361/2/3/5 cm^{-1}) Guanine (N7, B, Z-marker)*	*C*	113,141
1375.70	*(1376 cm^{-1}) Adenine (ring breathing modes of the DNA/RNA bases)*	*N*	104
1376.10		*N*	
1376.50		*N*	
1387.80	*(1388 cm^{-1}) Carbonyl and C-N-C stretch*	*C*	119
1389.60	*(?)*	*C*	
1390.50	*(1391 cm^{-1}) CH rocking*	*C*	106
1393.60	*(1393 cm^{-1}) CH rocking; δ(OH) + $δ(CH_3)$*	*N*	106,154
1396.80	*(?)*	*N*	
1399.00	*(1398 cm^{-1}) C=O symmetric stretch CH_2 deformation*	*C*	112,143
1399.50	*(1400 cm^{-1}) NH in-plane deformation Haemoglobin*	*C*	105,141
1400.40		*N*	
1401.70	*(1401 cm^{-1}) Bending modes of methyl groups (one of the vibrational modes of collagen)*	*N, C*	129
1402.20	*(1402 cm^{-1}) Δ5(CH_3) ω(CH_2)*	*N, C*	154
1402.60		*C*	
1406.20	*(1406 cm^{-1}) vsCOO− (IgG?)*	*N*	132
1408.90	*(1408 cm^{-1}) symmetric COO- found in hyaluronan*	*C*	100,132

USC UNIVERSIDADE DE SANTIAGO DE COMPOSTELA

	(1409 cm^{-1}) v5COO- B(CH_2) in stearic acid (fatty acids)		
1415.20	*(1413/16 cm^{-1}) symmetric COO- found in chondroitin-4-sulphate, and chondroitin-6-sulphate*	*C*	115
1416.50		*C*	
1417.90	*(1417 cm^{-1}) C=C stretching in quinoid ring*	*C*	149
1418.30	*(?)*	*N, C*	
1418.80	*(1419 cm^{-1}) B(CH_2) in mirystic acid (fatty acids)*	*C*	100,144,152,155
1419.20	*(1420-1450) CH_2 scissoring vibration (lipid band)*	*N*	
1419.70	*(1420-1470 cm^{-1}) CH_2 bending mode of proteins and lipids (1420-1421 cm^{-1}) Deoxyribose (B, Z-marker)*	*N*	
1447.50	*(1447 cm^{-1}) CH_2 bending mode of proteins and lipids; CH_2 deformation (protein vibration); a marker for protein concentration; δas (CH_3) δ(CH_2) of proteins*	*N*	122,132,143
1448.00	*(1448 cm^{-1}) CH_2CH_3 deformation*	*N*	112,117,123,150,154
1448.50	*CH_2 deformation*	*C*	
1448.90	*CH_2 Collagen CH deformation (in proteins, lipids and carbohydrates) CH_2 bending modes in lipids and proteins G,A CH deformation (DNA/RNA) (1449 cm^{-1}) δ as(CH_3) Δ(CH2)δ as (CH_3) in proteins C-H vibration (proteins) C-H vibration (lipids) Lipids*	*C*	
1458.80	*(1458 cm^{-1}) Nucleic acid modes Nucleic acid modes indicating the nucleic acid content in tissues Nucleic acid vibrational modes CH_2 deformation, amide (III) stretch*	*C*	119,146,156
1459.70	*(1459 cm^{-1}) Deoxyribose δ(CH_2) CH_2 deformation in chondroitin-6-sulfate B(CH_2/CH_3) in trilaurin (triacylglycerols)*	*N*	124,132
1460.10	*(1460 cm^{-1}) CH2/CH3 deformation of lipids and collagen*	*C*	100,112,124,154
1460.60	*CH2 wagging, CH2/CH3 deformation Deoxyribose Δ as(CH3)*	*C*	

USC UNIVERSIDADE DE SANTIAGO DE COMPOSTELA

	CH deformation in proteins and lipids		
1484.80	*(1485 cm^{-1}) G, A (ring breathing modes in the DNA bases) Nucleotide acid purine bases (guanine and adenine) 1485-550 cm−1 NH3+*	*N*	111,122,143
1485.30		*N*	
1486.20	*(1487/8 cm^{-1}) Guanine (N7)*	*N*	124
1553.60	*(?)*	*N, C*	
1554.10	*(1554 cm^{-1}) Amide II (1554 cm^{-1}) Tryptophan, tyrosine*	*C*	100,143
1576.50	*(1576 cm^{-1}) Nucleic acid mode Nucleic acid modes indicating the nucleic acid content in tiusses Nucleic acid vibrational mode Protein peak Tryptophan, nucleic acids (guanine, adenine), protein in tumours*	*N, C*	117,124,146,156
1577.00	*(1577 cm^{-1}) Bound and free NADH A,G in DNA*	*N, C*	100,150
1579.70	*(?)*	*C*	
1604.80	*(1604 cm^{-1}) C=C Phenylalanine, Tryptophan*	*N, C*	100
1605.30	*(1605 cm^{-1}) Cytosine (NH2) Ring C-C stretch of phenyl (1) Phenylalanine, tyrosine, C=C (protein) Retinoic acid*	*N, C*	106,124,125
1605.70	*(1606 cm^{-1}) C=C bending; Phenylalanine, Tyrosine*	*N*	118
1611.60	*1610 cm−1 Cytosine (NH2); C= C bending in phenylalanine and tyrosine*	*N*	120,124
1616.50	*(1616 cm^{-1}) C=C Tyrosine, tryptophane*	*N*	110,111
1617.00	*(1617 cm^{-1}) ν(CaCb), observed in the spectra of single human RBC (1618 cm^{-1}) ν(C=C), tryptophan and tyrosine (protein assignment) ν(C=C), porphirin Tryptophan Bound and free NADH*	*N, C*	127,128
1617.40		*N, C*	
1656.50	*(1656 cm^{-1}) (C=C) stretching in trilinolein, Tri-11-eicosenoin and tripalmitolein (triacylglycerols)*	*N, C*	102
1657.00	*(1657 cm^{-1}) Fatty acids Amide I (collagen assignment) Triglycerides (fatty acids) ν(C=C) in oleic acid, trilinolein, phosphatidylcholine and phosphatidylethanolamine (fatty acids, triacylglycerols, and membrane lipids)*	*C*	123,129,147,157
1657.90		*N*	

USC UNIVERSIDADE DE SANTIAGO DE COMPOSTELA

2328.40	*(2300-3800 cm^{-1}) Region of the OH-NH-CH stretching vibrations*	*N, C*	142
2719.80	*2700-3300 cm^{-1}) C-H stretches (2700-3500 cm^{-1}) stretching vibrations of CH, NH, and OH groups*	*C*	114,158
2721.60		*C*	
2723.40		*C*	
2723.80		*C*	
2724.30		*N, C*	
2725.20		*N*	
2727.40		*C*	
2728.30		*N, C*	
2729.20		*C*	
2730.60		*N, C*	
2731.50		*C*	
2733.30		*C*	
2733.70		*N, C*	
2735.10		*N*	
2736.00		*N*	
2736.40		*C*	
2737.80		*C*	
2846.50	*(2846 cm^{-1}) vs(=CH_2) in trimyristin, tripalmitin, cholesteryl palmitate, and cholesterol oleate (triacylglycerides and cholesterol and cholesterol ester)*	*C*	159
2847.40	*(2847 cm^{-1}) vs(=CH_2) in tricaprin, tristearin, triarachidin, tribehenin, trielaidin, phosphatidylcholine, phosphatidylethanolamine, and sphingomyelin (triacylglycerides and membrane lipids Symmetric methylene stretching*	*N, C*	134
2848.30	*(2848 cm^{-1}) vs(=CH_2) in palmitic acid, sialic acid, alpha-linoleic acid, trilaurin, tripetroselinin, trierucin, (fatty acids, triacylglycerides)*	*C*	100
2848.80		*N*	
2871.70	*(?)*	*N*	
2872.20	*(?)*	*N*	
2891.90	*(2889-2908 cm^{-1}) CH_2 assymetric stretch of lipids and proteins (2893/4/5 cm^{-1}) CH3 symmetric stretch Proteins/lipids CH2 and CH3 stretching (2895 cm^{-1}) vas(=CH_2) in palmitoleic acid (fatty acids) (2896 cm^{-1}) vas(=CH_2) in tripalmitolein and triolein (triacylglycerols) (2900 cm^{-1}) CH stretch*	*C*	100,102,134,160,161
2892.80		*N*	
2893.30		*N*	
2894.60		*C*	
2895.10		*C*	
2895.50		*C*	
2896.00		*C*	
2900.50		*C*	
2901.40		*N, C*	
2902.30		*C*	

USC UNIVERSIDADE DE SANTIAGO DE COMPOSTELA

2933.70	*(2931/40 cm^{-1}) Proteins/lipids CH_2 antisymmetric stretching, CH_3 symmetric stretching, CH_2 antisymmetric stretching, Lusine, glycogen (2933 cm^{-1}) (=CH_3) symmetric stretching in trymyristin, triarachidin, tripetroselinin and trilinolein (triacylglycerols)*	*N*	102,134
2934.20	*(2934 cm^{-1}) assymetric stretching of methoxy (=CH_3) symmetrical stretching in tricaproin, tricaprin, tristearin, trielaidin, trierucin and tripalmitin (triacylglycerides) (2934 cm^{-1}) found in collagen*	*N*	106
2934.60		*N, C*	102,162
2935.10	*(2935 cm^{-1}) Chain end CH_3 symmetric band vs(=CH_3) in trilaurin (triacylglycerols)*	*C*	113,114
2954.80	*(?)*	*C*	
2966.50	*(2960 -2980) CH_3 asymmetric stretch in proteins and lipids (2965 cm^{-1}) vas(=CH_3) in tricaprin (triacylglycerols)*	*C*	102,118
2967.40	*(2967 cm^{-1}) vas(=CH_3) in palmitic acid (triacylglycerols)*	*C*	102
2969.20		*C*	
2969.70	*(?)*	*N, C*	
2970.10	*(2970 cm^{-1}) v asCH_3, lipids, fatty acids Cholesterol and cholesterol ester (2971/3 cm^{-1}) asymmetric stretching of methoxy*	*N*	113
2970.60		*C*	106,114
2972.40	*(?)*	*N*	
2972.80	*(?)*	*C*	
2974.60	*(?)*	*N, C*	
2976.00	*(?)*	*C*	
2976.40	*(?)*	*N*	
2977.30	*(?)*	*N*	
2977.80	*(?)*	*C*	
2978.20	*(?)*	*C*	
2979.60	*(?)*	*C*	
2980.00	*(?)*	*C*	
3061.30	*(3060 cm^{-1}) Aromatics in DNA and proteins (3067 cm^{-1}) Nucleic acids/Proteins C-H aromatics*	*C*	118,134
3061.80		*N, C*	

N: Nucleus; C: Cytoplasm

USC UNIVERSIDADE DE SANTIAGO DE COMPOSTELA

The most prominent peaks appeared in the Raman spectra were the following ones:

- 480 cm^{-1}, attributed to C-C-C deformation of carbohydrates, glycogen, and DNA.
- 1339 cm^{-1} , attributed to CH_2/CH_3 wagging and twisting mode in collagen and lipids, nucleic acids, C-C stretching of phenyl and C_3-C_3 stretching and C_5-O_5 stretching CH alpha in-plane bending in tryptophan.
- 1448 cm^{-1} attributed to CH_2CH_3 deformation, collagen, CH deformation (in proteins, lipids, and carbohydrates), CH_2 bending modes in lipids and proteins, and guanine or adenine CH deformation (DNA/RNA).
- 1656 cm^{-1} attributed to (C=C) stretching in trilinolein, Tri-11-eicosenoin and tripalmitolein (triacylglycerols).
- 2800–3000 cm^{-1} interval, which correspond to the regions attributed to symmetric and asymmetric stretching of CH_2 and CH_3.

4.3.2 FABP4 modified the nuclear composition of hiPSC-derived atrial CMs

To investigate the molecular changes in atrial CMs associated with FABP4 treatment, we compared the spectra obtained from cell nuclei and cytoplasm (unlabelled samples (spectral ranges from 400 to 1800 $cm^{-1}$and from 2650 to 3100 cm^{-1})) of control and treated cells by multivariate analysis through OPLS-DA. This analysis can reveal the characteristic differences between groups[163].

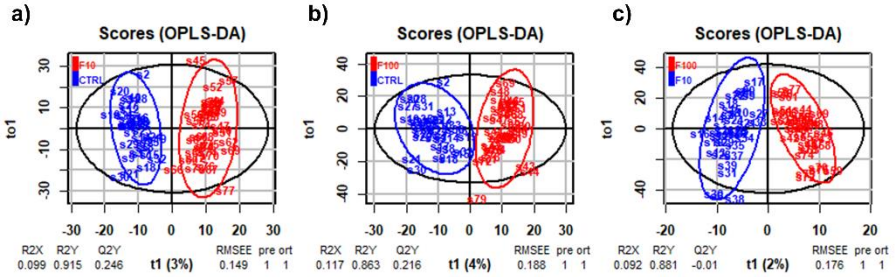


Figure 19. Multivariate analysis of the spectral regions from 400 to 1800 cm^{-1} and from 2650 to 3100 $cm^{-1}$of the Raman spectra obtained from unlabelled hiPSC-derived atrial CM nuclei.

USC UNIVERSIDADE DE SANTIAGO DE COMPOSTELA

Plot representation of OPLS-DA scores for spectra comparisons. Comparison between chronic treatment conditions (96h) of (a) control versus FABP4 at 10 ng/mL, (b) control versus FABP4 at 100 ng/mL and (c) FABP4 at 10 ng/mL versus FABP4 at 100 ng/mL from hiPSC-derived atrial CM nuclei.

The quality of the models is described by the cumulative modelled variation in the X matrix (Raman peaks) (R^2X), the cumulative modelled variation in the Y matrix (conditions) (R^2Y) and the cross validated predictive ability or Q^2Y values (Table 4). Values of R^2Y greater than 0.67 depict substantial differences, while $0.67<R^2Y>0.33$ depict moderate differences and $R^2Y<0.33$ represent weak differences[164]. In these analyses, we found substantial differences in the comparison of the different conditions ($R^2Y=0.915$ in control versus FABP4 at 10 ng/mL: $R^2Y=0.863$ in control versus FABP4 at 100 ng/mL and $R^2Y=0.881$ in FABP4 at 10 ng/mL versus FABP4 at 10 ng/mL). The corresponding peaks responsible for the separation of the groups are depicted in table supplementary Table 1 (see annex III).

Table 4. OPLS-DA results obtained for the different comparisons from the nuclei spectra of hiPSC-derived atrial CMs between conditions.

	R^2X	R^2Y	Q^2	t1	RMSEE	pre	ort	pR^2Y	pQ^2
Nucleus									
Control vs FABP4 10 ng/mL	0.099	0.915	0.246	3%	0.149	1	1	0.1	0.05
Control vs FABP4 100 ng/mL	0.117	0.863	0.216	4%	0.188	1	1	0.65	0.05
FABP4 10 ng/mL vs FABP4 100 ng/mL	0.092	0.881	-0.01	2%	0.176	1	1	0.5	0.2

Results from the collected Raman spectra for the intervals 400 to 1800 cm^{-1} and 2650 to 3100 cm^{-1} from the unlabelled samples. All comparisons showed moderate variance explained by the model, according to the classification: $1 \geq R^2Y \leq 0.67$; $0.67 > R^2Y \leq 0.33$; $0.33 > R^2Y \leq 0.19$.

Peaks in the following regions of the spectra resulted from these comparisons:

- Region I, with the peaks in the interval from 400 to 800 cm^{-1} corresponding to the deformation modes of CCO groups.

USC UNIVERSIDADE DE SANTIAGO DE COMPOSTELA

- Region II, with the interval from 800 to 1200 cm^{-1} associated with the stretching vibration of the O-C/C-C groups.
- Region III, with the interval from 1200 to 1800 cm^{-1} corresponding to the deformation modes of CH/CH_2 groups.
- Region IV, with the interval from 2650 to 3400 cm^{-1} associated with the stretching vibration of the CH/CH_2 groups.

The Variable Importance Parameter (VIP) values summarize the overall contribution of each X-variable to the model, summed over all components and weighted according to the Y variation accounted for by each component. Thus, VIP ranks the compounds (Raman peaks) according to their contribution to the model, and variable selection ensured the involvement of the most relevant VIP in the final model[165]. The corresponding peaks responsible for the separation of the groups resulted from the OPLS analysis (VIP)>1) are depicted in table 6.

Using two-way ANOVA followed by a post hoc test (Šídák's multiple comparisons test), we tested the significant differences between the intensities of the peaks defined by VIP>1 from the OPLS-DA analysis, for all our conditions (Control, FABP4 at 10 ng/mL, and FABP4 at 100 ng/mL). In these comparisons, statistically significant differences were found within hiPSC-derived atrial CM nucleus between control and FABP at 10 ng/mL; and between FABP4 at 10 ng/mL and FABP4 at 100 ng/mL (Figure 20).

USC
UNIVERSIDADE DE SANTIAGO DE COMPOSTELA

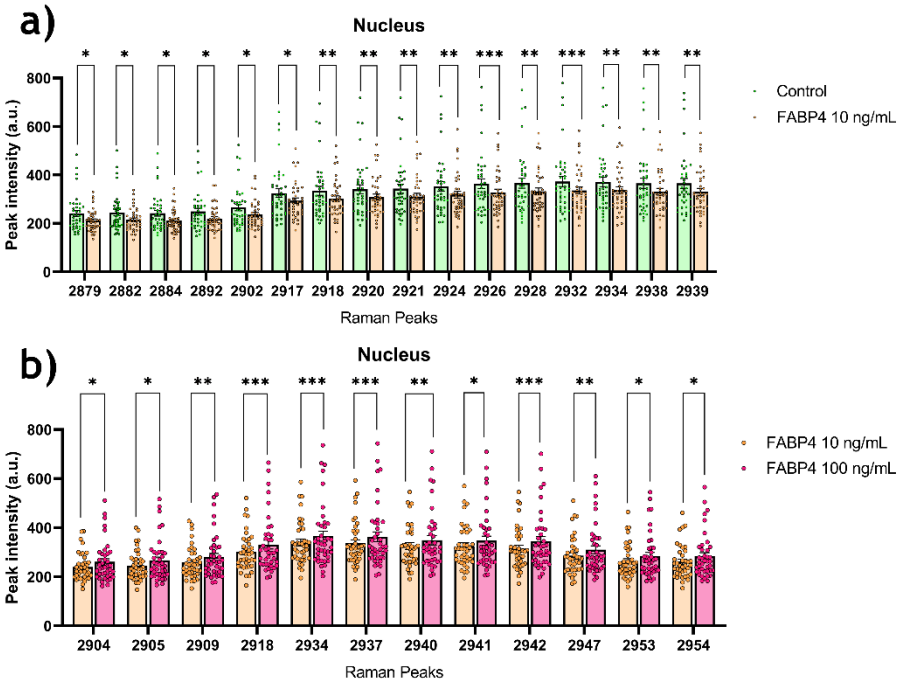


Figure 20. Differential Raman peaks found within CM nucleus attending FABP4.

Quality control of hiPSC-derived atrial CM intensity of the peaks responsible for the separation of the different groups of unlabelled samples found in the nucleus by OPLS-DA was measured in the corresponding Raman spectra. Graphs represent their mean intensity ± SEM from the spectra acquired in the interval from 0 to 1850 and from 2650 to 3100 cm^{-1}. (a) Values for the unique peaks appearing in the comparison between control and FABP4 at 10 ng/mL-treated atrial CMs. (b) Values for the unique peaks appearing in the comparison between atrial CMs treated with FABP4 at 10 ng/mL with those treated with FABP4 at 100 ng/mL. Two-way ANOVA followed by Šídák's multiple comparisons post hoc test, was performed, with *p< 0.05, **p< 0.01. and ***p< 0.001. The sampling distribution was first tested for normality using the Shapiro-Wilk test.

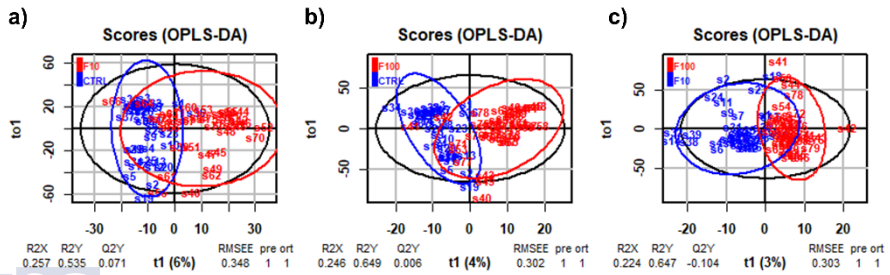
Using this approach, all the significantly different Raman peaks were in the Region IV, with the interval from 2650 to 3100 cm^{-1} associated with the stretching vibration of the CH/CH_2 groups. We found 16 peaks down-regulated in atrial CMs treated with FABP4 at 10 ng/mL in comparison with control cells. Our results showed that 12 peaks from the same region were up-regulated in FABP4 at 100 ng/mL-

USC UNIVERSIDADE DE SANTIAGO DE COMPOSTELA

treated cells regarding FABP4 at 10 ng/mL-treated cells. The significantly different peak intensities can be seen in the lipid-protein profiles in the region of 2800–3000 cm^{-1}, where the contribution from the monounsaturated FA that are common constituents of triacyl glycerides (TAG) of the AT dominates the Raman spectrum[166]. In fact, peaks at 2924, 2928 and 2934 cm^{-1} are related with the symmetrical stretching in $=CH_3$ of palmitoleic acid (2924 cm^{-1}), stearic acid (2928 cm^{-1}) and a variety of TAG, such as tricaprin, tripalmitin, tricaproin, trielaidin, and trierucin (2934 cm^{-1})[102]. To identify the dominating components of the samples in this spectral region, we studied a band at 3009 cm^{-1}, corresponding to H-C=C vibrations, which is clearly visible in FA, and weak in most proteins, according to one previous study[167]. Our results showed a non-significant trend to decrease the peak intensity of the band at 3009 cm^{-1} (from FA) in the profile of the cells treated with FABP4 in comparison with control cells (137.19 ± 4.93 in control *vs* 126.78 ± 3.18 in FABP4 at 10 ng/mL and 134.27 ± 4.53 in FABP4 at 100 ng/mL). The up-regulation in the intensity of the peaks from this region in FABP4 at 100 ng/mL regarding 10 ng/mL suggested the counter-balance of this high concentration with respect to the low FABP4 concentration (Figure 20).

4.3.3 FABP4 effect on the cytoplasmic composition of hiPSC-derived atrial CMs

In the cytoplasm analyses, we found moderate differences in the comparison of the different conditions (R^2Y=0.535 in control versus FABP4 at 10 ng/mL; R^2Y=0.649 in control versus FABP4 at 100 ng/mL and R^2Y=0.647 in FABP4 at 10 ng/mL versus FABP4 at 10 ng/mL) (Figure 21).



USC UNIVERSIDADE DE SANTIAGO DE COMPOSTELA

Figure 21. Multivariate analysis of the spectral regions from 400 to 1800 cm^{-1} and from 2650 to 3100 $cm^{-1}$of the Raman spectra obtained from unlabelled hiPSC-derived atrial CM cytoplasm.

Plot representation of OPLS-DA scores for spectra comparisons. Comparison between chronic treatment conditions (96h) of (a) control versus FABP4 at 10 ng/mL and (b) control versus FABP4 at 100 ng/mL and (c) FABP4 at 10 ng/mL versus FABP4 at 100 ng/mL from hiPSC-derived atrial CM cytoplasm.

The respective OPLS-DA scores for all comparisons from cytoplasm spectra are shown in Table 5.

Table 5. OPLS-DA results obtained for the different comparisons from the cytoplasm spectra of hiPSC-derived atrial CMs between conditions.

	R^2X	R^2Y	Q^2	*t1*	*RMSEE*	*pre*	*ort*	pR^2Y	pQ^2
Cytoplasm									
Control vs FABP4 10 ng/mL	0.257	0.535	0.071	6%	0.348	1	1	0.9	0.05
Control vs FABP4 100 ng/mL	0.246	0.649	0.006	4%	0.302	1	1	0.55	0.1
FABP4 10 ng/mL vs FABP4 100 ng/mL	0.224	0.647	-0.104	3%	0.303	1	1	0.5	0.45

Results from the collected Raman spectra for the intervals 400 to 1800 cm^{-1} and 2650 to 3100 cm^{-1} from the unlabelled samples. All comparisons showed moderate variance explained by the model, according to the classification: $1 \geq R2Y \leq 0.67$; $0.67 > R2Y \leq 0.33$; $0.33 > R2Y \leq 0.19$.

The corresponding peaks responsible for the separation of the groups resulted from the OPLS analysis (VIP)>1) are also depicted in supplementary table 1 (see Annex III).

The results of the subsequent analysis of the peaks with VIP>1 from the OPLS-DA of the cytoplasm did not show any statistical differences among control, FABP4 at 10 ng/mL, nor FABP4 at 100 ng/mL. We performed the specific analyses of the peak intensities of bands associated to lipids (C=C stretching at 1659 cm^{-1}, CH_2 deformation 1441 cm^{-1}, CH_2 twisting 1303 cm^{-1}), cytoplasmic regions likely to correspond to lipid bodies[168].

USC UNIVERSIDADE DE SANTIAGO DE COMPOSTELA

Table 6. Statistical analysis of the different comparisons from the Raman peaks typically assigned in the literature as lipids found in our unlabelled samples.

Two-way ANOVA, followed by post hoc Šídák's multiple comparisons test. Sample distribution was initially tested for normality using the Shapiro-Wilk test.

Wavelength (cm^{-1})	*Control Average peak intensity*	*Treatment Average peak intensity*	*p-value Post Hoc test*
1659.22	124.13 ± 3.54	***FABP4 10 ng/mL*** 125.94 ± 5.30	0.9878
		FABP4 100 ng/mL 130.49 ± 5.57	0.6712
1659.67	125.43 ± 3.57	***FABP4 10 ng/mL*** 126.06 ± 5.29	0.9994
		FABP4 100 ng/mL 129.80 ± 5.55	0.8570
1441.26	129.08 ± 3.76	***FABP4 10 ng/mL*** 128.79 ± 4.90	>0.9999
		FABP4 100 ng/mL 133.30 ± 5.82	0.9093
1441.71	130.06 ± 3.66	***FABP4 10 ng/mL*** 129.18 ± 4.97	0.9986
		FABP4 100 ng/mL 133.75 ± 5.76	0.9306
1303.3	126.63 ± 3.44	***FABP4 10 ng/mL*** 127.78 ± 4.86	0.9963
		FABP4 100 ng/mL 131.84 ± 5.27	0.8048
1303.74	126.41 ± 3.52	***FABP4 10 ng/mL*** 128.21 ± 4.86	0.9868
		FABP4 100 ng/mL 132.13 ± 5.33	0.7650

Our results showed a trend to increase the peak intensities of these lipid-associated bands under FABP4 treatment at 100 ng/mL (Table 6). However, we did not see statistically significant changes, may be due to data intra-variability or to high signal-to-noise ratio values of the acquired spectra under the specific selected conditions.

USC UNIVERSIDADE DE SANTIAGO DE COMPOSTELA

4.4 Effect of FABP4 on the differentiation of hiPSC into atrial CMs

The results in this subchapter were obtained in collaboration with the Signalling and Cardiovascular Pathophysiology Group, under the supervision of Dr. Laetitia Pereira, at the *Université Paris-Saclay, Institut national de la santé et de la recherche médicale* (INSERM) during a 3-month stay during the predoctoral period.

We wanted to know if FABP4 was affecting atrial CMs functioning by acting during the differentiation process from hiPSC. For that, we then worked with hiPSC cultures, performing in these cells the atrial CM differentiation, with a commercial kit. After this, as a quality control of the procedure, we performed immunocytochemistry (ICC) to visualize α-actinin. α-actinin is an actin-binding protein that belongs to the spectrin superfamily. In striated cardiac muscle cells, it is located in the Z discs, where it stabilizes the contractile apparatus of the muscle, forming a reticular structure that anchors the filaments of actinin[169]. Cells correctly differentiated into cardiomyocytes were counted as the percentage of cells labelled with α-actinin compared to the total number of nuclei visualized with the blue fluorescent DNA marker 4′,6-diamidino-2-phenylindole (DAPI).

Our results showed a high percentage of differentiated cells in control (91.95 ± 1.86% and under FABP4 100 ng/mL treatment (94.13 ± 1.09%). However, cells treated with FABP4 at 10 ng/mL showed a lower differentiation percentage, which was significantly different compared to the control (69.09 ± 2.07%, $p<0.001$) (Figure 22). In addition, in control and FABP4 100 ng/mL, we observed the presence of Inositol 1,4,5-Trisphosphate Receptor Type 3 (ITPR3), which is expressed to counteract the low expression of type 2 ryanodine receptors (RyR2), indicating an incomplete maturity of the cardiomyocytes[170].

USC UNIVERSIDADE DE SANTIAGO DE COMPOSTELA

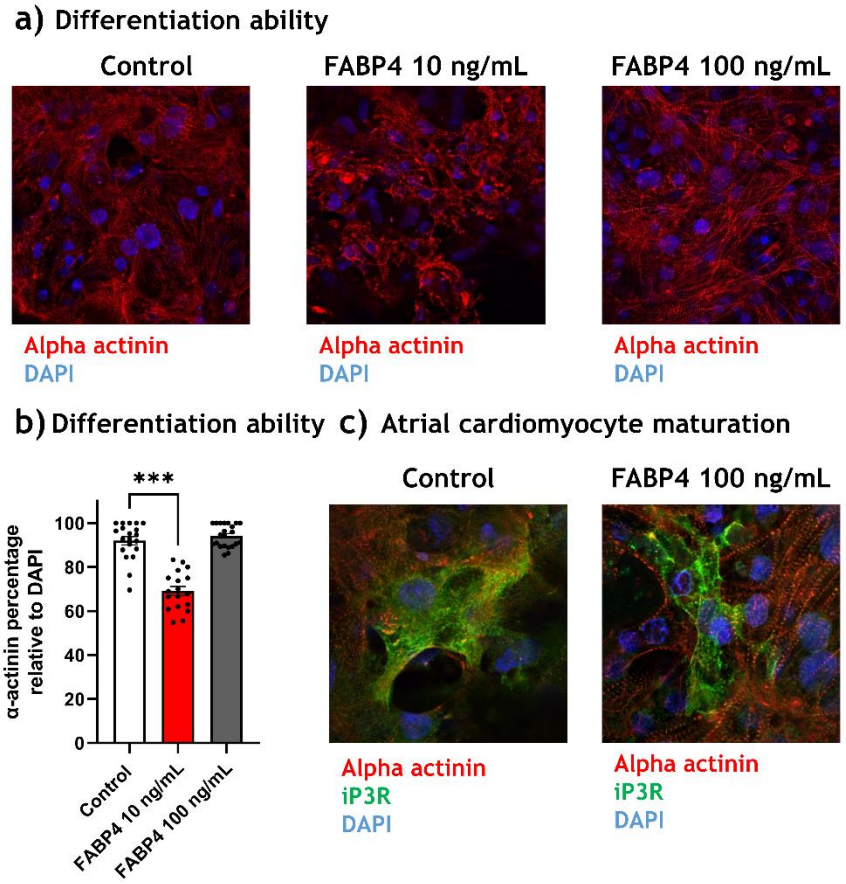


Figure 22. Quality control of hiPSC differentiation

a) Representative images of the ICQ performed on hiPSC-derived atrial CMs treated or not with FABP4 at 10 or 100 ng/mL during the differentiation process. b) Differentiation capacity of the hiPSCs according to the treatment c) Control of the maturation of the atrial CMs after the differentiation.

Images were acquired with an inverted Leica TCS SP8 microscope (Leica) (objective 60X) Data are presented as mean ± SEM ***p<0.001 versus control.

USC
UNIVERSIDADE DE SANTIAGO DE COMPOSTELA

4.4.1 Spontaneous [Ca^{2+}] transient interval from hiPSC-derived atrial CMs treated with FABP4 during its differentiation

To assess whether FABP4 exposure during hiPSC differentiation modifies atrial CMs behaviour, we analysed the spontaneous [Ca^{2+}] transient interval (without electrical stimulation), which reflects the time between CMs contractions. This analysis showed that FABP4 at low concentration increased the spontaneous [Ca^{2+}] transient interval compared to the vehicle (2.85 ± 0.37 s in control *vs* 5.25 ± 0.60 s in FABP4 10 ng/mL, p<0.001) (Figure 23).

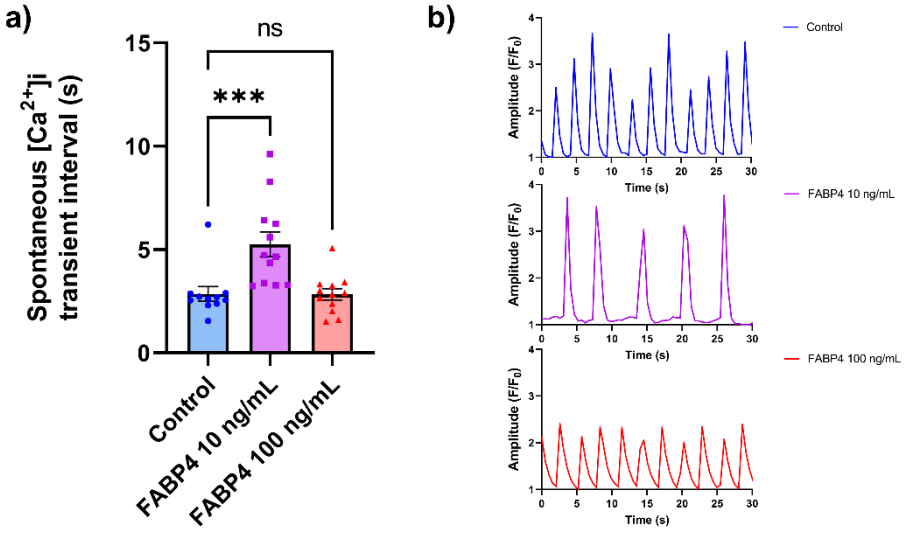


Figure 23. Spontaneous [Ca^{2+}] transient interval from hiPSC-derived atrial CMs treated with FABP4 during its differentiation

a) Mean values of spontaneous [Ca^{2+}] transient interval from hiPSC-derived atrial CMs treated with vehicle (n=43), FABP4 10 ng/mL (n=48) and FABP4 100 ng/mL (n=48). b) Representative amplitude profiles of the spontaneous [Ca^{2+}] transients from hiPSC-derived atrial CMs over 30 s.

Data are presented as mean ± SEM, ***p<0.001

USC UNIVERSIDADE DE SANTIAGO DE COMPOSTELA

4.4.2 $[Ca^{2+}]_i$ transient characteristics of hiPSC-derived atrial CMs submitted to FABP4 treatment during their differentiation

We investigated whether FABP4 modulates electrically evoked $[Ca^{2+}]_i$ transients in Calbryte™ 520 AM-loaded hiPSC-derived atrial CMs under electrical field stimulation at 1 Hz. Compared to vehicle, FABP4 at 100 ng/mL induced a significant increase in the amplitude of $[Ca^{2+}]_i$ transients (Figure 24b, $p<0.05$). Further analysis of time constants showed that FABP4 treatment changed the kinetic properties of $[Ca^{2+}]_i$ transients: Atrial CMs treated with FABP4 at 100 ng/mL during their differentiation exhibited a faster time decay constant, τ (Figure 24c; $p<0.01$) along with a significant decrease in the time to peak. This latter effect was also caused by FABP4 at 10 ng/mL (Figure. 24d; $p<0.001$), compared to vehicle-treated cells.

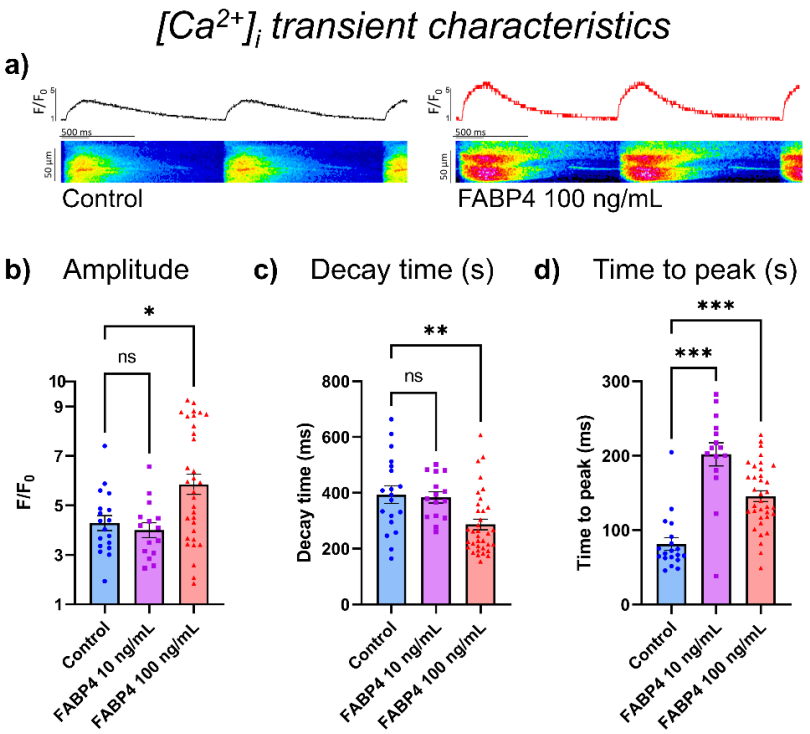


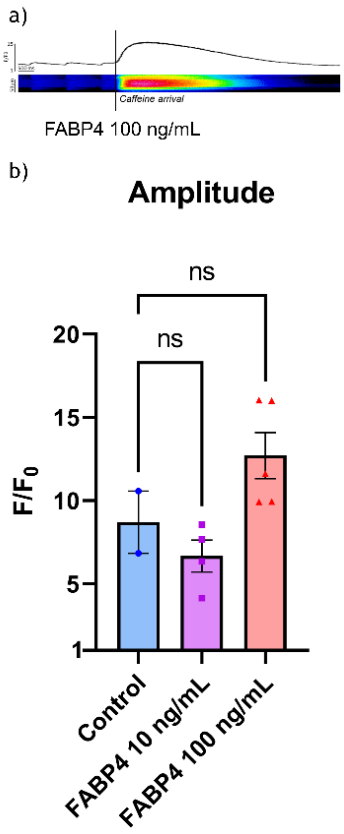
Figure 24. Characteristics of $[Ca^{2+}]_i$ transients from hiPSC-derived atrial CMs

Effect of FABP4 on electrically-evoked $[Ca^{2+}]_i$ transients of hiPSC-derived atrial CMs (a) Illustrative line-scan confocal image of single atrial CMs treated with vehicle (left) and FABP4 at 100 ng/mL (right) during their differentiation from hiPSC.

Individual and mean values ± SEM of (b) amplitude (F: F0), (c) decay constant (fitting time constant of the descending curve of fluorescence at a exponential function), τ, and (d) time to peak in hiPSC-derived atrial CMs treated with vehicle and FABP4 at 10 or 100 ng/mL during their differentiation (n=18,15 and 32 respectively).

*p<0.05, **p<0.01, ***p<0.001 versus control.

4.4.3 FABP4 treatment during the differentiation process could modulate diastolic Ca^{2+} content from SR in hiPSC-derived atrial CMs



We analysed whether FABP4 altered the $[Ca^{2+}]_i$ content of the sarcoplasmic reticulum (SR). After stimulating the atrial CMs to reach a steady state, caffeine was applied to deplete $[Ca^{2+}]_i$ from the RS. Due to the low number of results obtained with this procedure, we could not observe significant changes in the amplitude of the $[Ca^{2+}]_i$ transients evoked by caffeine. Nevertheless, our results showed a trend in amplitude increment in FABP4-treated atrial CMs during its differentiation (Figure 25).

Figure 25. Amplitude of $[Ca^{2+}]_i$ stored in the sarcoplasmic reticulum

a) Illustrative line-scan confocal image of a caffeine-induced $[Ca^{2+}]_i$ transient from a single hiPSC-derived atrial CMs treated with FABP4 100 ng/mL during its differentiation. (b) Individual and mean values ± SEM of amplitude (F:F0) from atrial CMs treated or not with FABP4 at 10 and 100 ng/ml during their differentiation from hiPSC.

USC UNIVERSIDADE DE SANTIAGO DE COMPOSTELA

4.5 ARTICLE 4 | HIGHER ACE2 EXPRESSION LEVELS IN EPICARDIAL CELLS THAN IN SUBCUTANEOUS STROMAL CELLS FROM PATIENTS WITH CARDIOVASCULAR DISEASE: DIABETES AND OBESITY AS POSSIBLE ENHANCERS

The results from this chapter have already been published as Marinela Couselo-Seijas[1,2], Cristina Almengló[2,3], Rosa M. Agra-Bermejo[3,4,5], Ángel L Fernández[2,5,6], Ezequiel Álvarez[2,3,5], José Ramón González-Juanatey[2,3,4,5], Sonia Eiras[1,5] Higher ACE2 expression levels in epicardial cells than subcutaneous stromal cells from patients with cardiovascular disease: Diabetes and obesity as possible enhancer. Eur J Clin Invest. 2021 May;51(5):e13463.

The study was approved by the Galician Research Ethics Committee (Registration Code 2019/439).

DOI: 10.1111/eci.13463., PMID: 33251580., ISSN: 0014-2972

Affiliations: [1]Grupo de Cardiología Traslacional, IDIS, Santiago de Compostela, España; [2]Universidad de Santiago de Compostela, Santiago de Compostela, España; [3]Grupo de Cardiología, IDIS, Santiago de Compostela, España; [4]Área Cardiovascular y Unidad Coronaria, Hospital Clínico Universitario, Santiago de Compostela, España; [5]CIBERCV, Madrid, España; [6]Departamento de Cirugía Cardíaca, Hospital Clínico Universitario, Santiago de Compostela, España

Link: https://onlinelibrary.wiley.com/doi/10.1111/eci.13463

5 DISCUSSION

The pathophysiological mechanisms that trigger the onset, burden, and maintenance of AF are complex, ranging from mechanical or structural and metabolic phenomena to electrical changes in cardiomyocytes. AF classification was performed according the presentation, duration, and spontaneous termination of its episodes[10], with the ability to become a permanent chronic disease. It is important to consider in this classification the so-called postoperative AF, which appears shortly after a surgical procedure. This type of AF is quite common (10% to 40% after surgical procedures)[9], and its consequences, related to increasing the risk of events, hospitalization times, and its associated costs; are not negligible. AF complexity is also accompanied by its multifactorial nature, as there are several risk factors and comorbidities associated with this arrhythmia.

For all these reasons, there is currently no effective treatment for AF. Within the different therapeutic strategies for rhythm control, recurrence of AF after cardioversion is estimated in approximately 70% of patients. After catheter ablation, being the first-line treatment for many patients, there is still a significant percentage of recurrence (20% to 45%)[171]. Therefore, selecting those patients who will benefit from a strategy based on the discovery of some specific marker is of vital importance to guarantee the success of the strategy chosen in each case. The urgent need for the improvement of AF management also comes from its increasing prevalence. As it was mentioned at the beginning of this doctoral thesis, in Europe, one out of three individuals over fifty-five years old will suffer from AF at some point in their life[10]. Besides, despite the improvement in the mortality rates in patients with AF, they still remain higher in comparison with people without AF[172].

The most described AF pathophysiological mechanisms focus on electrical remodelling (reduction of AP, shortening of the atrial refractory period, formation of re-entry circuits and conduction blockages), structural (accumulation of adipose tissue and fibrous tissue) and contractile (modification of contractile proteins and altered

USC
UNIVERSIDADE DE SANTIAGO DE COMPOSTELA

Ca^{2+} homeostasis). For this arrhythmia to be established, promoting events and a favourable substrate are needed. One of the promoting AF events is the alteration in the autonomic tone[173] and one of the supporting substrates is inflammation[174]. Thus, although the total contribution of the adrenergic or cholinergic system is unknown, it is known that there is altered atrial innervation. While the neurotransmitter of the parasympathetic system, ACh, is involved in hyperpolarizing and shortening the duration of the action potential, the neurotransmitter of the sympathetic nervous system, norepinephrine, maintains the arrhythmogenic effect through increased transient Ca^{2+}. In addition, inflammatory mediators may confer a prothrombotic state, partly mediated by endothelial injury and platelet activation, which promote fibrosis and contribute to structural remodelling. One of the tissues adjacent to the myocardium that secretes inflammatory mediators and has sympathetic and parasympathetic innervations is EAT[175].

This fat pad, being in direct contact and sharing the same microvasculature with the myocardium, could be playing an important role. The anatomical implication of EAT with AF has been widely described, relating parameters such as its volume, mass or thickness with this disease[176–180]. However, as it is a very metabolically active tissue[39,51], not only the quantity, but also the quality and functionality of EAT must be taken into account to understand its relationship with AF. Due to increasing advances and the availability of non-invasive imaging techniques, such as CT and CMR, there is currently more evidence of the risk of disease associated with different adipose tissue deposits. EAT is particularly relevant when it comes to CVD. This tissue is located on the myocardium, especially in atrioventricular branches, and under physiological conditions protects from excess circulating fatty acids and hypothermia, due to its high ability to incorporate fatty acids and the presence of UCP- 1[181], respectively. However, under pathological conditions this tissue secretes adipocytokines that induce fibrosis such as activin A[182], and inflammation, or reduces the expression and secretion of others that regulate arrhythmogenesis or atherogenic and inflammatory processes. Thus, the increase in its thickness or volume, as measured by the afore-

USC UNIVERSIDADE DE SANTIAGO DE COMPOSTELA

mentioned imaging techniques, has been linked to parameters of metabolic syndrome and cardiovascular disease, such as ischemic heart disease, heart failure, and AF[183].

EAT local effect, specifically in the LA, could be discerned from the effect caused by EAT depots located on other myocardial regions. In this sense, aEAT shows a specific transcriptomic profile with a greater expression of genes related to Ca^{2+} handling (muscular contraction and intracellular mobilization), compared to the expression levels found in EAT from other regions of the heart[184]. This comparison revealed the overexpression of Sarcoplasmic/Endoplasmic Reticulum Calcium ATPase 1 (SERCA1) in peri-atrial EAT, which codes for the protein of the adenosine triphosphate (ATP)-dependent intracellular pump of Ca^{2+}, and its association with the ECC[184]. These changes, as well as the expression of contractile proteins or proteins related to the cytoskeleton (such as gelsolin), could promote AF[185], since their absence induces an alteration of the I_{CaL}[186]. In addition to the transcriptomic level, it is important to know the protein secretion profile of EAT, given its paracrine activity on the myocardium. It has recently been shown that, in addition to its participation at the structural level in the interference in electrical conduction due to the infiltration of adipocytes or fibroblasts, there is an effect of the secretome of ovine or murine EAT on hiPSC-derived CMs or HL-1 electrophysiology. Specifically, by slowing down spontaneous contraction and prolonging the duration of the extracellular field potential, respectively[187].

Due to the difficulty in acquiring samples of EAT fat pads (healthy samples can only be acquired from autopsy or transplant procedures), we had to search alternatives to study the epicardial fat. One of these alternatives is the use of EAT samples from patients submitted to cardiac surgery. Besides, we acquired SAT samples from the same patient. Thus, it is possible to use SAT as control, and discard the effect of other possible co-morbidities in the control sample as it comes from the same individual. To verify the implication of EAT proximity to the focus of the disease, in this case the LA, our group has compared the protein secretion of aEAT and vEAT.

USC
UNIVERSIDADE DE SANTIAGO DE COMPOSTELA

Our results showed that both aEAT and vEAT secreted proteins into the extracellular medium, mostly related to metabolism, cell growth, transport, and immune response. Most of the secreted proteins were common to both tissues, and among the differential ones we found some ubiquitous proteins, such as hormone-sensitive lipase (HSL).

On the other hand, we observed a differential secretion protein profile in both tissues after treatment with ACh. In addition, more differences were found in vEAT than in aEAT. One of the most important reasons could be the greater vascularization and finding of blood proteins in aEAT, which could be masking other differentially secreted proteins in this tissue. Given that, regardless of its location, EAT behaviour is very similar at the protein secretion level, and it is modified after treatment with ACh. Our group decided to continue using this preclinical model to study the involvement of the ANS in AF, through EAT.

Along with the most studied relationship of the sympathetic nervous system (SNS)[188,189], the dysregulation of both (also the parasympathetic) has been highlighted in the onset and maintenance of AF[75]. Therefore, a better understanding of the factors that trigger the malfunction of the parasympathetic NS in the myocardium will be of valuable use for the clinical practice and, consequently, for the improvement in the prevention/diagnosis and/or treatment of AF patients. The main triggers that contribute to the AF initiation are located mostly in the pulmonary vein ostia. Around these structures, a higher thickness of epicardial fat was associated with AF burden[180].

In this sense, the first clinical study that evaluated the injection of botulinum toxin (which inhibits the secretion of the neurotransmitter ACh) in EAT fat pads, showed a reduction in AF recurrence in patients with a history of paroxysmal AF. Botulinum toxin injection in the fat pads adjacent to the PVs led to a significant reduction in both short-term[190,191] and long-term[192] AF recurrence.

A second trial including 130 patients undergoing cardiac surgery for coronary artery bypass grafting (CABG) and/or valve procedures with or without a history of paroxysmal AF demonstrated

USC UNIVERSIDADE DE SANTIAGO DE COMPOSTELA

an 11% absolute reduction in the occurrence of post-operative (in-hospital) AF, but this was not significant after a mean follow-up of 6 days. Still, the procedure was associated with shorter and less severe AF episodes, with no adverse safety outcomes compared to placebo[193].

Currently, and based on the previous two trials, the clinical study on Neurotoxin (botulinum toxin type A) for the prevention of Post-Operative Atrial Fibrillation, (NOVA), with the largest number (estimated approx. 330) of patients recruited in a project of this type, is taking place[194].

The variability in the results derived from these clinical studies, in addition to the factors that determined their design, may be related to the response of EAT itself to parasympathetic denervation, and understanding its functioning after cholinergic activity (ACh) could be helpful to determine the best follow-up strategy.

To this end, our group has demonstrated the presence of muscarinic receptors (muscarinic acetylcholine receptors, mAChR) in EAT. mAChRs are ACh receptors coupled to G proteins (G protein-coupled receptors, GPCRs). There are 5 subtypes of mAChR (1-5) depending on the type of G protein to which they are coupled with[195]. Within the different mAChR subtypes, mAChR 2 was the most expressed subtype, in the same way as in the myocardium, and as it had also been described in AT[196]. However, subtype 3 showed the most interesting results since its expression was upregulated after induction of adipogenic differentiation[197]. This receptor was considered a target for an anti-obesity drug[198]. In this sense, it could be related to the observed AF inhibition in cardiac surgery patients who have been injected with botulinum toxin in EAT[190–192], through the modulation of its activity and effects on mature adipocytes.

EAT SVF cells showed a greater cholinergic response (induced by ACh) than SAT SVF cells, regarding Ca^{2+} handling[199]. Thus, we observed an increase in $[Ca^{2+}]i$ of EAT stromal cells in response to ACh. This effect could be due to the mAChR presence in the tissue since mAChR 2 and mAChR 3 showed a greater expression in EAT in comparison with SAT SVF cells. However, mAChR2 is coupled to

USC UNIVERSIDADE DE SANTIAGO DE COMPOSTELA

inhibitory G proteins (Gi), which causes a decrease in heart rate in the myocardium, reduces the contractile force of the atrium, and the speed of conduction of the AV node, through the decrease in the conductance of K^+ and Ca^{2+}[200]. This would indicate that the mobilization of $[Ca^{2+}]i$ observed in EAT SVF cells could be mediated by subtype 3 coupled to a Gq, increasing phospholipase C (phospholipase C, PLC) and consequently inositol triphosphate and $[Ca^{2+}]i$. PLCβ1 stimulation occurs in both excitable and non-excitable cells[201]. The increased expression of mAChR 3 after adipogenic differentiation could indicate a greater response to cholinergic activity in patients with higher volume of EAT. In addition, the increase in $[Ca^{2+}]i$ caused by this receptor, is important for the regulation of several cellular responses, including enzyme activation or transcriptional modifications[201].

The different types of AF could have differential components, in such a way that postoperative or paroxysmal AF could be more related to inflammation and cardiomyocyte electrical activity; while long-term persistent or permanent AF would be more associated with structural changes, fibrosis, adipocyte infiltration, and metabolic cellular activity.

Inflammatory conditions, such as pericarditis or myocarditis, are associated with AF[202,203]. A recent study has shown that $CD45^+$ and $CD3^+$ cell infiltration in the atrium is increased in patients with paroxysmal AF compared to samples from non-paroxysmal AF patients[204]. The pro-inflammatory activity of adipocytes has been shown to modify the ion currents and contractility of cardiomyocytes[205]. In line with this, the pro-inflammatory profile of EAT SVF might participate in the initiation of AF. This could be due to the activity of the many other cell types that are included in the SVF (fibroblasts, mesenchymal cells, ADSC, pericytes, vascular cells and immune system (myeloid and lymphoid) cells[206]. Our results showed higher levels of inflammatory cytokines and chemokines in EAT SVF compared to SAT SVF. However, no differences were observed regarding AF presence. On the other hand, acute cholinergic activity increased the mRNA expression levels of the chemokine MCP-1 in EAT SVF cells. This gene, together with IL-6, showed a higher base-

USC
UNIVERSIDADE DE SANTIAGO DE COMPOSTELA

line gene expression in EAT compared to SAT, indicating a more pro-inflammatory profile of this local fat pad. These results suggest that the cholinergic activity modulation in EAT from patients undergoing cardiac surgery could prevent the acute inflammatory response and the recruitment of immune cells caused by MCP1. In this line, MCP1 has been shown to increase the recruitment of neutrophils in response to a bacterial lung infection studied in a murine model[207]. It has been shown that ACh activity modulates the macrophage-induced inflammation response through nicotinic ACh receptor α7 subunit[208] and it also stimulates the pro-inflammatory cytokine secretion and neutrophil recruitment through mAChRs[209]. Thus, the reduction of cholinergic activity on EAT pads during open-heart surgery might prevent the acute inflammatory response and neutrophil infiltration, in a similar mechanism to the evoked under colchicine treatment, used as a preventive strategy for post-operative AF[210].

After comparing the atrial and ventricle epicardial fat pads, we observed that both fat pads have a similar endocrine activity after ACh treatment. Some of these proteins were involved on inflammation, detoxification, and structural composition. Intriguingly, we observed a lower secretion of IL-6 and DEFA3 after ACh treatment.

Defensins are small cationic peptides between 18 and 45 amino acids. There are three subfamilies of defensins (α, β and θ), of which α-defensins are only found in mammals and marsupials. There are 6 peptides of α-defensins, encoded by 5 genes (human neutrophil peptide, HNP 1-5). The HNP3 gene is missing in about 10% of people, so their neutrophils contain only HNP1 and HNP2[211]. α-defensins are stored in the azurophilic granules of polymorphonuclear cells (PMNs), in the same way as myeloperoxidase (MPO). HNP1-3 represent 5 to 7% of the total protein of a human PMN, and 30-50% of the total protein of their granules. As components of neutrophils, their main functions are antimicrobial, antiviral, antitoxic, and cell adhesion. The binding of α-defensins is neither specific nor covalent, and it is easily reversible[212].

The ability of α-defensins to dimerize, oligomerize, and/or multimerize provides them with additional molecular complexity, contributing to a greater structural diversity and functional versatility.

USC UNIVERSIDADE DE SANTIAGO DE COMPOSTELA

Therefore, the interaction between their hydrophobicity and their cationicity gives them a wide range of functional properties and allows them to participate in many diverse biological processes[212]. In contrast to the higher concentration of DEFA3, which was interpreted as a marker in the progression of HF or CAD[213,214], a decrease in this molecule may also imply a reduced protection against external agents[215,216]. Thus, postoperative infections increase the probability of developing postoperative AF[217].

On the other hand, in long-term ACh treatments, the effect in EAT SVF cells was found to be more associated with lipid accumulation. It was shown in a recent study that the expression levels of genes related to FA metabolism and autophagy were up-regulated in patients with permanent AF[218]. The hyperactivity of FA uptake induces mitochondrial dysfunction and metabolism dysregulation. These results allowed Katoh H. *et al* to speculate with a FA metabolism dysregulation in AF atrial myocardium. This lipotoxicity could be counteracted by autophagy in a process termed "lipophagy"[218].

FABPs are a family of 14–15 kDa proteins, known as intracellular lipid chaperones, that regulate lipid trafficking and response in cells. FABPs can reversibly bind to hydrophobic ligands, such as saturated and unsaturated long-chain fatty acids (LCFA), eicosanoids, and other lipids, with high affinity and broad selectivity[219]. FABP isoforms are uniquely expressed in different tissues involved in lipid metabolism. Thus, FABP4 or AP2 is mainly expressed in AT, although it is also expressed in macrophages and endothelial cells[220]. In addition to its main function of intracellular FA transport, FABP4 has recently been described with hormonal functions[67], such that this chaperone could play a role in metabolic maintenance and dysregulation. Thus, our group has found that FABP4 peripheral and local plasma levels distinguished left atrial adipose tissue (LAAT) volume in permanent from paroxysmal AF patients. Besides, within the permanent AF patients, FABP4 was associated with those at higher risk of recurrence after pulmonary vein isolation[93].

In this line, our results showed an increased expression of FABP4 in EAT SVF cells from patients with long-standing persistent

USC UNIVERSIDADE DE SANTIAGO DE COMPOSTELA

AF. In addition, we demonstrated its long-term parasympathetic regulation through a vagotomised rat model, in which we observed that after denervation of the vague nerve, FABP4 plasma levels were reduced in a body weight-independent manner[199]. FABP4 is secreted by adipocytes and macrophages through a calcium-dependent pathway, and independent of the classical pathway of the endoplasmic reticulum and the Golgi apparatus[221]. A recent study has shown the role of some adipokines in blocking the differentiation of CM precursor cells and in the apoptosis of mature CMs[222].

To understand the effect that FABP4 could be exerting on myocardial function, our group has initiated a series of procedures in hiPSC-derived atrial CMs. Embryonic stem (ES) cells are pluripotent cells that grow indefinitely, derived from the inner cell mass of mammalian blastocysts. However, their use become challenging overall in terms of ethical issues because they need to be obtained from human embryos[223]. Thanks to the discoveries of Takahashi *et al*. back in 2006, the scientific community is now able to work with iPSC derived from somatic cells. By the ectopic expression of a set of four determined transcription factors, named Oct3/4, Sox2, c-Myc and Klf4, they were able to generate iPSC from mouse and human adult somatic cells[223,224]. iPSC can be generated from patients' own cells, solving the problem of tissue rejection after transplantation when they are generated in the context of cell transplantation therapy or regenerative medicine. Besides, in the context of human disease modelling, patient-specific iPSCs offer advantages over ES cells since hiPSC sustain the genetic and epigenetic background of the subject from which they were obtained[225]. After de-differentiation, hiPSC have the ability differentiate into cells of any of the three germ layers (endo-, ecto- and mesoderm), including cardiomyocytes, like ES cells[225].

In this line, hiPSC have been extremely useful in the investigation of the pathophysiology of CVD. Differentiation of hiPSC to CMs have been developed by adding, as in the de-differentiation process, specific factors at different determined times to the culture media (Rho-associated kinase (ROCK) inhibitor, (Y-27632), B-27, insulin, GSK3 inhibitor, Wnt signaling pathway activator

USC UNIVERSIDADE DE SANTIAGO DE COMPOSTELA

(CHIR99021), Wnt inhibitors (IWP4 or IWR-1))[224,225]. Modulation of the retinoic acid signaling pathway by adding retinoic acid during the early differentiation process directed hiPSC towards an atrial CM phenotype[226]. Atrial CMs differentiated from hiPSC become a powerful tool to study the mechanisms of atrial-specific diseases or to test the efficacy of atrial-selective drugs. Thus, this cells can be used to unravel the mechanisms, pathophysiology, and treatment options of AF[226]. For these reasons, we selected hiPSC and hiPSC-derived atrial CMs to test the effect of FABP4.

To find out if FABP4 effect on CMs is caused during the differentiation process, we carried out experiments including FABP4 in the cell culture medium of hiPSC during its differentiation, and we analysed the behaviour of intracellular calcium currents, comparing differentiated cells subjected or not to treatment with FABP4 at 10 and at 100 ng/mL during the early stages (day 0 to 4) of the process. Ca^{2+} regulates contraction through the ECC in CMs. For each heartbeat, sarcolemmal L type Ca^{2+} channels open during the AP, leading to Ca^{2+} influx that activates Ca^{2+} release from the RyRs located at the SR. This release of Ca^{2+} by the RyR (visualized as a $[Ca^{2+}]_i$ transient) activates contractile myofibrils to generate CM contraction. After the contraction, the Ca^{2+} is re-uptaken into the SR by the SERCA pump and extruded outside the CM mainly by the Na^+/Ca^{2+} exchanger, resulting in cardiomyocyte relaxation[227]. There are several Ca^{2+}-dependent mechanisms involved in the control of APD[228]. In this line, it was demonstrated that in diabetic cardiomyopathy, cardiac dysfunction is associated with Ca^{2+} mishandling. Indeed, glucose-induced arrhythmogenic Ca^{2+} waves occur through a CaMKII and O-GlcNAc dependent mechanism[229]. For this reason, we aimed to further characterize, as the already demonstrated glucose-induced arrhythmogenic mechanism, the lipid effect on human CM contractility but also in its differentiation ability.

Our results indicated that FABP4 at low concentration increased the time interval between spontaneous $[Ca^{2+}]i$ currents from hiPSC-derived atrial CMs. This result could be explained by the lower degree of differentiation in FABP4-treated atrial CMs with 10 ng/mL,

USC UNIVERSIDADE DE SANTIAGO DE COMPOSTELA

measured by the expression of α-actinin. A higher number of undifferentiated cells could promote a disruption in impulse propagation and/or affect the contraction rate of mature cells. As IP3R-mediated Ca^{2+} release is one of the major counter-balancing methods for Ca^{2+} cycling in human CMs with RyR_2 deficiency[230], the positive result for IP3R should be taken into account to consider increasing the cell culture maintenance time, to guarantee the complete maturation process of the atrial CMs. An analysis of the expression of a) troponin and GAP junctions with connexin 43 (Cx43) or connexin 40 (Cx40) (specific to the atrium), which suggest the formation of electrically coupled multicellular units, or b) genes related to structural development, such as the heavy chain of the myosin[231] could help to confirm this hypothesis. The expression of the Myosin regulatory light chain 2 (MYL2), being an atrial-specific isoform[232], would also confirm the correct differentiation of the cells.

FABP4 at 100 ng/mL increased the amplitude and time to peak of electrically evoked $[Ca^{2+}]i$ transients in hiPSC-derived atrial CMs, compared to control. The increased amplitude of $[Ca^{2+}]i$ release could indicate a modulation of the RyRs, since it has previously been demonstrated that FABP4 did not modify the activity of I_{CaL}, the main responsible for its cellular internalization[94]. The decay constant of transient $[Ca^{2+}]i$ reflects the disappearance of Ca^{2+} from the cytosol by reinternalization in the SR through (sarco(endo)plasmic reticulum calcium-ATPase 2 (SERCA2), and to a lesser extent by its extrusion through NCX. FABP4 at 100 ng/mL during differentiation decreased the decay constant of transient $[Ca^{2+}]i$ in atrial CMs, which could indicate an improvement in the activation or functioning of SERCA2. The total SR Ca^{2+} load, which is suggested by the amplitude of the transient $[Ca^{2+}]i$ evoked by caffeine showed a trend to be up-regulated after FABP4 treatment. These results went in line with the increase in the amplitude of the electrically evoked $[Ca^{2+}]i$ transient; since a higher concentration of Ca^{2+} in the SR would allow an increase in its release into the cytosol by RyR, and its reuptake into the SR by SERCA2.

During relaxation, Ca^{2+} release into the cytosol does not occur under normal conditions, since RyRs are closed. However, there are

USC UNIVERSIDADE DE SANTIAGO DE COMPOSTELA

Ca^{2+} leaks, known as sparks, which are Ca^{2+} releases from the SR, mediated by the spontaneous activation of a variable number of RyRs. The analysis of the modulation of these Ca^{2+} leaks after treatment with FABP4, could reveal its involvement in the appearance of these pro-arrhythmogenic events, relating the activity of FABP4 with AF.

Among the different FABP4 exogenous effects described (enhanced hepatic glucose production, inhibited activation/expression of endothelial nitric oxide synthase in vascular endothelial cells, increased proliferation/migration in vascular smooth muscle cells or glucose-stimulated insulin secretion in pancreatic β-cells)[220]; it has already been described that FABP4 exerts a cardiodepressive effect in murine mature ventricular CMs, reducing cell shortening and $[Ca^{2+}]i$ fluorescence peak[94]. Therefore, we wanted to test the effect of FABP4 on already differentiated hiPSC-derived atrial CMs. We performed Raman spectroscopy to test the intracellular modifications evoked by FABP4 treatment in this cell type. We developed an OPLS-DA model using Raman spectra of 118 atrial CMs treated or not with FABP4 at 10 and 100 ng/mL for ninety-six hours. Due to the high spatial resolution of the technique, we were allowed to collect the spectra from the nucleus and the cytoplasm from each measured cell. The OPLS-DA model using the scores of the VIP>1 showed substantial differences in the comparison of the different conditions, being the most distinguishable among control and FABP4 at 10 ng/mL (R^2Y=0.915) within the nucleus of atrial CMs (n=78 spectra). However, the values of the other parameters (t1, pR^2Y) suggest that these models could not be correctly discerning the groups. For this reason, we analysed the statistical differences of some peak intensities apart from the resulted significant peaks of the OPLS-DA analysis, based on the previous literature. Besides, other analysis approaches will be performed in collaboration with statistic specialists to find models with the ability to better discern the cells regarding FABP4 treatment, and to ensure the characterization of the Raman peaks responsible for these changes.

The Raman bands identified in the OPLS-DA model indicated that the marked distinctions were found within the nucleus. The spectral differences between control atrial CMs and atrial CMs treated with

USC UNIVERSIDADE DE SANTIAGO DE COMPOSTELA

FABP4 at 10 ng/mL were mainly attributed to the highest wavenumber region. FABP4 carries FA to different organelles within the cell (mitochondrion, peroxisome, endoplasmic reticulum). Although the primary sequence of FABP4 does not harbour a nuclear localization signal, its 3D structure shows this signal, allowing FABP4 to deliver ligands from the cytosol to different receptors, such as PPARγ in the nucleus[233]. Our results showed that the significant peak intensities were found in the lipid-protein profiles in the region of 2800–3000 cm^{-1}. The main challenge in the interpretation of the Raman bands in the region of 2800–3000 cm^{-1} is due to the fact that the spectral region of the bands of FA and lipids overlap with the bands of proteins. The main protein band near 2940 cm^{-1} attributed to aromatic and aliphatic amino acids and many other amino acids overlaps with the known C-H bands of FA[113,234] attributed to a myriad of CH, CH_2, and CH_3 groups in the side chains. Thus, we performed the analysis of specific Raman peaks associated with lipids in the literature (3009 cm^{-1} [167], 1659 cm^{-1}, 1441 cm^{-1}, and 1303 cm^{-1} [168]). Our results showed a non-significant trend to decrease the peak intensity of the band at 3009 cm-1 (from FA) in the profile of the cells treated with FABP4 at 10 ng/mL in comparison with control cells.

The OPLS-DA analysis of the cytoplasm spectra did not show statistical differences among cells regarding FABP4 treatment. However, our results showed a trend to increase the peak intensities of lipid-associated bands in cells treated with FABP4 at 100 ng/mL. It has been demonstrated that exogenous FABP4 effects can differ according to its binding to FA. In macrophages and in human coronary artery smooth muscle and endothelial cells, treatment with FABP4 significantly increased the gene expression of inflammatory markers, such as MCP1, IL-6, TNFα, only under palmitic acid presence. On the other side, FABP4 ligand-independent effects included a dose-dependent increment in the proliferation of human coronary artery smooth muscle cells and a reduction in endothelial nitric oxide synthase activation[235]. Further studies will be necessary to achieve a complete assignment of the Raman bands, which should include treatment in the presence/absence of FA (such as palmitic acid), to better discern if the effects of FABP4 in CMs are ligand-dependent or independent.

USC UNIVERSIDADE DE SANTIAGO DE COMPOSTELA

Besides, this molecule has the ability to interact with itself to potentially form oligomeric structures[233], which could relate its differential behaviour to its concentration and/or ligand dependency. To advance this assignment, further studies comparing Raman spectral images corresponding to the selected Raman bands identified in the OPLS-DA loadings with the immunostaining of FABP4 would shed light on its intracellular localization. Besides, the results obtained from these procedures would help to show relevant biomolecules associated with FABP4 directly from hiPSC-derived atrial CMs. This label-free, non-invasive analytical technique can be further developed to aid in the identification of the effects of FABP4 in hiPSC differentiation to CMs. The ability to noninvasively monitor time-dependent molecular changes in hiPSC treated with FABP4 during the differentiation to atrial CMs may have a huge beneficial impact on this study.

Currently, it does not exist non-invasive plasma predictors of AF recurrence after radiofrequency ablation or cardiac surgery. The results obtained from our experiments would help us to increase our knowledge about the mechanistic relating CMs dysfunction in AF through EAT activity. Since we already demonstrated that EAT SVF cells modified its endocrine activity, lipid accumulation and Ca^{2+} mobilization in response to ACh, our future perspectives aim to elucidate the specific effects of FABP4, on cardiomyocyte intracellular composition and electrophysiological functioning. Finding the molecular mechanisms responsible of contractile dysfunction and arrhythmogenesis, through EAT, will help us in the stratification of patients and the development of therapeutic targets that will improve AF prognosis and/or efficient diagnosis. Knowing that FABP4 acts hormonally provides the opportunity to target FABP4 as a therapeutic approach. Some of the different approaches targeting this lipid chaperone, such as constitutive genetic deletion, temporal genetic manipulation, small-molecule inhibitors, or neutralizing antibodies; has already showed remarkable consistency in the improvement of metabolic features. The specific FABP4 inhibitor, BMS309403, inhibits lipid binding and reduce the activity of FABP4 both intracellularly and presumably in circulation[236]. The ligand dependency of FABP4 on the effect in CMs behaviour requires further clarification

USC UNIVERSIDADE DE SANTIAGO DE COMPOSTELA

in order to select the best approach to target this molecule in the context of AF.

Due to SARS-CoV-2 outbreak last year, our group wanted to collaborate in the knowledge about the behaviour of the virus, which could be useful in patient's treatments and in the prevention of possible cardiovascular consequences generated by this disease. To this end, we studied the expression of one of its main receptors, angiotensin-converting enzyme 2 (ACE2), and the main enzyme responsible for its cleavage, A disintegrin and metalloprotease 17 (ADAM17), in EAT. Then, we compared both gene expressions according to different cardiovascular pathologies.

We observed a higher gene expression of both molecules in EAT compared to SAT SVF cells. In addition, our results showed that, after evaluating the main risk factors associated with COVID-19 in CVD patients, the main contributor to the up-regulation of ACE2 levels in EAT was T2DM. Within these patients, those who presented obesity showed the highest levels. Therefore, both factors, diabetes, and obesity, could be contributing to the increased risk of contracting the disease through the higher expression of ACE2 in EAT.

USC
UNIVERSIDADE DE SANTIAGO DE COMPOSTELA

USC
UNIVERSIDADE
DE SANTIAGO
DE COMPOSTELA

6 CONCLUSIONS

The results obtained from the procedures carried out during this doctoral thesis have allowed us to reach the following conclusions:

1. The secretory activity of vEAT and aEAT is very similar, and both can be used as preclinical models to study their relationship with AF.

2. EAT stromal cells express muscarinic receptors, being subtype 3 the one that is modified and increases with adipogenesis.

3. The presence of inflammatory molecules in EAT and its regulation by ACh could indicate its participation in postoperative AF.

4. Long-term cholinergic imbalance could favour lipid accumulation in epicardial stroma and, consequently, it would increase FABP4.

5. FABP4 levels affect differentiation and calcium mobilization of hiPSC-derived atrial cardiomyocytes.

6. EAT stromal cells express higher levels of ACE2 compared to those of SAT, increasing in the presence of obesity and T2DM in CVD patients. Both could be risk factors for SARS-CoV-2 infection susceptibility.

.

USC
UNIVERSIDADE DE SANTIAGO DE COMPOSTELA

USC
UNIVERSIDADE
DE SANTIAGO
DE COMPOSTELA

7 REFERENCES

1. Timmis A, Townsend N, Gale CP, et al. European society of cardiology: Cardiovascular disease statistics 2019. *Eur Heart J*. 2020;41(1):12-85. doi:10.1093/eurheartj/ehz859

2. INEbase / Sociedad /Salud /Estadística de defunciones según la causa de muerte / Últimos datos. https://www.ine.es/dyngs/INEbase/es/operacion.htm?c=Estadistica_C&cid=1254736176780&menu=ultiDatos&idp=1254735573175. Accessed May 16, 2022.

3. Paulk EA. Clinical disorders of the heart beat. *Am J Cardiol*. 1972;30(6):707. doi:10.1016/0002-9149(72)90620-0

4. Gavaghan M. Cardiac anatomy and physiology: a review. *AORN J*. 1998;67(4):800. doi:10.1016/S0001-2092(06)62644-6

5. Gordan R, Gwathmey JK, Xie L-H. Autonomic and endocrine control of cardiovascular function. *World J Cardiol*. 2015;7(4):204. doi:10.4330/WJC.V7.I4.204

6. Escudero-Martínez I, Morales-Caba L, Segura T. Atrial fibrillation and stroke: A review and new insights. *Trends Cardiovasc Med*. December 2021. doi:10.1016/J.TCM.2021.12.001

7. Mulder BA, Rienstra M, Van Gelder IC, Blaauw Y. Update on management of atrial fibrillation in heart failure: a focus on ablation. *Heart*. 2021;0:1-7. doi:10.1136/HEARTJNL-2020-318081

8. Dai H, Zhang Q, Much AA, et al. Global, regional, and national prevalence, incidence, mortality, and risk factors for atrial fibrillation, 1990–2017: results from the Global Burden of Disease Study 2017. *Eur Hear J - Qual Care Clin Outcomes*. 2021;7(6):574-582. doi:10.1093/EHJQCCO/QCAA061

9. Dobrev D, Aguilar M, Heijman J, Guichard JB, Nattel S.

USC UNIVERSIDADE DE SANTIAGO DE COMPOSTELA

Postoperative atrial fibrillation: mechanisms, manifestations and management. *Nat Rev Cardiol*. 2019;16(7):417-436. doi:10.1038/s41569-019-0166-5

10. Arbelo E, Bax JJ, Blomström m-Lundqvist C, et al. 2020 ESC Guidelines for the diagnosis and management of atrial fibrillation developed in collaboration with the European Association of Cardio-Thoracic Surgery (EACTS) ESC Committee for Practice Guidelines (CPG) and National Cardiac Societies document reviewers, and Author/Task Force Member affiliations: listed in the Appendix. doi:10.1093/eurheartj/ehaa612

11. Timmis A, Townsend N, Gale CP, et al. European Society of Cardiology: Cardiovascular Disease Statistics 2019. *Eur Heart J*. 2020;41(1):12-85. doi:10.1093/EURHEARTJ/EHZ859

12. Nanda A, Kabra R. Racial Differences in Atrial Fibrillation Epidemiology, Management, and Outcomes. *Curr Treat Options Cardiovasc Med*. 2019;21(12):1-11. doi:10.1007/s11936-019-0793-5

13. Rodriguez CJ, Soliman EZ, Alonso A, et al. Atrial fibrillation incidence and risk factors in relation to race-ethnicity and the population attributable fraction of atrial fibrillation risk factors: The Multi-Ethnic Study of Atherosclerosis. *Ann Epidemiol*. 2015;25(2):71-76.e1. doi:10.1016/j.annepidem.2014.11.024

14. Heckbert SR, Austin TR, Jensen PN, et al. Differences by Race/Ethnicity in the Prevalence of Clinically Detected and Monitor-Detected Atrial Fibrillation: MESA. *Circ Arrhythm Electrophysiol*. 2020;13(1):e007698. doi:10.1161/CIRCEP.119.007698

15. Blum S, Meyre P, Aeschbacher S, et al. Incidence and predictors of atrial fibrillation progression: A systematic review and meta-analysis. *Hear Rhythm*. 2019;16(4):502-510. doi:10.1016/j.hrthm.2018.10.022

USC
UNIVERSIDADE DE SANTIAGO DE COMPOSTELA

16. Watanabe I. Smoking and risk of atrial fibrillation. *J Cardiol*. 2018;71(2):111-112. doi:10.1016/j.jjcc.2017.08.001

17. Voskoboinik A, Kalman JM, De Silva A, et al. Alcohol Abstinence in Drinkers with Atrial Fibrillation. *N Engl J Med*. 2020;382(1):20-28. doi:10.1056/NEJMoa1817591

18. Valenzuela PL, Santos-Lozano A, Morales JS, et al. Physical activity, sports and risk of atrial fibrillation: umbrella review of meta-analyses. *Eur J Prev Cardiol*. May 2020:204748732092318. doi:10.1177/2047487320923183

19. Lozano-Velasco E, Franco D, Aranega A, Daimi H. Genetics and Epigenetics of Atrial Fibrillation. *Int J Mol Sci*. 2020;21(16). doi:10.3390/ijms21165717

20. Herraiz-Martínez A, Llach A, Tarifa C, et al. The 4q25 variant rs13143308T links risk of atrial fibrillation to defective calcium homoeostasis. *Cardiovasc Res*. 2019;115(3):578-589. doi:10.1093/cvr/cvy215

21. Verdecchia P, Angeli F, Reboldi G. Hypertension and atrial fibrillation: Doubts and certainties from basic and clinical studies. *Circ Res*. 2018;122(2):352-368. doi:10.1161/CIRCRESAHA.117.311402

22. Gumprecht J, Domek M, Lip GYH, Shantsila A. Invited review: hypertension and atrial fibrillation: epidemiology, pathophysiology, and implications for management. *J Hum Hypertens*. 2019;33(12):824-836. doi:10.1038/s41371-019-0279-7

23. Soliman EZ, Rahman AF, Zhang Z, et al. Effect of Intensive Blood Pressure Lowering on the Risk of Atrial Fibrillation. *Hypertension*. 2020;75(6):1491-1496. doi:10.1161/HYPERTENSIONAHA.120.14766

24. Sharashova E, Wilsgaard T, Ball J, et al. Long-term blood pressure trajectories and incident atrial fibrillation in women and men: the Tromsø Study. doi:10.1093/eurheartj/ehz374

USC UNIVERSIDADE DE SANTIAGO DE COMPOSTELA

25. Zathar Z, Karunatilleke A, Fawzy AM, Lip GYH. Atrial Fibrillation in Older People: Concepts and Controversies. *Front Med*. 2019;6:175. doi:10.3389/fmed.2019.00175

26. Laredo M, Waldmann V, Khairy P, Nattel S. Age as a Critical Determinant of Atrial Fibrillation: A Two-sided Relationship. *Can J Cardiol*. 2018;34(11):1396-1406. doi:10.1016/j.cjca.2018.08.007

27. BUNCH TJ, MAY HT, BAIR TL, et al. The Impact of Age on 5-Year Outcomes After Atrial Fibrillation Catheter Ablation. *J Cardiovasc Electrophysiol*. 2016;27(2):141-146. doi:10.1111/jce.12849

28. Aune D, Feng T, Schlesinger S, Janszky I, Norat T, Riboli E. Diabetes mellitus, blood glucose and the risk of atrial fibrillation: A systematic review and meta-analysis of cohort studies. *J Diabetes Complications*. 2018;32(5):501-511. doi:10.1016/j.jdiacomp.2018.02.004

29. Kim YG, Han K Do, Choi J Il, et al. The impact of body weight and diabetes on new-onset atrial fibrillation: a nationwide population based study. *Cardiovasc Diabetol*. 2019;18(1):128. doi:10.1186/s12933-019-0932-z

30. Shantha G, Pelosi F, Morady F. Relationship between obstructive sleep apnoea and AF. *Arrhythmia Electrophysiol Rev*. 2019;8(3):180-183. doi:10.15420/aer.2019.35.2

31. Takagi T, Nakamura K, Hashimoto H, et al. The impact of sleep apnea on right atrial structural remodeling with atrial fibrillation. *J Cardiol*. 2020;75(6):665-672. doi:10.1016/j.jjcc.2019.12.012

32. Lux JC, Channaveerappa D, Aslebagh R, et al. Identification of dysregulation of atrial proteins in rats with chronic obstructive apnea using two-dimensional polyacrylamide gel electrophoresis and mass spectrometry. *J Cell Mol Med*. 2019;23(4):3016-3020. doi:10.1111/jcmm.14131

33. Huxley RR, Lopez FL, Folsom AR, et al. Absolute and

USC UNIVERSIDADE DE SANTIAGO DE COMPOSTELA

attributable risks of atrial fibrillation in relation to optimal and borderline risk factors: The atherosclerosis risk in communities (ARIC) study. *Circulation*. 2011;123(14):1501-1508. doi:10.1161/CIRCULATIONAHA.110.009035

34. Feng T, Vegard M, Strand LB, et al. Weight and weight change and risk of atrial fibrillation: the HUNT study. *Eur Heart J*. 2019;40(34):2859-2866. doi:10.1093/eurheartj/ehz390

35. Rodríguez A, Becerril S, Hernández-Pardos AW, Frühbeck G. Adipose tissue depot differences in adipokines and effects on skeletal and cardiac muscle. *Curr Opin Pharmacol*. 2020;52:1-8. doi:10.1016/J.COPH.2020.04.003

36. Herter CA. AN EXPERIMENTAL STUDY OF FAT STARVATION WITH ESPECIAL REFERENCE TO THE PRODUCTION OF SEROUS ATROPHY OF FAT. *J Exp Med*. 1898;3(3):293-314. doi:10.1084/JEM.3.3.293

37. Iacobellis G, Ribaudo MC, Assael F, et al. Echocardiographic epicardial adipose tissue is related to anthropometric and clinical parameters of metabolic syndrome: a new indicator of cardiovascular risk. *J Clin Endocrinol Metab*. 2003;88(11):5163-5168. doi:10.1210/JC.2003-030698

38. Iacobellis G, Ribaudo MC, Zappaterreno A, Iannucci CV, Leonetti F. Relation between epicardial adipose tissue and left ventricular mass. *Am J Cardiol*. 2004;94(8):1084-1087. doi:10.1016/J.AMJCARD.2004.06.075

39. Iacobellis G, Corradi D, Sharma AM. Epicardial adipose tissue: Anatomic, biomolecular and clinical relationships with the heart. *Nat Clin Pract Cardiovasc Med*. 2005;2(10):536-543. doi:10.1038/NCPCARDIO0319

40. Iacobellis G, Leonetti F. Epicardial adipose tissue and insulin resistance in obese subjects. *J Clin Endocrinol Metab*. 2005;90(11):6300-6302. doi:10.1210/JC.2005-1087

41. Iacobellis G. Imaging of visceral adipose tissue: an emerging

USC UNIVERSIDADE DE SANTIAGO DE COMPOSTELA

diagnostic tool and therapeutic target. *Curr Drug Targets Cardiovasc Haematol Disord*. 2005;5(4):345-353. doi:10.2174/1568006054553408

42. Iacobellis G, ed. *Epicardial Adipose Tissue*. Cham: Springer International Publishing; 2020. doi:10.1007/978-3-030-40570-0

43. Iacobellis G. Epicardial and Pericardial Fat: Close, but Very Different. *Obesity*. 2009;17(4):625-625. doi:10.1038/OBY.2008.575

44. Talman AH, Psaltis PJ, Cameron JD, Meredith IT, Seneviratne SK, Wong DTL. Epicardial adipose tissue: far more than a fat depot. *Cardiovasc Diagn Ther*. 2014;4(6):416-429. doi:10.3978/j.issn.2223-3652.2014.11.05

45. Ramakrishnan VM, Boyd NL. The Adipose Stromal Vascular Fraction as a Complex Cellular Source for Tissue Engineering Applications. *Tissue Eng - Part B Rev*. 2018;24(4):289-299. doi:10.1089/ten.teb.2017.0061

46. Iacobellis G, Assael F, Ribaudo MC, et al. Epicardial Fat from Echocardiography: A New Method for Visceral Adipose Tissue Prediction. *Obes Res*. 2003;11(2):304-310. doi:10.1038/OBY.2003.45

47. Singh N, Singh H, Khanijoun HK, Iacobellis G. Echocardiographic Assessment of Epicardial Adipose Tissue - A Marker of Visceral Adiposity. *McGill J Med MJM*. 2007;10(1):26. doi:10.26443/mjm.v10i1.469

48. Meenakshi K, Rajendran M, Srikumar S, Chidambaram S. Epicardial fat thickness: A surrogate marker of coronary artery disease – Assessment by echocardiography. *Indian Heart J*. 2016;68(3):336-341. doi:10.1016/J.IHJ.2015.08.005

49. Marwan M, Achenbach S. Quantification of epicardial fat by computed tomography: why, when and how? *J Cardiovasc Comput Tomogr*. 2013;7(1):3-10. doi:10.1016/J.JCCT.2013.01.002

USC
UNIVERSIDADE DE SANTIAGO DE COMPOSTELA

50. Flüchter S, Haghi D, Dinter D, et al. Volumetric assessment of epicardial adipose tissue with cardiovascular magnetic resonance imaging. *Obesity (Silver Spring)*. 2007;15(4):870-878. doi:10.1038/OBY.2007.591

51. Rabkin SW. Epicardial fat: properties, function and relationship to obesity. *Obes Rev*. 2007;8(3):253-261. doi:10.1111/J.1467-789X.2006.00293.X

52. Prati F, Arbustinib E, Labellarte A, et al. Eccentric atherosclerotic plaques with positive remodelling have a pericardial distribution: a permissive role of epicardial fat? A three-dimensional intravascular ultrasound study of left anterior descending artery lesions. *Eur Heart J*. 2003;24(4):329-336. doi:10.1016/S0195-668X(02)00426-8

53. Kolwicz SC, Purohit S, Tian R. Characteristics of Fuel Metabolism in the Heart Capacity and Flexibility of Substrate Metabolism for ATP Production Cardiac Metabolism and its Interactions With Contraction, Growth, and Survival of Cardiomyocytes. 2013. doi:10.1161/CIRCRESAHA.113.302095

54. Opie LH. Cardiac metabolism--emergence, decline, and resurgence. Part II. *Cardiovasc Res*. 1992;26(9):817-830. http://www.ncbi.nlm.nih.gov/pubmed/1451158. Accessed November 23, 2018.

55. Iacobellis G. Local and systemic effects of the multifaceted epicardial adipose tissue depot. *Nat Rev Endocrinol*. 2015;11(6):363-371. doi:10.1038/nrendo.2015.58

56. Marchington JM, Mattacks CA, Pond CM. Adipose tissue in the mammalian heart and pericardium: structure, foetal development and biochemical properties. *Comp Biochem Physiol B*. 1989;94(2):225-232. doi:10.1016/0305-0491(89)90337-4

57. Cannon B, Nedergaard J. Brown adipose tissue: function and physiological significance. *Physiol Rev*. 2004;84(1):277-359.

USC UNIVERSIDADE DE SANTIAGO DE COMPOSTELA

doi:10.1152/PHYSREV.00015.2003

58. Cypess AM, Lehman S, Williams G, et al. Identification and Importance of Brown Adipose Tissue in Adult Humans. *N Engl J Med*. 2009;360(15):1509-1517. doi:10.1056/NEJMOA0810780/SUPPL_FILE/NEJM_CYPESS_1509SA1.PDF

59. Chechi K, Voisine P, Mathieu P, et al. Functional characterization of the Ucp1-Associated oxidative phenotype of human epicardial adipose tissue. *Sci Rep*. 2017;7(1):1-15. doi:10.1038/s41598-017-15501-7

60. Sacks HS, Fain JN, Holman B, et al. Uncoupling Protein-1 and Related Messenger Ribonucleic Acids in Human Epicardial and Other Adipose Tissues: Epicardial Fat Functioning as Brown Fat. *J Clin Endocrinol Metab*. 2009;94(9):3611-3615. doi:10.1210/JC.2009-0571

61. Mazurek T, Zhang LF, Zalewski A, et al. Human Epicardial Adipose Tissue Is a Source of Inflammatory Mediators. *Circulation*. 2003;108(20):2460-2466. doi:10.1161/01.CIR.0000099542.57313.C5

62. Greenstein AS, Khavandi K, Withers SB, et al. Local inflammation and hypoxia abolish the protective anticontractile properties of perivascular fat in obese patients. *Circulation*. 2009;119(12):1661-1670. doi:10.1161/CIRCULATIONAHA.108.821181

63. Iacobellis G, Pistilli D, Gucciardo M, et al. Adiponectin expression in human epicardial adipose tissue in vivo is lower in patients with coronary artery disease. *Cytokine*. 2005;29(6):251-255. doi:10.1016/J.CYTO.2004.11.002

64. Iglesias MJ, Eiras S, Piñeiro R, et al. Gender Differences in Adiponectin and Leptin Expression in Epicardial and Subcutaneous Adipose Tissue. Findings in Patients Undergoing Cardiac Surgery. *Rev Española Cardiol (English Ed*.

USC
UNIVERSIDADE DE SANTIAGO DE COMPOSTELA

2006;59(12):1252-1260. doi:10.1016/S1885-5857(07)60081-4

65. Silaghi A, Achard V, Paulmyer-Lacroix O, et al. Expression of adrenomedullin in human epicardial adipose tissue: role of coronary status. *Am J Physiol Endocrinol Metab*. 2007;293(5). doi:10.1152/AJPENDO.00273.2007

66. Hamid SA, Baxter GF. A critical cytoprotective role of endogenous adrenomedullin in acute myocardial infarction. *J Mol Cell Cardiol*. 2006;41(2):360-363. doi:10.1016/J.YJMCC.2006.05.017

67. Prentice KJ, Saksi J, Hotamisligil GS. Adipokine FABP4 integrates energy stores and counterregulatory metabolic responses. *J Lipid Res*. 2019;60(4):734-740. doi:10.1194/JLR.S091793

68. Stern JH, Rutkowski JM, Scherer PE. Adiponectin, Leptin, and Fatty Acids in the Maintenance of Metabolic Homeostasis through Adipose Tissue Crosstalk. *Cell Metab*. 2016;23(5):770-784. doi:10.1016/J.CMET.2016.04.011

69. Fain JN, Sacks HS, Buehrer B, et al. Identification of omentin mRNA in human epicardial adipose tissue: comparison to omentin in subcutaneous, internal mammary artery periadventitial and visceral abdominal depots. *Int J Obes 2008 325*. 2008;32(5):810-815. doi:10.1038/sj.ijo.0803790

70. Fernández-Trasancos Á, Agra RM, García-Acuña JM, Fernández ÁL, González-Juanatey JR, Eiras S. Omentin treatment of epicardial fat improves its anti-inflammatory activity and paracrine benefit on smooth muscle cells. *Obesity*. 2017;25(6):1042-1049. doi:10.1002/oby.21832

71. Sawicka M, Janowska J, Chudek J. Potential beneficial effect of some adipokines positively correlated with the adipose tissue content on the cardiovascular system. *Int J Cardiol*. 2016;222:581-589. doi:10.1016/j.ijcard.2016.07.054

72. Zhang T, Yang P, Li T, Gao J, Zhang Y. Leptin Expression in

USC UNIVERSIDADE DE SANTIAGO DE COMPOSTELA

Human Epicardial Adipose Tissue Is Associated with Local Coronary Atherosclerosis. *Med Sci Monit*. 2019;25:9913. doi:10.12659/MSM.918390

73. Venteclef N, Guglielmi V, Balse E, et al. Human epicardial adipose tissue induces fibrosis of the atrial myocardium through the secretion of adipo-fibrokines. *Eur Heart J*. 2015;36(13):795-805. doi:10.1093/eurheartj/eht099

74. Wang Q, Min J, Jia L, et al. Human Epicardial Adipose Tissue Activin A Expression Predicts Occurrence of Postoperative Atrial Fibrillation in Patients Receiving Cardiac Surgery. *Heart Lung and Circulation*. 2018.

75. Linz D, Elliott AD, Hohl M, et al. Role of autonomic nervous system in atrial fibrillation. *Int J Cardiol*. 2019;287:181-188. doi:10.1016/j.ijcard.2018.11.091

76. Grant AO. Cardiac ion channels. *Circ Arrhythmia Electrophysiol*. 2009;2(2):185-194. doi:10.1161/CIRCEP.108.789081

77. Bosch RF, Zeng X, Grammer JB, Popovic K, Mewis C, Kühlkamp V. Ionic mechanisms of electrical remodeling in human atrial fibrillation. *Cardiovasc Res*. 1999;44(1):121-131. doi:10.1016/S0008-6363(99)00178-9

78. Molina CE, Abu-Taha IH, Wang Q, et al. Profibrotic, Electrical, and Calcium-Handling Remodeling of the Atria in Heart Failure Patients With and Without Atrial Fibrillation. *Front Physiol*. 2018;9(OCT):1383. doi:10.3389/fphys.2018.01383

79. Dobrev D, Wettwer E, Kortner A, Knaut M, Schüler S, Ravens U. Human inward rectifier potassium channels in chronic and postoperative atrial fibrillation. *Cardiovasc Res*. 2002;54(2):397-404. doi:10.1016/S0008-6363(01)00555-7

80. Schmidt C, Wiedmann F, Voigt N, et al. Upregulation of K2P 3.1 K + Current Causes Action Potential Shortening in Patients with Chronic Atrial Fibrillation. *Circulation*. 2015;132(2):82-

USC UNIVERSIDADE DE SANTIAGO DE COMPOSTELA

92. doi:10.1161/CIRCULATIONAHA.114.012657

81. Caballero R, de la Fuente MG, Gómez R, et al. In humans, chronic atrial fibrillation decreases the transient outward current and ultrarapid component of the delayed rectifier current differentially on each atria and increases the slow component of the delayed rectifier current in both. *J Am Coll Cardiol*. 2010;55(21):2346-2354. doi:10.1016/J.JACC.2010.02.028

82. Eisner DA, Caldwell JL, Kistamás K, Trafford AW. Calcium and Excitation-Contraction Coupling in the Heart. *Circ Res*. 2017;121(2):181-195. doi:10.1161/CIRCRESAHA.117.310230

83. Calderón JC, Bolaños P, Caputo C. The excitation-contraction coupling mechanism in skeletal muscle. *Biophys Rev*. 2014;6(1):133-160. doi:10.1007/S12551-013-0135-X

84. Alsina KM, Hulsurkar M, Brandenburg S, et al. Loss of Protein Phosphatase 1 Regulatory Subunit PPP1R3A Promotes Atrial Fibrillation. *Circulation*. 2019;140(8):681-693. doi:10.1161/CIRCULATIONAHA.119.039642

85. Dobrev D, Wehrens XHT. Calcium-mediated cellular triggered activity in atrial fibrillation. *J Physiol*. 2017;595(12):4001. doi:10.1113/JP273048

86. Voigt N, Heijman J, Wang Q, et al. Cellular and molecular mechanisms of atrial arrhythmogenesis in patients with paroxysmal atrial fibrillation. *Circulation*. 2014;129(2):145-156. doi:10.1161/CIRCULATIONAHA.113.006641

87. Voigt N, Li N, Wang Q, et al. Enhanced sarcoplasmic reticulum Ca2+ leak and increased Na+-Ca2+ exchanger function underlie delayed afterdepolarizations in patients with chronic atrial fibrillation. *Circulation*. 2012;125(17):2059-2070. doi:10.1161/CIRCULATIONAHA.111.067306

88. Zimmermann M, Kalusche D. Fluctuation in autonomic tone is a major determinant of sustained atrial arrhythmias in patients with focal ectopy originating from the pulmonary veins. *J Cardiovasc*

USC UNIVERSIDADE DE SANTIAGO DE COMPOSTELA

Electrophysiol. 2001;12(3):285-291. doi:10.1046/J.1540-8167.2001.00285.X

89. Yin L, Zahradnikova A, Rizzetto R, et al. Impaired Binding to Junctophilin-2 and Nanostructural Alteration in CPVT Mutation. *Circ Res*. 2021:35-52. doi:10.1161/CIRCRESAHA.121.319094

90. Chaichi A, Prasad A, Ranjan Gartia M. Raman Spectroscopy and Microscopy Applications in Cardiovascular Diseases: From Molecules to Organs. *Biosens 2018, Vol 8, Page 107*. 2018;8(4):107. doi:10.3390/BIOS8040107

91. Rueden CT, Schindelin J, Hiner MC, et al. ImageJ2: ImageJ for the next generation of scientific image data. *BMC Bioinformatics*. 2017;18(1):529. doi:10.1186/s12859-017-1934-z

92. Navarro-García JA, Delgado C, Fernández-Velasco M, et al. Fibroblast growth factor-23 promotes rhythm alterations and contractile dysfunction in adult ventricular cardiomyocytes. *Nephrol Dial Transplant*. 2019;34(11):1864-1875. doi:10.1093/NDT/GFY392

93. Lopez-Canoa JN, Baluja A, Couselo-Seijas M, et al. Plasma FABP4 levels are associated with left atrial fat volume in persistent atrial fibrillation and predict recurrence after catheter ablation. *Int J Cardiol*. 2019;292:131-135. doi:10.1016/j.ijcard.2019.04.031

94. Lamounier-Zepter V, Look C, Alvarez J, et al. Adipocyte fatty acid-binding protein suppresses cardiomyocyte contraction: A new link between obesity and heart disease. *Circ Res*. 2009;105(4):326-334. doi:10.1161/CIRCRESAHA.109.200501

95. Matthews Q, Jirasek A, Lum J, Duan X, Brolo AG. Variability in Raman Spectra of Single Human Tumor Cells Cultured in Vitro: Correlation with Cell Cycle and Culture Confluency.

96. Ichimura T, Chiu L Da, Fujita K, et al. Non-label immune cell state prediction using Raman spectroscopy. *Sci Reports 2016 61*.

USC UNIVERSIDADE DE SANTIAGO DE COMPOSTELA

2016;6(1):1-7. doi:10.1038/srep37562

97. Hsu CC, Xu J, Brinkhof B, et al. A single-cell Raman-based platform to identify developmental stages of human pluripotent stem cell-derived neurons. *Proc Natl Acad Sci U S A*. 2020;117(31):18412-18423. doi:10.1073/PNAS.2001906117/-/DCSUPPLEMENTAL

98. De Gelder J, De Gussem K, Vandenabeele P, Moens L. Reference database of Raman spectra of biological molecules. *J Raman Spectrosc*. 2007;38(9):1133-1147. doi:10.1002/JRS.1734

99. Wiercigroch E, Szafraniec E, Czamara K, et al. Raman and infrared spectroscopy of carbohydrates: A review. *Spectrochim Acta Part A Mol Biomol Spectrosc*. 2017;185:317-335. doi:10.1016/J.SAA.2017.05.045

100. Talari ACS, Movasaghi Z, Rehman S, Rehman IU. Raman Spectroscopy of Biological Tissues. *http://dx.doi.org/101080/057049282014923902*. 2014;50(1):46-111. doi:10.1080/05704928.2014.923902

101. Essendoubi M, Gobinet C, Reynaud R, Angiboust JF, Manfait M, Piot O. Human skin penetration of hyaluronic acid of different molecular weights as probed by Raman spectroscopy. *Skin Res Technol*. 2016;22(1):55-62. doi:10.1111/SRT.12228

102. Czamara K, Majzner K, Pacia MZ, Kochan K, Kaczor A, Baranska M. Raman spectroscopy of lipids: a review. *J Raman Spectrosc*. 2015;46(1):4-20. doi:10.1002/JRS.4607

103. Morawski M, Brückner G, Arendt T, Matthews RT. Aggrecan: Beyond cartilage and into the brain. *Int J Biochem Cell Biol*. 2012;44(5):690-693. doi:10.1016/J.BIOCEL.2012.01.010

104. Cˆıntcˆınt ˇ S, Pˆınzaru P, Andronie LM, Domsa I, Cozar O, Astilean S. Rapid Communication Bridging biomolecules with nanoparticles: surface-enhanced Raman scattering from colon carcinoma and normal tissue. *J RAMAN Spectrosc J Raman*

USC UNIVERSIDADE DE SANTIAGO DE COMPOSTELA

Spectrosc. 2008;39:331-334. doi:10.1002/jrs.1907

105. Shende C, Shende CA, Farquharson S, Inscore FE, Maksymiuk P, Gift A. Analysis of 5-fluorouracil in saliva using surface-enhanced Raman spectroscopy Cite this paper Related papers Surface-enhanced Raman Spect ral Measurement s of 5Fluorouracil in Saliva Analysis of 5-fluorouracil in saliva using surface-enhanced Raman spectroscopy. *J Raman Spectrosc*. 2005;36:208-212. doi:10.1002/jrs.1277

106. Schulz H, Baranska M. Identification and quantification of valuable plant substances by IR and Raman spectroscopy. *Vib Spectrosc*. 2007;43(1):13-25. doi:10.1016/J.VIBSPEC.2006.06.001

107. Wu H, Volponi J V., Oliver AE, Parikh AN, Simmons BA, Singh S. In vivo lipidomics using single-cell Raman spectroscopy. *Proc Natl Acad Sci U S A*. 2011;108(9):3809-3814. doi:10.1073/PNAS.1009043108/-/DCSUPPLEMENTAL

108. Binoy J, Abraham JP, Joe IH, Jayakumar VS, Pettit GR, Nielsen OF. NIR-FT Raman and FT-IR spectral studies and ab initio calculations of the anti-cancer drug combretastatin-A4. *J Raman Spectrosc*. 2004;35(11):939-946. doi:10.1002/JRS.1236

109. Pascut FC, Goh HT, Welch N, Buttery LD, Denning C, Notingher I. Noninvasive Detection and Imaging of Molecular Markers in Live Cardiomyocytes Derived from Human Embryonic Stem Cells. *Biophys J*. 2011;100(1):251. doi:10.1016/J.BPJ.2010.11.043

110. Stone N, Kendall C, Shepherd N, Crow P, Barr H. Near-infrared Raman spectroscopy for the classification of epithelial pre-cancers and cancers. *J Raman Spectrosc*. 2002;33(7):564-573. doi:10.1002/JRS.882

111. Stone N, Kendall C, Smith J, Crow P, Barr H. Raman spectroscopy for identification of epithelial cancers. *Faraday Discuss*. 2004;126(1):141-157. doi:10.1039/B304992B

USC
UNIVERSIDADE DE SANTIAGO DE COMPOSTELA

112. Cheng WT, Liu MT, Liu HN, Lin SY. Micro-Raman spectroscopy used to identify and grade human skin pilomatrixoma. *Microsc Res Tech*. 2005;68(2):75-79. doi:10.1002/JEMT.20229

113. Shetty G, Kendall C, Shepherd N, Stone N, Barr H. Raman spectroscopy: elucidation of biochemical changes in carcinogenesis of oesophagus. *Br J Cancer*. 2006;94(10):1460-1464. doi:10.1038/SJ.BJC.6603102

114. Krafft C, Neudert L, Simat T, Salzer R. Near infrared Raman spectra of human brain lipids. *Spectrochim Acta A Mol Biomol Spectrosc*. 2005;61(7):1529-1535. doi:10.1016/J.SAA.2004.11.017

115. Ellis R, Green E, Winlove CP. Structural analysis of glycosaminoglycans and proteoglycans by means of Raman microspectrometry. *Connect Tissue Res*. 2009;50(1):29-36. doi:10.1080/03008200802398422

116. De Miranda Marzullo AC, Neto OP, Bitar RA, Da Silva Martinho H, Martin AA. FT-Raman Spectra of the Border of Infiltrating Ductal Carcinoma Lesions. *https://home.liebertpub.com/pho*. 2007;25(5):455-460. doi:10.1089/PHO.2007.2094

117. Kast RE, Serhatkulu GK, Cao A, et al. Raman spectroscopy can differentiate malignant tumors from normal breast tissue and detect early neoplastic changes in a mouse model. *Biopolymers*. 2008;89(3):235-241. doi:10.1002/BIP.20899

118. Syed A, Smith EA. Raman Imaging in Cell Membranes, Lipid-Rich Organelles, and Lipid Bilayers. *Annu Rev Anal Chem (Palo Alto Calif)*. 2017;10(1):271-291. doi:10.1146/ANNUREV-ANCHEM-061516-045317

119. Cipriani P, Smith CY. Characterization of Thalidomide using Raman Spectroscopy. *Spectrochim Acta Part A Mol Biomol Spectrosc*. 2008;69(2):333-337.

USC UNIVERSIDADE DE SANTIAGO DE COMPOSTELA

doi:10.1016/J.SAA.2007.04.002

120. Jess PRT, Smith DDW, Mazilu M, Dholakia K, Riches AC, Herrington CS. Early detection of cervical neoplasia by Raman spectroscopy. *Int J cancer*. 2007;121(12):2723-2728. doi:10.1002/IJC.23046

121. Deng JL, Wei Q, Zhang MH, Wang YZ, Li YQ. Study of the effect of alcohol on single human red blood cells using near-infrared laser tweezers Raman spectroscopy. *J Raman Spectrosc*. 2005;36(3):257-261. doi:10.1002/JRS.1301

122. Chan JW, Taylor DS, Zwerdling T, Lane SM, Ihara K, Huser T. Micro-Raman spectroscopy detects individual neoplastic and normal hematopoietic cells. *Biophys J*. 2006;90(2):648-656. doi:10.1529/BIOPHYSJ.105.066761

123. Frank CJ, McCreary RL, Redd DCB. Raman Spectroscopy of Normal and Diseased Human Breast Tissues. *Anal Chem*. 2002;67(5):777-783. doi:10.1021/AC00101A001

124. Ruiz-Chica AJ, Medina MA, Sánchez-Jiménez F, Ramírez FJ. Characterization by Raman spectroscopy of conformational changes on guanine–cytosine and adenine–thymine oligonucleotides induced by aminooxy analogues of spermidine. *J Raman Spectrosc*. 2004;35(2):93-100. doi:10.1002/JRS.1107

125. Takanezawa S, Morita SI, Ozaki Y, Sako Y. Raman spectral dynamics of single cells in the early stages of growth factor stimulation. *Biophys J*. 2015;108(9):2148-2157. doi:10.1016/J.BPJ.2015.03.037

126. Krishna CM, Prathima NB, Malini R, et al. Raman spectroscopy studies for diagnosis of cancers in human uterine cervix. *Vib Spectrosc*. 2006;41(1):136-141. doi:10.1016/J.VIBSPEC.2006.01.011

127. Huang Z, McWilliams A, Lui H, McLean DI, Lam S, Zeng H. Near-infrared Raman spectroscopy for optical diagnosis of lung cancer. *Int J cancer*. 2003;107(6):1047-1052.

USC UNIVERSIDADE DE SANTIAGO DE COMPOSTELA

doi:10.1002/IJC.11500

128. Naumann D. Infrared and NIR Raman spectroscopy in medical microbiology. *https://doi.org/101117/12306089*. 1998;3257:245-257. doi:10.1117/12.306089

129. Dukor RK. Vibrational Spectroscopy in the Detection of Cancer. *Handb Vib Spectrosc*. August 2006. doi:10.1002/0470027320.S8107

130. Bansil R, Yannas I V., Stanley HE. Raman Spectroscopy: A structural probe of glycosaminoglycans. *Biochim Biophys Acta - Gen Subj*. 1978;541(4):535-542. doi:10.1016/0304-4165(78)90163-0

131. Maheedhar K, Bhat RA, Malini R, et al. Diagnosis of ovarian cancer by Raman spectroscopy: a pilot study. *Photomed Laser Surg*. 2008;26(2):83-90. doi:10.1089/PHO.2007.2128

132. Lakshmi RJ, Kartha VB, Krishna CM, Solomon JGR, Ullas G, Devi PU. Tissue Raman Spectroscopy for the Study of Radiation Damage: Brain Irradiation of Mice. *https://doi.org/101667/0033-7587(2002)157[0175:TRSFTS]20CO;2*. 2002;157(2):175-182. doi:10.1667/0033-7587(2002)157

133. Sekhar PK, Ramgir NS, Bhansali S. Metal-decorated silica nano wires: An active surface-enhanced Raman substrate for cancer biomarker detection. *J Phys Chem C*. 2008;112(6):1729-1734. doi:10.1021/JP077698O/SUPPL_FILE/JP077698O-FILE002.PDF

134. Kopec M, Imiela A, Abramczyk H. Monitoring glycosylation metabolism in brain and breast cancer by Raman imaging. *Sci Reports 2019 91*. 2019;9(1):1-13. doi:10.1038/s41598-018-36622-7

135. Pichardo-Molina JL, Frausto-Reyes C, Barbosa-García O, et al. Raman spectroscopy and multivariate analysis of serum samples from breast cancer patients. *Lasers Med Sci*. 2007;22(4):229-

USC UNIVERSIDADE DE SANTIAGO DE COMPOSTELA

236. doi:10.1007/S10103-006-0432-8

136. Huang Z, Lui H, McLean DI, Korbelik M, Zeng H. Raman Spectroscopy in Combination with Background Near-infrared Autofluorescence Enhances the In Vivo Assessment of Malignant Tissues. *Photochem Photobiol*. 2005;81(5):1219-1226. doi:10.1562/2005-02-24-RA-449

137. Germond A, Panina Y, Shiga M, Niioka H, Watanabe TM. Following Embryonic Stem Cells, Their Differentiated Progeny, and Cell-State Changes during iPS Reprogramming by Raman Spectroscopy. *Anal Chem*. 2020;92(22):14915-14923. doi:10.1021/ACS.ANALCHEM.0C01800/SUPPL_FILE/AC0C01800_SI_002.XLSX

138. Teh SK, Zheng W, Ho KY, Teh M, Yeoh KG, Huang Z. Diagnostic potential of near-infrared Raman spectroscopy in the stomach: differentiating dysplasia from normal tissue. *Br J Cancer*. 2008;98(2):457-465. doi:10.1038/SJ.BJC.6604176

139. Onogi C, Motoyama M, Hamaguchi HO. High concentration trans form unsaturated lipids detected in a HeLa cell by Raman microspectroscopy. *J Raman Spectrosc*. 2008;39(5):555-556. doi:10.1002/JRS.1900

140. Lord RC, Yu N teng. Laser-excited Raman spectroscopy of biomolecules: I. Native lysozyme and its constituent amino acids. *J Mol Biol*. 1970;50(2):509-524. doi:10.1016/0022-2836(70)90208-1

141. Hu Y, Shen A, Jiang T, Ai Y, Hu J. Classification of normal and malignant human gastric mucosa tissue with confocal Raman microspectroscopy and wavelet analysis. *Spectrochim Acta Part A Mol Biomol Spectrosc*. 2008;69(2):378-382. doi:10.1016/J.SAA.2007.04.009

142. Dovbeshko GI, Gridina NY, Kruglova EB, Pashchuk OP. FTIR spectroscopy studies of nucleic acid damage. *Talanta*. 2000;53(1):233-246. doi:10.1016/S0039-9140(00)00462-8

USC
UNIVERSIDADE DE SANTIAGO DE COMPOSTELA

143. Ó Faoláin E, Hunter MB, Byrne JM, et al. A study examining the effects of tissue processing on human tissue sections using vibrational spectroscopy. *Vib Spectrosc*. 2005;38(1-2):121-127. doi:10.1016/J.VIBSPEC.2005.02.013

144. Khanmohammadi M, Nasiri R, Ghasemi K, Samani S, Bagheri Garmarudi A. Diagnosis of basal cell carcinoma by infrared spectroscopy of whole blood samples applying soft independent modeling class analogy. *J Cancer Res Clin Oncol*. 2007;133(12):1001-1010. doi:10.1007/S00432-007-0286-X

145. Yano K, Ohoshima S, Gotou Y, Kumaido K, Moriguchi T, Katayama H. Direct measurement of human lung cancerous and noncancerous tissues by fourier transform infrared microscopy: can an infrared microscope be used as a clinical tool? *Anal Biochem*. 2000;287(2):218-225. doi:10.1006/ABIO.2000.4872

146. Mahadevan-Jansen A, Richards-Kortum R. Raman spectroscopy for cancer detection: a review. *Annu Int Conf IEEE Eng Med Biol - Proc*. 1997;6:2722-2728. doi:10.1109/IEMBS.1997.756895

147. Silveira L, Sathaiah S, Zngaro RA, Pacheco MTT, Chavantes MC, Pasqualucci CAG. Correlation between near-infrared Raman spectroscopy and the histopathological analysis of atherosclerosis in human coronary arteries. *Lasers Surg Med*. 2002;30(4):290-297. doi:10.1002/LSM.10053

148. Puppels GJ, Garritsen HSP, Kummer JA, Greve J. Carotenoids located in human lymphocyte subpopulations and natural killer cells by Raman microspectroscopy. *Cytometry*. 1993;14(3):251-256. doi:10.1002/CYTO.990140303

149. Laska J, Widlarz J. Spectroscopic and structural characterization of low molecular weight fractions of polyaniline. *Polymer (Guildf)*. 2005;5(46):1485-1495. doi:10.1016/J.POLYMER.2004.12.008

150. Malini R, Venkatakrishna K, Kurien J, et al. Discrimination of normal, inflammatory, premalignant, and malignant oral tissue:

USC UNIVERSIDADE DE SANTIAGO DE COMPOSTELA

A Raman spectroscopy study. *Biopolymers*. 2006;81(3):179-193. doi:10.1002/BIP.20398

151. Takai Y, Masuko T, Takeuchi H. Lipid structure of cytotoxic granules in living human killer T lymphocytes studied by Raman microspectroscopy. *Biochim Biophys Acta*. 1997;1335(1-2):199-208. doi:10.1016/S0304-4165(96)00138-9

152. Lau DP, Huang Z, Lui H, et al. Raman spectroscopy for optical diagnosis in normal and cancerous tissue of the nasopharynx-preliminary findings. *Lasers Surg Med*. 2003;32(3):210-214. doi:10.1002/LSM.10084

153. Pudlas M, Brauchle E, Klein TJ, Hutmacher DW, Schenke-Layland K. Non-invasive identification of proteoglycans and chondrocyte differentiation state by Raman microspectroscopy. *J Biophotonics*. 2013;6(2):205-211. doi:10.1002/JBIO.201200064

154. Calheiros R, Machado NFL, Fiuza SM, et al. Antioxidant phenolic esters with potential anticancer activity: A Raman spectroscopy study. *J RAMAN Spectrosc J Raman Spectrosc*. 2008;39:95-107. doi:10.1002/jrs.1822

155. Gniadecka M, Wulf HC, Mortensen NN, Nielsen OF, Christensen DH. Diagnosis of Basal Cell Carcinoma by Raman Spectroscopy. *J RAMAN Spectrosc*. 1997;28:125-129.

156. Barr H, Dix T, Stone N. Optical spectroscopy for the early diagnosis of gastrointestinal malignancy. *Lasers Med Sci 1998 131*. 1998;13(1):3-13. doi:10.1007/BF00592955

157. Hanlon EB, Manoharan R, Koo TW, et al. Prospects for in vivo Raman spectroscopy. *Phys Med Biol*. 2000;45(2). doi:10.1088/0031-9155/45/2/201

158. Conroy J, Ryder AG, Leger MN, Hennessey K, Madden MG. Qualitative and quantitative analysis of chlorinated solvents using Raman spectroscopy and machine learning. *https://doi.org/101117/12605056*. 2005;5826:131-142.

USC UNIVERSIDADE DE SANTIAGO DE COMPOSTELA

doi:10.1117/12.605056

159. Rinia HA, Burger KNJ, Bonn M, Müller M. Quantitative label-free imaging of lipid composition and packing of individual cellular lipid droplets using multiplex CARS microscopy. *Biophys J*. 2008;95(10):4908-4914. doi:10.1529/BIOPHYSJ.108.137737/ATTACHMENT/8C4085FD-5A9A-485C-A11F-C671AB070FD2/MMC2.PDF

160. Agarwal R, Tandon P, Gupta VD. Phonon dispersion in poly(dimethylsilane). *J Organomet Chem*. 2006;13(691):2902-2908. doi:10.1016/J.JORGANCHEM.2006.02.032

161. Collard L, Sinjab F, Notingher I. Raman Spectroscopy Study of Curvature-Mediated Lipid Packing and Sorting in Single Lipid Vesicles. *Biophys J*. 2019;117(9):1589-1598. doi:10.1016/J.BPJ.2019.09.020

162. Yamamoto T, Minamikawa T, Harada Y, et al. Label-free Evaluation of Myocardial Infarct in Surgically Excised Ventricular Myocardium by Raman Spectroscopy. *Sci Reports 2018 81*. 2018;8(1):1-10. doi:10.1038/s41598-018-33025-6

163. Eriksson L, Rosén J, Johansson E, Trygg J. Orthogonal PLS (OPLS) Modeling for Improved Analysis and Interpretation in Drug Design. *Mol Inform*. 2012;31(6-7):414-419. doi:10.1002/MINF.201200158

164. Modern Methods for Business Research. *Mod Methods Bus Res*. March 1998. doi:10.4324/9781410604385/MODERN-METHODS-BUSINESS-RESEARCH

165. Blasco H, Błaszczyński J, Billaut JC, et al. Comparative analysis of targeted metabolomics: Dominance-based rough set approach versus orthogonal partial least square-discriminant analysis. *J Biomed Inform*. 2015;53:291-299. doi:10.1016/J.JBI.2014.12.001

166. Brozek-Pluska B, Jablonska-Gajewicz J, Kordek R, Abramczyk H. Phase transitions in oleic acid and in human breast tissue as

USC UNIVERSIDADE DE SANTIAGO DE COMPOSTELA

studied by raman spectroscopy and raman imaging. *J Med Chem*. 2011;54(9):3386-3392. doi:10.1021/JM200180F/ASSET/IMAGES/JM200180F.SOCIAL.JPEG_V03

167. Surmacki J, Musial J, Kordek R, Abramczyk H. Raman imaging at biological interfaces: applications in breast cancer diagnosis. *Mol Cancer*. 2013;12(1):48. doi:10.1186/1476-4598-12-48

168. FC P, HT G, V G, C D, I N. Toward label-free Raman-activated cell sorting of cardiomyocytes derived from human embryonic stem cells. *J Biomed Opt*. 2011;16(4):045002. doi:10.1117/1.3570302

169. Luther PK. The vertebrate muscle Z-disc: sarcomere anchor for structure and signalling. *J Muscle Res Cell Motil*. 2009;30(5-6):171-185. doi:10.1007/S10974-009-9189-6

170. Luo X, Li W, Künzel K, et al. IP3R-Mediated Compensatory Mechanism for Calcium Handling in Human Induced Pluripotent Stem Cell-Derived Cardiomyocytes With Cardiac Ryanodine Receptor Deficiency. *Front cell Dev Biol*. 2020;8. doi:10.3389/FCELL.2020.00772

171. Dretzke J, Chuchu N, Agarwal R, et al. Predicting recurrent atrial fibrillation after catheter ablation: a systematic review of prognostic models. *EP Eur*. 2020;22(5):748-760. doi:10.1093/EUROPACE/EUAA041

172. Alonso A, Almuwaqqat Z, Chamberlain A. Mortality in atrial fibrillation. Is it changing? *Trends Cardiovasc Med*. 2021;31(8):469-473. doi:10.1016/J.TCM.2020.10.010

173. Khan AA, Lip GYH, Shantsila A. Heart rate variability in atrial fibrillation: The balance between sympathetic and parasympathetic nervous system. *Eur J Clin Invest*. 2019;49(11). doi:10.1111/eci.13174

174. Scott L, Li N, Dobrev D. Role of inflammatory signaling in atrial fibrillation. *Int J Cardiol*. 2019;287:195-200.

USC UNIVERSIDADE DE SANTIAGO DE COMPOSTELA

doi:10.1016/j.ijcard.2018.10.020

175. Mazurek T, Kiliszek M, Kobylecka M, et al. Relation of proinflammatory activity of epicardial adipose tissue to the occurrence of atrial fibrillation. *Am J Cardiol*. 2014;113(9):1505-1508. doi:10.1016/j.amjcard.2014.02.005

176. Maeda M, Oba K, Yamaguchi S, et al. Usefulness of Epicardial Adipose Tissue Volume to Predict Recurrent Atrial Fibrillation After Radiofrequency Catheter Ablation. *Am J Cardiol*. 2018;122(10):1694-1700. doi:10.1016/j.amjcard.2018.08.005

177. Chao TF, Hung CL, Tsao HM, et al. Epicardial Adipose Tissue Thickness and Ablation Outcome of Atrial Fibrillation. *PLoS One*. 2013;8(9). doi:10.1371/journal.pone.0074926

178. Kurt M, Tanboğa İH, Aksakal E, Karakoyun S. Relation between epicardial fat tissue and atrial fibrillation. *J Clin Exp Investig*. 2012;3(1):13-17. doi:10.5799/ahinjs.01.2012.01.0103

179. Van Rosendael AR, Dimitriu-Leen AC, Van Rosendael PJ, et al. Association between posterior left atrial adipose tissue mass and atrial fibrillation. *Circ Arrhythmia Electrophysiol*. 2017;10(2). doi:10.1161/CIRCEP.116.004614

180. Batal O, Schoenhagen P, Shao M, et al. Left Atrial epicardial adiposity and Atrial fibrillation. *Circ Arrhythmia Electrophysiol*. 2010;3(3):230-236. doi:10.1161/CIRCEP.110.957241

181. Sacks HS, Fain JN, Holman B, et al. Uncoupling protein-1 and related messenger ribonucleic acids in human epicardial and other adipose tissues: epicardial fat functioning as brown fat. *J Clin Endocrinol Metab*. 2009;94(9):3611-3615. doi:10.1210/JC.2009-0571

182. Venteclef N, Guglielmi V, Balse E, et al. Human epicardial adipose tissue induces fibrosis of the atrial myocardium through the secretion of adipo-fibrokines. *Eur Heart J*. 2015;36(13):795-805. doi:10.1093/eurheartj/eht099

USC UNIVERSIDADE DE SANTIAGO DE COMPOSTELA

183. Ansaldo AM, Montecucco F, Sahebkar A, Dallegri F, Carbone F. Epicardial adipose tissue and cardiovascular diseases. *Int J Cardiol*. 2019;278:254-260. doi:10.1016/j.ijcard.2018.09.089

184. Gaborit B, Venteclef N, Ancel P, et al. Human epicardial adipose tissue has a specific transcriptomic signature depending on its anatomical peri-atrial, peri-ventricular, or peri-coronary location. *Cardiovasc Res*. 2015;108(1):62-73. doi:10.1093/cvr/cvv208

185. Viviano A, Yin X, Zampetaki A, et al. Proteomics of the epicardial fat secretome and its role in post-operative atrial fibrillation. *Europace*. 2018;20(7):1201-1208. doi:10.1093/europace/eux113

186. Schrickel JW, Fink K, Meyer R, et al. Lack of gelsolin promotes perpetuation of atrial fibrillation in the mouse heart. *J Interv Card Electrophysiol*. 2009;26(1):3-10. doi:10.1007/s10840-009-9425-4

187. Nalliah CJ, Bell JR, Raaijmakers AJA, et al. Epicardial Adipose Tissue Accumulation Confers Atrial Conduction Abnormality. *J Am Coll Cardiol*. 2020;76(10):1197-1211. doi:10.1016/j.jacc.2020.07.017

188. Feyz L, Theuns DA, Bhagwandien R, et al. Atrial fibrillation reduction by renal sympathetic denervation: 12 months' results of the AFFORD study. *Clin Res Cardiol*. 2019;108(6):634-642. doi:10.1007/s00392-018-1391-3

189. Kawasaki M, Yamada T, Furukawa Y, et al. Are cardiac sympathetic nerve activity and epicardial adipose tissue associated with atrial fibrillation recurrence after catheter ablation in patients without heart failure? *Int J Cardiol*. 2020;303:41-48. doi:10.1016/j.ijcard.2019.11.092

190. Pokushalov E, Kozlov B, Romanov A, et al. Botulinum toxin injection in epicardial fat pads can prevent recurrences of atrial fibrillation after cardiac surgery: results of a randomized pilot

USC
UNIVERSIDADE DE SANTIAGO DE COMPOSTELA

study. *J Am Coll Cardiol*. 2014;64(6):628-629. doi:10.1016/j.jacc.2014.04.062

191. Pokushalov E, Kozlov B, Romanov A, et al. Long-Term Suppression of Atrial Fibrillation by Botulinum Toxin Injection Into Epicardial Fat Pads in Patients Undergoing Cardiac Surgery: One-Year Follow-Up of a Randomized Pilot Study. *Circ Arrhythm Electrophysiol*. 2015;8(6):1334-1341. doi:10.1161/CIRCEP.115.003199

192. Romanov A, Pokushalov E, Ponomarev D, et al. Long-term suppression of atrial fibrillation by botulinum toxin injection into epicardial fat pads in patients undergoing cardiac surgery: Three-year follow-up of a randomized study. *Hear Rhythm*. 2019;16(2):172-177. doi:10.1016/j.hrthm.2018.08.019

193. Waldron NH, Cooter M, Haney JC, et al. Temporary autonomic modulation with botulinum toxin type A to reduce atrial fibrillation after cardiac surgery. *Hear Rhythm*. 2019;16(2):178-184. doi:10.1016/J.HRTHM.2018.08.021

194. Piccini JP, Ahlsson A, Dorian P, et al. Design and Rationale of a Phase 2 Study of NeurOtoxin (Botulinum Toxin Type A) for the PreVention of Post-Operative Atrial Fibrillation – The NOVA Study. *Am Heart J*. October 2021. doi:10.1016/J.AHJ.2021.10.114

195. Kruse AC, Kobilka BK, Gautam D, Sexton PM, Christopoulos A, Wess J. Muscarinic acetylcholine receptors: novel opportunities for drug development. *Nat Rev Drug Discov 2014 137*. 2014;13(7):549-560. doi:10.1038/nrd4295

196. Piovesana R, Melfi S, Fiore M, Magnaghi V, Tata AM. M2 muscarinic receptor activation inhibits cell proliferation and migration of rat adipose-mesenchymal stem cells. *J Cell Physiol*. 2018;233(7):5348-5360. doi:10.1002/jcp.26350

197. Couselo-Seijas M, López-Canoa JN, Agra-Bermejo RM, et al. Cholinergic activity regulates the secretome of epicardial

USC UNIVERSIDADE DE SANTIAGO DE COMPOSTELA

adipose tissue: Association with atrial fibrillation. *J Cell Physiol*. 2018. doi:10.1002/jcp.27723

198. Gautam D, Gavrilova O, Jeon J, et al. Beneficial metabolic effects of M3 muscarinic acetylcholine receptor deficiency. *Cell Metab*. 2006;4(5):363-375. doi:10.1016/j.cmet.2006.09.008

199. M Couselo-Seijas, JN Lopez-Canoa, AL Fernandez, L González-Melchor, LM Seoane, D Duran- Muñoz, A Rozados-Luis, JR González-Juanatey MR-MSE. Inflammatory and lipid regulation by cholinergic activity in epicardial stromal cells from patients who underwent open-heart surgery. *J Cell Mol Med*. 2020.

200. Qin K, Dong C, Wu G, Lambert NA. Inactive-state preassembly of Gq-coupled receptors and Gq heterotrimers. *Nat Chem Biol*. 2011;7(10):740. doi:10.1038/NCHEMBIO.642

201. Carroll RC, Peralta EG. The m3 muscarinic acetylcholine receptor differentially regulates calcium influx and release through modulation of monovalent cation channels. *EMBO J*. 1998;17(11):3036. doi:10.1093/EMBOJ/17.11.3036

202. Mayosi BM. Pericarditis-associated atrial fibrillation. *Heart*. 2015;101(18):1439-1440. doi:10.1136/heartjnl-2015-307917

203. Subahi A, Akintoye E, Yassin AS, et al. Impact of atrial fibrillation on patients hospitalized for acute myocarditis: Insights from a nationally-representative United States cohort. *Clin Cardiol*. 2019;42(1):26-31. doi:10.1002/clc.23088

204. Wu L, Emmens RW, van Wezenbeek J, et al. Atrial inflammation in different atrial fibrillation subtypes and its relation with clinical risk factors. *Clin Res Cardiol*. February 2020:1-11. doi:10.1007/s00392-020-01619-8

205. Lin YK, Chen YC, Chen JH, Chen SA, Chen YJ. Adipocytes modulate the electrophysiology of atrial myocytes: Implications in obesity-induced atrial fibrillation. *Basic Res Cardiol*. 2012;107(5). doi:10.1007/s00395-012-0293-1

USC
UNIVERSIDADE DE SANTIAGO DE COMPOSTELA

206. Ramakrishnan VM, Boyd NL. The Adipose Stromal Vascular Fraction as a Complex Cellular Source for Tissue Engineering Applications. *Tissue Eng Part B Rev*. 2018;24(4):289-299. doi:10.1089/ten.teb.2017.0061

207. Balamayooran G, Batra S, Balamayooran T, Cai S, Jeyaseelan S. Monocyte Chemoattractant Protein 1 Regulates Pulmonary Host Defense via Neutrophil Recruitment during Escherichia coli Infection. *Infect Immun*. 2011;79(7):2567. doi:10.1128/IAI.00067-11

208. Wang H, Yu M, Ochani M, et al. Nicotinic acetylcholine receptor α7 subunit is an essential regulator of inflammation. *Nature*. 2003;421(6921):384-388. doi:10.1038/nature01339

209. Koarai A, Traves SL, Fenwick PS, et al. Expression of muscarinic receptors by human macrophages. *Eur Respir J*. 2012;39(3):698-704. doi:10.1183/09031936.00136710

210. Lennerz C, Barman M, Tantawy M, Sopher M, Whittaker P. Colchicine for primary prevention of atrial fibrillation after open-heart surgery: Systematic review and meta-analysis. *Int J Cardiol*. 2017;249:127-137. doi:10.1016/j.ijcard.2017.08.039

211. Aldred PMR, Hollox EJ, Armour JAL. Copy number polymorphism and expression level variation of the human alpha-defensin genes DEFA1 and DEFA3. *Hum Mol Genet*. 2005;14(14):2045-2052. doi:10.1093/HMG/DDI209

212. Lehrer RI, Lu W. α-Defensins in human innate immunity. *Immunol Rev*. 2012;245(1):84-112. doi:10.1111/J.1600-065X.2011.01082.X

213. Christensen HM, Frystyk J, Faber J, et al. α-Defensins and outcome in patients with chronic heart failure. *Eur J Heart Fail*. 2012;14(4):387-394. doi:10.1093/eurjhf/hfs021

214. Maneerat Y, Prasongsukarn K, Benjathummarak S, Dechkhajorn W, Chaisri U. Increased alpha-defensin expression is associated with risk of coronary heart disease: A feasible predictive

USC UNIVERSIDADE DE SANTIAGO DE COMPOSTELA

inflammatory biomarker of coronary heart disease in hyperlipidemia patients. *Lipids Health Dis*. 2016;15(1):1-12. doi:10.1186/S12944-016-0285-5/FIGURES/4

215. Németh BC, Várkonyi T, Somogyvári F, et al. Relevance of α-defensins (HNP1-3) and defensin β-1 in diabetes. *World J Gastroenterol*. 2014;20(27):9128-9137. doi:10.3748/wjg.v20.i27.9128

216. Wehkamp J, Wang G, Kübler I, et al. The Paneth Cell α-Defensin Deficiency of Ileal Crohn's Disease Is Linked to Wnt/Tcf-4. *J Immunol*. 2007;179(5):3109-3118. doi:10.4049/jimmunol.179.5.3109

217. Attaran S, Shaw M, Bond L, Pullan MD, Fabri BM. Atrial fibrillation postcardiac surgery: a common but a morbid complication. *Interact Cardiovasc Thorac Surg*. 2011;12(5):772-777. doi:10.1510/ICVTS.2010.243782

218. Shingu Y, Takada S, Yokota T, et al. Correlation between increased atrial expression of genes related to fatty acid metabolism and autophagy in patients with chronic atrial fibrillation. Ai T, ed. *PLoS One*. 2020;15(4):e0224713. doi:10.1371/journal.pone.0224713

219. Furuhashi M, Saitoh S, Shimamoto K, Miura T. Fatty Acid-Binding Protein 4 (FABP4): Pathophysiological Insights and Potent Clinical Biomarker of Metabolic and Cardiovascular Diseases. *Clin Med Insights Cardiol*. 2014;8(Suppl 3):23. doi:10.4137/CMC.S17067

220. Furuhashi M. Fatty Acid-Binding Protein 4 in Cardiovascular and Metabolic Diseases. *J Atheroscler Thromb*. 2019;26(3):216-232. doi:10.5551/JAT.48710

221. Schlottmann I, Ehrhart-Bornstein M, Wabitsch M, Bornstein SR, Lamounier-Zepter V. Calcium-dependent release of adipocyte fatty acid binding protein from human adipocytes. *Int J Obes (Lond)*. 2014;38(9):1221-1227. doi:10.1038/IJO.2013.241

USC
UNIVERSIDADE DE SANTIAGO DE COMPOSTELA

222. Pérez LM, de Lucas B, Bernal A, Gálvez BG. Adipokines disrupt cardiac differentiation and cardiomyocyte survival. *Int J Obes*. 2020;44(4):908-919. doi:10.1038/s41366-019-0455-4

223. Takahashi K, Yamanaka S. Induction of pluripotent stem cells from mouse embryonic and adult fibroblast cultures by defined factors. *Cell*. 2006;126(4):663-676. doi:10.1016/J.CELL.2006.07.024

224. Takahashi K, Tanabe K, Ohnuki M, et al. Induction of Pluripotent Stem Cells from Adult Human Fibroblasts by Defined Factors. *Cell*. 2007;131(5):861-872. doi:10.1016/J.CELL.2007.11.019

225. Parrotta E, De Angelis MT, Scalise S, et al. Two sides of the same coin? Unraveling subtle differences between human embryonic and induced pluripotent stem cells by Raman spectroscopy. *Stem Cell Res Ther*. 2017;8(1). doi:10.1186/S13287-017-0720-1

226. Gharanei M, Shafaattalab S, Sangha S, et al. Atrial-specific hiPSC-derived cardiomyocytes in drug discovery and disease modeling. *Methods*. June 2021. doi:10.1016/J.YMETH.2021.06.009

227. Delgado C, Gomez A-M, Samia El Hayek M, Ruiz-Hurtado G, Pereira L. Gender-Dependent Alteration of Ca2+ and TNFα Signaling in db/db Mice, an Obesity-Linked Type 2 Diabetic Model. *Front Physiol*. 2019;10(FEB):40. doi:10.3389/fphys.2019.00040

228. Richard S, Perrier E, Fauconnier J, et al. "Ca2+-induced Ca2+ entry" or how the L-type Ca 2+ channel remodels its own signalling pathway in cardiac cells. In: *Progress in Biophysics and Molecular Biology*. Vol 90. Pergamon; 2006:118-135. doi:10.1016/j.pbiomolbio.2005.05.005

229. Erickson JR, Pereira L, Wang L, et al. Diabetic hyperglycaemia activates CaMKII and arrhythmias by O-linked glycosylation.

USC UNIVERSIDADE DE SANTIAGO DE COMPOSTELA

Nature. 2013;502(7471):372-376. doi:10.1038/nature12537

230. Luo X, Li W, Künzel K, et al. IP3R-Mediated Compensatory Mechanism for Calcium Handling in Human Induced Pluripotent Stem Cell-Derived Cardiomyocytes With Cardiac Ryanodine Receptor Deficiency. *Front cell Dev Biol*. 2020;8. doi:10.3389/FCELL.2020.00772

231. Eng G, Lee BW, Protas L, et al. Autonomous beating rate adaptation in human stem cell-derived cardiomyocytes. *Nat Commun*. 2016;7. doi:10.1038/NCOMMS10312

232. Franco D, Lamers WH, Moorman AFM. Patterns of expression in the developing myocardium: Towards a morphologically integrated transcriptional model. *Cardiovasc Res*. 1998;38(1):25-53. doi:10.1016/S0008-6363(97)00321-0/2/38-1-25-FIG9.GIF

233. Gillilan RE, Ayers SD, Noy N. Structural basis for activation of fatty acid-binding protein 4. *J Mol Biol*. 2007;372(5):1246-1260. doi:10.1016/J.JMB.2007.07.040

234. Sigurdsson S, Philipsen PA, Hansen LK, Larsen J, Gniadecka M, Christian Wulf H. Detection of skin cancer by classification of Raman spectra. *IEEE Trans Biomed Eng*. 2004;51(10):1784-1793. doi:10.1109/TBME.2004.831538

235. Furuhashi M, Fuseya T, Murata M, et al. Local production of fatty acid-binding protein 4 in epicardial/perivascular fat and macrophages is linked to coronary atherosclerosis. *Arterioscler Thromb Vasc Biol*. 2016;36(5):825-834. doi:10.1161/ATVBAHA.116.307225

236. Prentice KJ, Saksi J, Hotamisligil GS. Adipokine FABP4 integrates energy stores and counterregulatory metabolic responses. *J Lipid Res*. 2019;60(4):734-740. doi:10.1194/JLR.S091793

USC
UNIVERSIDADE DE SANTIAGO DE COMPOSTELA

8 ANNEXES

8.1 ANNEX I. DOCTORAL STUDENT PUBLICATIONS

Publications included in this doctoral thesis:

1. **Couselo-Seijas M**; Nicolás Lopez Canoa; Rosa María Agra Bermejo; Esther Díaz Rodríguez; Angel Luis Fernandez; JM Martinez Cereijo; Darío Duran Muñoz; Susana Bravo; Alba Velo; L González Melchor; XA Fernández López; JL Martínez Sande; Javier García Seara; José Ramón González Juanatey; Moisés Rodríguez Mañero; Sonia Eiras. *Cholinergic activity regulates the secretome of epicardial adipose tissue: Association with atrial fibrillation*. *Journal of Cellular Physiology*. 27/11/2018. DOI: 10.1002/jcp.27723

2. **Couselo-Seijas M**, Lopez-Canoa JN, Fernandez ÁL, González-Melchor L, Seoane LM, Duran-Muñoz D, Rozados-Luis A, González-Juanatey JR, Rodríguez-Mañero M, Eiras S. *Inflammatory and lipid regulation by cholinergic activity in epicardial stromal cells from patients who underwent open-heart surgery*. *J Cell Mol Med*. 2020 Sep;24(18):10958-10969. doi: 10.1111/jcmm.15727

3. **Couselo-Seijas M**, Almengló C, M Agra-Bermejo R, Luis Fernandez Á, Alvarez E, R González-Juanatey J, Eiras S. *Higher ACE2 expression levels in epicardial cells than subcutaneous stromal cells from patients with cardiovascular disease: Diabetes and obesity as possible enhancer*. *Eur J Clin Invest*. 2020 Nov 29:e13463. doi: 10.1111/eci.13463

4. **Couselo-Seijas M**, Rodríguez-Mañero M, González-Juanatey JR, Eiras S. *Updates on epicardial adipose tissue mechanisms on atrial fibrillation*, 2021 May 17. *Obesity Reviews*. doi:10.1111/obr.13277

USC UNIVERSIDADE DE SANTIAGO DE COMPOSTELA

Other doctoral student's publications as main author:

1. **Couselo-Seijas M**, Rosa María Agra-Bermejo, Angel Luis Fernández, José Manuel Martínez-Cereijo, Juan Sierra, Maeve Soto-Pérez, Adriana Rozados-Luis, José Ramón González-Juanatey, SoniaEiras. *High released lactate by epicardial fat from coronary artery disease patients is reduced by dapagliflozin treatment*. *Atherosclerosis.* Jan, 2020. DOI: 10.1016/j.atherosclerosis.2019.11.016

Other publications:

1. Ricardo Lage; Isabel Moscoso; Ángel Fernández Trasancos; María Cebro; **Couselo M**; Rubén Fandiño Vaquero; Susana B Bravo; Juan Sierra; José Ramón González Juanatey; Sonia Eiras. *Differential behaviour of epicardial adipose tissue-secretomes with high and low orosomucoid levels from patients with cardiovascular disease in H9C2 cells*. *Molecular and cellular endocrinology*. 416, pp. 77 - 87. (Irlanda): 15/11/2015. ISSN 1872-8057 DOI:10.1016/j.mce.2015.08.025

2. Nicolás Lopez Canoa; Aurora Baluja; **Couselo-Seijas M**; Anaberta Bermudez Naveira; Laila Gonzalez-Melchor; Adriana Rozados; Luis Martínez-Sande; , Javier García-Seara; X. Alberte Fernandez-Lopez; A.L. Fernandez; Jose Ramon Gonzalez-Juanatey; Sonia Eiras; Moisés Rodriguez-Mañero. *Plasma FABP4 levels are associated with left atrial fat volume in persistent atrial fibrillation and predict recurrence after catheter ablation*. *International Journal of Cardiology*. 10/04/2019. DOI: 10.1016/j.ijcard.2019.04.031

3. Agra-Bermejo RM, Cacho-Antonio C, Rozados-Luis A, **Couselo-Seijas M**, Fernandez AL, Martinez-Cereijo JM, Bravo SB, Gonzalez-Juanatey JR, Eiras S. *CD5L, Macrophage*

USC UNIVERSIDADE DE SANTIAGO DE COMPOSTELA

Apoptosis Inhibitor, Was Identified in Epicardial Fat-Secretome and Regulated by Isoproterenol From Patients With Heart Failure. Front Physiol. 2020 Jun 30;11:620. doi: 10.3389/fphys.2020.00620.

4. López-Canoa JN, **Couselo-Seijas M**, Baluja A, González-Melchor L, Rozados A, Llorente-Cortés V, de Gonzalo-Calvo D, Guerra JM, Vilades D, Leta R, Martínez-Sande JL, García-Seara FJ, Fernández-López XA, González-Juanatey JR, Eiras S, Rodríguez-Mañero M. *Sex-related differences of fatty acid-binding protein 4 and leptin levels in atrial fibrillation*. *Europace*. 2020 Dec 15. doi: 10.1093/europace/euaa284.

5. Almengló C, **Couselo-Seijas M**, Agra RM, et al. *Soluble angiotensin-converting enzyme levels in heart failure or acute coronary syndrome: revisiting its modulation and prognosis value*. *J Mol Med* (Berl). 2021;99(12):1741-1753. doi:10.1007/s00109-021-02129-4

USC UNIVERSIDADE DE SANTIAGO DE COMPOSTELA

USC
UNIVERSIDADE
DE SANTIAGO
DE COMPOSTELA

8.2 ANNEX II. DECLARATIONS: PUBLISHED CONTENT

Article 1. *Updates on epicardial adipose tissue mechanisms on atrial fibrillation*

Obesity reviews, volume 22, issue 9, pages 15

DOI: 10.1111/obr.13277

Specific contribution in the publication:

Conceptualization, methodology and research: Acquisition and analysis of data. Writing of the original manuscript.

Quality index:

The journal where chapter 1.4.5 was published currently has an impact index of 9.213 (2020 Journal Impact Factor) and the following positions in the following categories: quartile 1 (Q1) decile 1 (D1) in ENDOCRINOLOGY & METABOLISM calculated by Clarivate™.

Journal's authorization:

The Journal of *Obesity Reviews*, owned by John Wiley and Sons, where Chapter 1.4.5 has been published, allows the author to reuse the article as part of her thesis.

License Number: 5300760868013

Article 2. *Cholinergic activity regulates the secretome of epicardial adipose tissue: association with atrial fibrillation*

Journal of Cellular Physiology, volume *234*, issue *7*, pages *10512–10522.*

DOI: 10.1002/jcp.27723

Specific contribution in the publication:

USC UNIVERSIDADE DE SANTIAGO DE COMPOSTELA

Methodology and research: Approach and development of laboratory procedures and techniques. Acquisition and analysis of data. Writing of the original manuscript.

Quality index:

The journal where chapter 4.1 was published currently has an impact index of 6.384 (2020 Journal Impact Factor) and the following positions in the following categories: quartile 2 (Q2) in CELL BIOLOGY and quartile 1 (Q1) decile 1 (D1) in PHYSIOLOGY calculated by Clarivate™.

Journal's authorization:

The Journal of *Journal of Cellular Physiology*, owned by John Wiley and Sons, where Chapter 4.1 has been published, allows the author to reuse the article as part of her thesis.

License Number: 5300760357766

Article 3. *Inflammatory and lipid regulation by cholinergic activity in epicardial stromal cells from patients who underwent open-heart surgery*

Journal of Cellular and Molecular Medicine, volume *24*, issue *18*, pages *10958–10969*.

DOI: 10.1111/jcmm.15727

Specific contribution in the publication:

Conceptualization, methodology and research: Approach and development of laboratory procedures and techniques. Acquisition and analysis of data. Writing of the original manuscript.

Quality index:

The journal where chapter 4.2 was published currently has an impact index of 5.310 (2020 Journal Impact Factor) and the following positions in the following categories: quartile 2 (Q2) in CELL BIOLOGY and

USC UNIVERSIDADE DE SANTIAGO DE COMPOSTELA

quartile 2 (Q2) in MEDICINE, RESEARCH & EXPERIMENTAL calculated by Clarivate™.

Journal's authorization:

The Journal of *Journal of Cellular and Molecular Medicine* is an open access article under the terms of the Creative Commons Attribution License, which permits use, distribution, and reproduction in any medium, provided the original work is properly cited.

©2020 The Authors. *Journal of Cellular and Molecular Medicine* published by Foundation for Cellular and Molecular Medicine and John Wiley & Sons Ltd.

Article 4. *Higher ACE2 expression levels in epicardial cells tan subcutaneous stromal cells from patients with cardiovascular disease: diabetes and obesity as possible enhancer*

European Journal of Clinical Investigation, volume *51*, issue *5*, pages X

DOI:10.1111/eci.13463

Specific contribution in the publication:

Conceptualization, methodology and research: Approach and development of laboratory procedures and techniques. Acquisition and analysis of data. Writing of the original manuscript.

Quality index:

The journal where chapter 4.5 was published currently has an impact index of 4.686 (2020 Journal Impact Factor) and the following positions in the following categories: quartile 1 (Q1) in MEDICINE, GENERAL & INTERNAL and quartile 2 (Q2) in MEDICINE, RESEARCH & EXPERIMENTAL calculated by Clarivate™.

Journal's authorization:

USC UNIVERSIDADE DE SANTIAGO DE COMPOSTELA

The Journal of *European Journal of Clinical Investigation*, owned by John Wiley and Sons, where Chapter 4.5 has been published, allows the author to reuse the article as part of her thesis.

License Number: 5300760724815

USC
UNIVERSIDADE DE SANTIAGO DE COMPOSTELA

8.3 ANNEX III. SUPPLEMENTARY TABLE 1

Supplementary table 1. Raman peaks appearing in the coefficient loading plots from the spectra acquired in intervals 400-2650 and 2650-3400 cm^{-1} from the unlabelled samples.

	Nucleus			*Cytoplasm*		
Wavenumbers (cm^{-1})	*Control vs FABP4 10 ng/mL*	*Control vs FABP4 100 ng/mL*	*FABP4 10 ng/mL vs FABP4 100 ng/mL*	*Control vs FABP4 10 ng/mL*	*Control vs FABP4 100 ng/mL*	*FABP4 10 ng/mL vs FABP4 100 ng/mL*
Region I (400-800)	401	400	400	400	408	400
	404	404	401	401	417	401
	410	405	402	402	424	402
	415	407	404	403	426	403
	420	408	405	404	435	404
	422	412	406	405	436	405
	423	413	410	406	437	406
	424	414	411	407	463	407
	425	416	412	408	466	408
	426	417	413	409	510	409
	427	418	415	410	542	410
	434	419	416	411	549	411
	435	424	417	412	560	412
	439	437	418	413	562	413
	442	443	423	414	564	414
	465	446	427	415	565	415
	470	453	430	416	567	416
	473	454	433	417	568	417
	480	457	434	418	570	418
	484	459	437	419	575	419
	489	462	438	420	590	420
	494	470	442	421	594	421
	496	471	444	422	595	422
	507	472	449	423	597	423
	521	483	453	424	608	424
	533	485	454	425	614	425
	537	486	457	426	615	426
	541	488	461	427	616	427
	552	490	462	428	617	428
	555	491	465	429	620	429
	556	493	466	430	621	430
	565	504	469	431	623	431
	567	505	470	432	625	432
	570	507	471	434	636	433
	577	508	472	436	638	434
	582	511	473	437	641	435
	583	513	480	438	642	436
	586	514	482	439	643	437
	588	516	484	440	644	438
	595	518	485	444	645	439

USC UNIVERSIDADE DE SANTIAGO DE COMPOSTELA

	606	522	486	445	654	440
	608	523	487	449	656	441
	609	526	488	451	657	442
	614	527	489	452	662	443
	616	528	490	453	670	444
	620	534	491	456	671	445
	624	535	495	457	674	446
	628	537	496	458	676	447
	636	538	499	459	681	448
	639	542	500	461	684	449
	640	544	501	462	685	451
	642	546	504	463	688	452
	643	549	505	510	689	453
	646	551	507	515	692	454
	651	552	508	518	693	455
	662	557	510	520	695	456
	670	562	511	521	697	457
	679	567	514	523	698	458
	687	568	515	526	699	459
	693	570	516	527	700	460
	694	575	517	528	701	461
	697	581	518	529	703	462
	698	582	521	530	704	463
	705	583	522	531	706	464
	713	593	523	532	708	465
	716	605	524	533	710	466
	717	606	527	534	711	467
	718	607	528	535	714	468
	724	616	530	536	716	469
	726	630	531	537	717	470
	727	631	532	538	719	471
	728	640	533	540	720	475
	732	643	534	541	721	490
	733	648	535	542	724	491
	735	651	540	543	726	493
	736	666	541	545	727	494
	737	670	542	546	728	495
	738	673	544	547	731	496
	739	676	546	549	732	497
	742	685	549	550	736	498
	744	687	550	552	737	500
	745	688	552	554	738	501
	757	697	554	555	740	502
	758	698	555	556	746	503
	768	701	556	559	753	504
	769	704	559	563	754	505
	774	713	561	565	758	506
	776	714	562	568	763	507
	777	717	564	587	767	508
	778	718	565	588	773	510
	779	722	566	589	778	511
	780	726	567	590	779	512
	781	727	568	593	781	513
	782	728	571	594	784	514

USC UNIVERSIDADE DE SANTIAGO DE COMPOSTELA

	783	736	572	595	785	515
	784	738	575	597	786	516
	785	742	576	604	787	517
	786	750	577	605	790	518
	787	758	578	608	791	519
	789	764	579	611	795	520
	790	765	580	612	797	521
	791	766	581	613		522
	799	774	586	615		523
		776	588	623		526
		777	589	626		527
		778	590	628		528
		779	591	629		529
		780	595	630		530
		781	596	636		531
		782	598	638		532
		783	599	648		533
		785	601	649		534
		786	603	661		535
		787	604	663		536
		789	607	666		537
		790	613	681		539
		799	614	682		540
			617	684		541
			618	693		542
			622	694		543
			629	701		544
			630	702		545
			631	703		546
			634	705		547
			635	706		548
			639	707		549
			640	710		550
			641	711		551
			642	717		552
			645	719		553
			646	724		554
			647	728		555
			654	732		556
			657	740		557
			660	744		559
			662	758		561
			664	759		562
			668	761		563
			669	775		564
			671	779		565
			672	781		569
			675	782		570
			676	783		572
			677	784		578
			678	785		587
			679	786		588
			680	788		589
			681	789		592

USC
UNIVERSIDADE
DE SANTIAGO
DE COMPOSTELA

			682	790		593
			683	794		594
			685	795		597
			687	796		599
			688			600
			689			601
			690			602
			691			605
			692			608
			693			609
			694			610
			696			611
			698			612
			701			613
			703			614
			704			615
			705			616
			708			617
			713			619
			714			620
			715			621
			716			629
			718			630
			719			633
			720			635
			721			636
			722			637
			723			641
			724			642
			726			643
			727			648
			732			649
			733			651
			735			653
			737			654
			739			655
			740			657
			742			658
			743			661
			745			662
			746			663
			750			664
			755			665
			757			670
			758			672
			759			674
			760			677
			762			679
			764			682
			765			683
			766			684
			770			685
			773			686
			774			687

USC UNIVERSIDADE DE SANTIAGO DE COMPOSTELA

			777 778 779 780 781 782 785 786 787 789 790 791 794 795 796 797 799			689 691 692 697 701 702 703 705 706 707 710 711 714 715 716 717 719 731 737 741 744 745 756 757 758 759 761 766 767 768 769 771 773 775 776 777 779 780 782 783 784 785 786 788 789 790 792 794 795 796 798 799
Region II *(800-1200)*	813 818	830 831	801 804	800 802	810 811	800 801

USC
UNIVERSIDADE DE SANTIAGO DE COMPOSTELA

	819	834	805	804	813	802
	820	835	806	807	814	803
	821	836	807	808	816	804
	828	837	808	809	822	805
	832	840	810	810	845	807
	833	841	812	811	846	808
	836	842	815	812	869	809
	837	847	818	813	877	811
	840	848	819	814	882	815
	841	851	821	815	885	817
	842	852	826	817	886	819
	846	853	828	819	887	820
	847	855	831	820	892	821
	848	857	834	821	903	823
	849	859	835	822	904	824
	850	860	839	823	913	826
	853	875	844	824	920	827
	854	882	846	825	926	828
	857	884	847	827	935	830
	861	889	848	830	938	831
	871	894	849	834	941	832
	876	895	851	845	961	833
	884	899	852	881	975	834
	889	902	853	889	982	835
	890	905	854	891	986	836
	899	907	855	896	989	837
	902	925	856	897	991	838
	905	929	857	901	993	839
	907	932	858	921	1000	840
	908	933	859	937	1001	843
	910	934	860	941	1002	844
	914	935	861	952	1003	846
	915	936	862	954	1004	852
	924	937	866	955	1005	853
	930	939	867	957	1006	856
	932	942	872	959	1007	858
	933	950	875	960	1008	861
	934	951	876	961	1009	868
	936	953	878	962	1010	869
	937	954	879	966	1011	878
	940	955	880	968	1014	881
	941	958	882	970	1017	882
	951	959	884	972	1022	883
	952	963	886	975	1024	884
	954	966	890	983	1030	885
	959	967	892	984	1048	886
	961	971	896	987	1054	888
	963	972	898	988	1056	889
	964	973	902	990	1057	891
	966	974	906	994	1058	895
	970	975	908	995	1062	896
	974	976	910	997	1063	897
	983	977	913	999	1064	901
	986	980	915	1000	1065	902

USC UNIVERSIDADE DE SANTIAGO DE COMPOSTELA

	995	981	916	1001	1066	903
	1017	982	918	1002	1067	905
	1021	986	922	1003	1068	906
	1022	989	924	1004	1071	908
	1023	993	925	1006	1072	910
	1025	996	929	1010	1073	911
	1040	997	931	1013	1075	914
	1058	998	932	1017	1078	916
	1059	999	935	1021	1079	919
	1061	1000	936	1022	1088	921
	1065	1001	937	1023	1097	924
	1070	1004	938	1024	1099	925
	1072	1017	939	1025	1128	930
	1073	1018	942	1031	1129	932
	1074	1019	943	1032	1136	933
	1077	1021	945	1033	1157	937
	1088	1026	946	1034	1178	938
	1094	1035	948	1035	1183	946
	1101	1037	950	1036	1185	950
	1103	1041	951	1038	1186	951
	1105	1042	952	1039	1190	952
	1106	1046	954	1042	1197	953
	1113	1051	955	1043	1198	956
	1114	1052	956	1044		957
	1115	1056	958	1045		958
	1117	1057	959	1046		959
	1119	1063	961	1047		961
	1120	1064	962	1048		962
	1121	1066	963	1049		967
	1122	1073	964	1051		968
	1126	1079	966	1052		970
	1127	1092	967	1053		973
	1135	1105	969	1054		974
	1142	1110	970	1055		975
	1143	1118	971	1056		977
	1144	1133	972	1057		978
	1146	1134	973	1058		980
	1151	1135	975	1059		981
	1162	1137	976	1060		983
	1170	1146	977	1061		984
	1171	1153	978	1062		987
	1172	1169	980	1063		989
	1173	1177	982	1064		990
	1176	1194	983	1065		994
	1177	1199	985	1066		996
	1184		987	1067		997
			988	1068		1003
			989	1069		1009
			990	1070		1013
			995	1071		1015
			996	1072		1017
			997	1073		1018
			998	1074		1019
			999	1075		1020

USC
UNIVERSIDADE
DE SANTIAGO
DE COMPOSTELA

			1003	1077		1021
			1004	1078		1022
			1005	1079		1024
			1006	1080		1025
			1009	1081		1027
			1012	1082		1029
			1014	1083		1030
			1015	1084		1032
			1017	1085		1033
			1019	1086		1034
			1022	1087		1035
			1023	1088		1036
			1024	1089		1039
			1025	1090		1041
			1026	1091		1042
			1027	1092		1043
			1029	1093		1044
			1030	1094		1045
			1031	1095		1046
			1033	1096		1047
			1034	1097		1048
			1035	1098		1049
			1040	1099		1052
			1042	1102		1053
			1044	1103		1054
			1046	1104		1055
			1047	1105		1056
			1049	1108		1057
			1050	1109		1059
			1051	1110		1060
			1052	1111		1061
			1055	1112		1062
			1056	1113		1064
			1059	1114		1065
			1061	1115		1066
			1062	1116		1067
			1066	1117		1068
			1068	1118		1069
			1070	1119		1070
			1071	1120		1071
			1074	1121		1073
			1078	1129		1074
			1080	1130		1088
			1085	1131		1090
			1086	1132		1091
			1087	1133		1097
			1088	1134		1098
			1089	1136		1101
			1090	1137		1104
			1092	1138		1108
			1094	1139		1110
			1095	1141		1129
			1097	1142		1132
			1098	1144		1138

USC
UNIVERSIDADE DE SANTIAGO DE COMPOSTELA

			1101 1102 1103 1104 1106 1108 1110 1111 1113 1118 1119 1121 1122 1123 1124 1125 1126 1127 1128 1133 1134 1136 1137 1140 1142 1143 1144 1151 1153 1155 1156 1157 1158 1161 1162 1167 1168 1169 1170 1172 1173 1179 1184 1186 1187 1188 1190 1192 1195 1196 1199	1146 1148 1149 1150 1151 1152 1154 1175 1176 1178 1188 1199		1146 1150 1152 1167 1168 1171 1176 1179 1184 1185 1187 1188 1191 1194 1196 1198 1199
Region III (1200-1800)	1200 1203 1214	1202 1204 1205	1200 1202 1203	1203 1204 1206	1201 1202 1203	1200 1209 1214

USC
UNIVERSIDADE DE SANTIAGO DE COMPOSTELA

	1215	1206	1204	1207	1205	1229
	1217	1207	1206	1212	1206	1231
	1220	1208	1208	1215	1207	1236
	1221	1214	1210	1216	1209	1247
	1222	1215	1212	1217	1211	1253
	1223	1216	1214	1219	1213	1276
	1225	1218	1217	1220	1215	1279
	1226	1219	1218	1221	1216	1285
	1227	1220	1221	1222	1219	1292
	1228	1221	1224	1224	1220	1294
	1229	1222	1226	1226	1222	1299
	1230	1223	1228	1227	1224	1305
	1231	1225	1229	1228	1225	1315
	1232	1226	1237	1229	1226	1316
	1234	1227	1238	1230	1227	1317
	1235	1228	1239	1231	1228	1329
	1236	1229	1240	1232	1229	1331
	1237	1230	1241	1233	1230	1337
	1238	1231	1245	1234	1231	1339
	1239	1232	1248	1235	1232	1340
	1240	1233	1250	1236	1233	1341
	1241	1234	1251	1237	1234	1348
	1242	1235	1252	1238	1235	1349
	1244	1236	1253	1239	1236	1351
	1246	1237	1254	1240	1237	1358
	1248	1238	1255	1241	1238	1360
	1249	1239	1257	1242	1239	1361
	1250	1240	1258	1243	1240	1367
	1251	1241	1261	1244	1241	1380
	1252	1242	1262	1245	1242	1386
	1255	1243	1268	1246	1243	1387
	1261	1244	1270	1248	1244	1389
	1263	1245	1271	1250	1245	1392
	1264	1246	1272	1254	1246	1393
	1266	1247	1273	1272	1247	1394
	1270	1248	1274	1275	1248	1395
	1271	1249	1280	1279	1249	1396
	1274	1252	1281	1288	1250	1398
	1276	1253	1283	1291	1251	1399
	1278	1254	1284	1305	1252	1400
	1279	1255	1285	1308	1253	1405
	1280	1256	1286	1309	1254	1407
	1286	1257	1288	1310	1256	1411
	1288	1263	1289	1311	1258	1412
	1289	1276	1290	1312	1261	1413
	1301	1277	1293	1313	1262	1417
	1305	1280	1295	1314	1277	1420
	1307	1281	1297	1315	1281	1421
	1308	1283	1302	1316	1286	1423
	1309	1284	1303	1317	1288	1427
	1310	1289	1304	1318	1299	1429
	1311	1290	1305	1319	1302	1430
	1312	1297	1306	1320	1310	1431
	1313	1307	1307	1321	1311	1432

USC UNIVERSIDADE DE SANTIAGO DE COMPOSTELA

	1314	1308	1308	1322	1312	1434
	1315	1309	1314	1323	1314	1435
	1316	1310	1316	1325	1315	1436
	1317	1311	1317	1327	1316	1437
	1318	1312	1318	1329	1317	1438
	1320	1313	1319	1337	1318	1439
	1321	1314	1320	1423	1319	1446
	1322	1315	1323	1429	1320	1448
	1323	1316	1327	1431	1321	1452
	1324	1317	1328	1432	1322	1453
	1325	1318	1329	1434	1323	1454
	1326	1319	1332	1437	1325	1455
	1327	1320	1340	1438	1326	1458
	1328	1321	1345	1439	1327	1459
	1329	1322	1346	1461	1328	1461
	1330	1323	1350	1470	1329	1466
	1331	1324	1353	1474	1330	1467
	1332	1325	1354	1477	1331	1471
	1333	1326	1357	1478	1332	1472
	1334	1327	1359	1479	1335	1475
	1335	1328	1361	1480	1338	1492
	1336	1329	1362	1481	1341	1494
	1337	1330	1363	1483	1342	1495
	1338	1331	1364	1484	1343	1496
	1339	1332	1365	1486	1359	1499
	1340	1333	1367	1490	1389	1501
	1341	1334	1371	1491	1396	1502
	1342	1335	1375	1492	1399	1505
	1343	1336	1376	1495	1405	1506
	1345	1337	1377	1502	1416	1507
	1346	1338	1378	1510	1424	1508
	1347	1339	1379	1530	1428	1510
	1348	1340	1384	1531	1429	1512
	1349	1341	1386	1532	1431	1515
	1350	1342	1388	1536	1432	1523
	1351	1343	1390	1537	1433	1526
	1352	1345	1394	1540	1434	1527
	1353	1346	1397	1541	1435	1529
	1354	1347	1398	1542	1436	1530
	1355	1348	1399	1543	1437	1531
	1356	1349	1400	1545	1438	1533
	1357	1350	1401	1546	1439	1538
	1358	1351	1402	1547	1440	1543
	1359	1352	1403	1548	1441	1544
	1360	1353	1406	1549	1442	1545
	1361	1354	1407	1550	1453	1551
	1362	1355	1408	1551	1456	1552
	1363	1356	1409	1552	1459	1553
	1364	1357	1410	1553	1465	1554
	1365	1358	1411	1554	1466	1555
	1366	1359	1412	1555	1470	1557
	1367	1360	1413	1556	1474	1558
	1368	1361	1414	1557	1475	1563
	1369	1362	1415	1558	1477	1566

USC
UNIVERSIDADE
DE SANTIAGO
DE COMPOSTELA

	1370	1363	1418	1559	1479	1567
	1372	1365	1419	1560	1480	1569
	1373	1367	1420	1561	1481	1570
	1374	1368	1421	1562	1482	1571
	1376	1369	1422	1563	1483	1572
	1377	1370	1423	1564	1484	1576
	1378	1371	1424	1565	1485	1577
	1380	1373	1425	1566	1486	1578
	1381	1374	1426	1567	1488	1579
	1382	1375	1428	1568	1489	1580
	1383	1376	1429	1569	1495	1582
	1384	1377	1433	1570	1501	1585
	1385	1378	1434	1571	1506	1586
	1386	1379	1437	1572	1508	1588
	1387	1380	1439	1573	1510	1589
	1388	1381	1440	1574	1520	1593
	1390	1382	1441	1575	1523	1594
	1391	1383	1443	1576	1525	1596
	1392	1384	1446	1577	1532	1604
	1393	1385	1447	1578	1533	1607
	1394	1386	1448	1579	1534	1608
	1395	1387	1449	1580	1535	1612
	1396	1388	1450	1581	1536	1614
	1397	1390	1452	1582	1537	1621
	1398	1391	1453	1583	1538	1624
	1399	1392	1454	1584	1539	1643
	1400	1393	1455	1585	1541	1679
	1401	1394	1457	1586	1542	1692
	1402	1395	1460	1587	1543	1696
	1403	1396	1461	1588	1544	1703
	1404	1397	1465	1589	1545	1707
	1406	1399	1468	1591	1547	1708
	1407	1401	1470	1592	1548	1709
	1408	1402	1471	1593	1549	1710
	1409	1403	1472	1594	1550	1713
	1410	1404	1473	1596	1551	1714
	1411	1406	1479	1597	1552	1717
	1412	1410	1480	1598	1553	1718
	1413	1411	1481	1599	1554	1719
	1414	1414	1486	1600	1556	1720
	1415	1416	1487	1602	1558	1721
	1416	1427	1489	1603	1559	1725
	1424	1428	1491	1604	1560	1727
	1425	1432	1492	1605	1561	1728
	1426	1433	1493	1606	1564	1731
	1430	1434	1494	1607	1566	1732
	1432	1435	1495	1608	1567	1734
	1433	1436	1496	1609	1568	1735
	1434	1437	1497	1610	1569	1736
	1435	1438	1498	1611	1570	1737
	1436	1439	1500	1612	1572	1739
	1437	1440	1501	1614	1573	1740
	1438	1441	1502	1615	1574	1741
	1439	1442	1503	1616	1575	1743

USC UNIVERSIDADE DE SANTIAGO DE COMPOSTELA

	1440	1443	1504	1617	1576	1745
	1441	1446	1505	1618	1577	1748
	1442	1448	1506	1619	1582	1750
	1443	1450	1507	1620	1583	1751
	1445	1452	1509	1621	1584	1754
	1446	1455	1510	1622	1585	1757
	1448	1456	1511	1626	1588	1758
	1450	1457	1513	1629	1591	1760
	1452	1461	1514	1637	1592	1761
	1456	1465	1515	1639	1597	1766
	1459	1471	1516	1640	1599	1770
	1461	1473	1517	1644	1600	1771
	1465	1475	1518	1645	1601	1772
	1468	1476	1520	1647	1602	1773
	1471	1477	1521	1669	1603	1775
	1474	1479	1522	1672	1608	1779
	1475	1480	1523	1673	1610	1781
	1476	1481	1524	1674	1611	1785
	1477	1482	1528	1676	1612	1786
	1478	1483	1533	1677	1613	1787
	1479	1484	1535	1678	1614	1788
	1480	1485	1537	1679	1616	1790
	1481	1486	1539	1680	1617	1794
	1482	1487	1541	1681	1618	1795
	1483	1488	1543	1682	1622	1796
	1484	1489	1546	1683	1648	1798
	1485	1491	1547	1684	1671	
	1486	1492	1549	1685	1672	
	1488	1493	1553	1686	1673	
	1489	1497	1555	1687	1674	
	1491	1499	1557	1688	1676	
	1496	1502	1558	1690	1677	
	1502	1508	1559	1691	1678	
	1506	1510	1560	1692	1679	
	1509	1511	1562	1694	1680	
	1512	1513	1563	1696	1681	
	1516	1514	1564	1697	1682	
	1530	1516	1565	1698	1683	
	1543	1518	1571	1701	1684	
	1544	1529	1573	1702	1685	
	1545	1533	1577	1704	1686	
	1549	1537	1578	1717	1687	
	1552	1539	1585	1724	1688	
	1553	1541	1588	1725	1689	
	1554	1543	1592	1728	1690	
	1555	1544	1594	1729	1691	
	1557	1545	1595	1731	1692	
	1559	1546	1596	1735	1694	
	1560	1547	1597	1736	1695	
	1561	1548	1598	1737	1696	
	1562	1549	1600	1739	1697	
	1563	1551	1604	1740	1698	
	1564	1552	1605	1741	1699	
	1565	1553	1606	1743	1701	

USC
UNIVERSIDADE
DE SANTIAGO
DE COMPOSTELA

	1566	1554	1608	1745	1702	
	1567	1557	1610	1747	1703	
	1568	1559	1611	1748	1704	
	1569	1560	1612	1749	1705	
	1570	1561	1613	1750	1711	
	1571	1562	1614	1752	1714	
	1572	1563	1615	1754	1716	
	1573	1564	1617	1755	1717	
	1574	1565	1618	1756	1718	
	1575	1566	1621	1757	1721	
	1576	1567	1622	1758	1723	
	1577	1568	1624	1760	1724	
	1578	1569	1625	1761	1727	
	1579	1570	1626	1763	1729	
	1580	1571	1627	1765	1731	
	1581	1572	1631	1766	1732	
	1582	1573	1633	1770	1734	
	1583	1574	1634	1773	1735	
	1584	1575	1636	1775	1736	
	1585	1576	1637	1779	1737	
	1588	1577	1639	1781	1738	
	1589	1578	1640	1782	1739	
	1590	1580	1641	1783	1741	
	1593	1581	1643	1785	1742	
	1599	1582	1646	1786	1743	
	1600	1583	1648	1787	1744	
	1601	1584	1651	1788	1745	
	1602	1586	1653	1790	1746	
	1603	1587	1656	1794	1747	
	1604	1589	1658	1799	1748	
	1606	1590	1661		1749	
	1614	1594	1663		1750	
	1615	1597	1664		1752	
	1616	1599	1665		1753	
	1618	1600	1666		1755	
	1621	1602	1668		1756	
	1623	1603	1669		1760	
	1625	1604	1670		1761	
	1638	1606	1672		1765	
	1639	1607	1673		1767	
	1640	1609	1674		1768	
	1642	1613	1676		1770	
	1646	1615	1677		1771	
	1649	1616	1680		1774	
	1650	1617	1682		1775	
	1651	1621	1686		1777	
	1652	1628	1689		1778	
	1653	1629	1693		1779	
	1654	1630	1694		1781	
	1655	1641	1696		1782	
	1656	1649	1701		1783	
	1657	1650	1703		1784	
	1658	1653	1705		1786	
	1659	1654	1706		1787	

USC UNIVERSIDADE DE SANTIAGO DE COMPOSTELA

	1660	1655	1707		1789	
	1661	1656	1708		1791	
	1662	1657	1709		1792	
	1663	1658	1710		1797	
	1664	1659	1711		1798	
	1665	1660	1714		1799	
	1666	1661	1716			
	1668	1662	1717			
	1671	1663	1718			
	1674	1672	1720			
	1676	1673	1726			
	1683	1674	1728			
	1688	1676	1729			
	1691	1678	1731			
	1692	1679	1732			
	1695	1680	1733			
	1696	1681	1734			
	1698	1682	1735			
	1702	1683	1736			
	1708	1684	1737			
	1715	1685	1738			
	1721	1686	1740			
	1730	1688	1741			
	1731	1689	1743			
	1732	1691	1745			
	1733	1692	1748			
	1735	1693	1750			
	1736	1694	1751			
	1740	1695	1754			
	1741	1696	1755			
	1742	1702	1757			
	1743	1703	1759			
	1744	1704	1760			
	1745	1705	1763			
	1746	1708	1766			
	1747	1709	1767			
	1749	1715	1769			
	1750	1716	1771			
	1751	1717	1772			
	1752	1721	1774			
	1753	1728	1775			
	1754	1730	1776			
	1755	1732	1777			
	1757	1733	1778			
	1758	1736	1781			
	1759	1737	1782			
	1760	1740	1783			
	1761	1741	1785			
	1762	1742	1786			
	1765	1743	1788			
	1767	1744	1789			
	1768	1745	1790			
	1772	1746	1791			
	1776	1747	1794			

USC
UNIVERSIDADE
DE SANTIAGO
DE COMPOSTELA

	1780 1781 1782 1784 1787 1790 1792 1794 1798	1748 1749 1750 1751 1752 1753 1754 1755 1761 1762 1764 1767 1768 1771 1774 1775 1778 1780 1784 1787 1790 1791 1794 1797 1798	1795 1796 1797 1798			
Region IV (2650-3100)	2653 2656 2667 2669 2677 2682 2684 2690 2692 2698 2700 2704 2707 2710 2714 2716 2717 2718 2721 2722 2723 2724 2726 2727 2728 2731 2733 2734 2737	2660 2664 2675 2679 2682 2683 2689 2698 2704 2706 2707 2712 2714 2716 2718 2721 2722 2723 2728 2731 2734 2737 2743 2753 2768 2775 2780 2785 2789	2651 2653 2655 2656 2658 2660 2661 2662 2663 2664 2666 2667 2668 2669 2670 2672 2673 2674 2675 2676 2677 2678 2681 2682 2683 2684 2686 2687 2688	2655 2660 2662 2663 2665 2674 2684 2691 2701 2703 2704 2714 2716 2717 2719 2722 2724 2729 2740 2743 2746 2749 2766 2767 2788 2789 2792 2794 2799	2655 2659 2660 2662 2664 2673 2678 2683 2684 2685 2689 2691 2694 2695 2697 2698 2700 2701 2704 2708 2709 2710 2714 2716 2717 2720 2722 2725 2726	2654 2655 2657 2658 2660 2661 2663 2665 2666 2668 2669 2670 2673 2674 2676 2678 2683 2689 2691 2695 2699 2700 2701 2702 2703 2705 2706 2711 2712

USC UNIVERSIDADE DE SANTIAGO DE COMPOSTELA

	2738	2795	2692	2802	2727	2713
	2740	2797	2693	2803	2728	2714
	2746	2798	2695	2806	2729	2715
	2749	2802	2696	2807	2748	2716
	2756	2808	2697	2808	2750	2717
	2761	2812	2698	2809	2765	2718
	2762	2813	2699	2810	2768	2719
	2764	2814	2701	2811	2773	2720
	2766	2815	2703	2812	2778	2721
	2771	2818	2704	2813	2783	2722
	2775	2820	2707	2814	2789	2724
	2777	2821	2710	2815	2792	2726
	2780	2822	2711	2816	2796	2727
	2782	2823	2713	2817	2797	2728
	2787	2824	2714	2818	2798	2729
	2791	2825	2717	2819	2802	2739
	2792	2826	2719	2820	2804	2740
	2795	2827	2720	2821	2809	2742
	2797	2828	2721	2822	2810	2743
	2798	2829	2724	2823	2811	2744
	2806	2830	2727	2824	2812	2748
	2809	2831	2728	2825	2814	2749
	2814	2832	2733	2826	2815	2751
	2820	2833	2735	2827	2816	2757
	2822	2834	2736	2828	2817	2766
	2823	2835	2737	2829	2818	2767
	2824	2836	2741	2830	2819	2771
	2825	2837	2742	2831	2820	2772
	2826	2838	2743	2832	2821	2776
	2827	2839	2746	2833	2822	2781
	2828	2840	2749	2834	2823	2786
	2829	2841	2750	2835	2824	2787
	2830	2842	2752	2836	2825	2789
	2831	2843	2754	2837	2826	2802
	2832	2844	2756	2838	2827	2803
	2833	2845	2758	2839	2828	2805
	2834	2846	2759	2840	2829	2806
	2835	2847	2760	2841	2830	2809
	2836	2848	2761	2842	2831	2810
	2837	2849	2762	2843	2832	2811
	2838	2850	2763	2844	2833	2813
	2839	2851	2764	2845	2834	2816
	2840	2852	2765	2846	2835	2818
	2841	2853	2766	2847	2836	2819
	2842	2854	2767	2848	2837	2822
	2843	2855	2768	2849	2838	2824
	2844	2856	2771	2850	2839	2825
	2845	2857	2773	2851	2840	2826
	2846	2858	2774	2852	2841	2827
	2847	2859	2775	2853	2842	2828
	2848	2860	2777	2854	2843	2829
	2849	2861	2778	2855	2844	2830
	2850	2862	2780	2856	2845	2831
	2851	2863	2782	2857	2846	2832

USC
UNIVERSIDADE DE SANTIAGO DE COMPOSTELA

	2852	2864	2784	2858	2847	2833
	2853	2865	2787	2859	2848	2834
	2854	2866	2788	2860	2849	2835
	2855	2867	2789	2861	2850	2836
	2856	2868	2790	2862	2851	2837
	2857	2869	2791	2863	2852	2838
	2858	2870	2792	2864	2853	2839
	2859	2871	2795	2865	2854	2840
	2860	2872	2796	2866	2855	2841
	2861	2873	2797	2867	2856	2842
	2862	2874	2798	2868	2857	2843
	2863	2875	2799	2869	2858	2844
	2864	2876	2801	2871	2859	2845
	2865	2877	2802	2872	2860	2846
	2866	2878	2804	2873	2861	2847
	2867	2879	2806	2874	2862	2848
	2868	2880	2809	2875	2863	2849
	2869	2881	2812	2876	2864	2850
	2870	2882	2814	2877	2865	2851
	2871	2883	2815	2878	2866	2852
	2872	2884	2818	2879	2867	2853
	2873	2885	2819	2880	2868	2854
	2874	2886	2821	2881	2869	2855
	2875	2887	2825	2882	2870	2856
	2876	2888	2826	2883	2871	2857
	2877	2889	2828	2884	2872	2858
	2878	2890	2829	2885	2873	2859
	2879	2891	2832	2886	2874	2860
	2880	2892	2836	2887	2875	2861
	2881	2893	2839	2888	2876	2862
	2882	2894	2859	2889	2877	2863
	2883	2895	2860	2890	2878	2864
	2884	2896	2863	2891	2879	2865
	2885	2897	2864	2892	2880	2866
	2886	2898	2865	2893	2881	2867
	2887	2899	2867	2894	2882	2868
	2888	2900	2872	2895	2883	2869
	2889	2901	2876	2896	2884	2870
	2890	2902	2881	2897	2885	2871
	2891	2903	2882	2898	2886	2872
	2892	2904	2883	2899	2887	2873
	2893	2905	2885	2900	2888	2874
	2894	2906	2903	2901	2889	2875
	2895	2907	2905	2902	2890	2876
	2896	2908	2909	2903	2891	2877
	2897	2910	2918	2904	2892	2878
	2898	2942	2933	2905	2893	2879
	2899	2943	2937	2906	2894	2880
	2900	2947	2940	2907	2895	2881
	2901	2948	2942	2908	2896	2882
	2902	2949	2947	2909	2897	2883
	2903	2950	2949	2910	2898	2884
	2904	2952	2950	2911	2899	2885
	2905	2953	2951	2912	2900	2886

USC
UNIVERSIDADE DE SANTIAGO DE COMPOSTELA

	2906	2954	2953	2913	2901	2887
	2907	2955	2954	2914	2902	2888
	2908	2956	2955	2915	2903	2889
	2909	2957	2957	2916	2904	2890
	2910	2958	2958	2917	2905	2891
	2911	2959	2959	2918	2906	2892
	2912	2960	2962	2963	2907	2893
	2916	2961	2964	2974	2908	2894
	2917	2962	2968	2976	2909	2895
	2918	2963	2975	2980	2910	2896
	2919	2964	2976	2981	2911	2897
	2920	2965	2987	2982	2912	2898
	2923	2966	2988	2983	2913	2899
	2926	2967	2989	2984	2920	2900
	2927	2968	2990	2985	2925	2901
	2931	2969	2992	2994	2931	2902
	2934	2970	2993	3005	2932	2903
	2938	2971	2997	3006	2935	2904
	2949	2972	2999	3007	2937	2905
	2950	2973	3001	3008	2938	2906
	2954	2974	3002	3009	2940	2907
	2956	2975	3004	3010	2941	2908
	2957	2976	3005	3011	2942	2909
	2958	2977	3006	3012	2943	2910
	2959	2978	3007	3013	2944	2911
	2960	2979	3008	3014	2945	2912
	2962	2980	3013	3015	2946	2913
	2964	2981	3015	3016	2947	2914
	2965	2982	3016	3017	2948	2915
	2966	2983	3022	3018	2949	2916
	2967	2984	3024	3019	2950	2917
	2968	2985	3025	3020	2951	2918
	2969	2986	3027	3021	2952	2919
	2971	2987	3030	3022	2953	2920
	2972	2988	3031	3024	2954	2921
	2973	2989	3032	3026	2955	2922
	2974	2990	3033	3029	2956	2923
	2975	2991	3035	3030	2957	2924
	2976	2992	3038	3032	2959	2925
	2977	2993	3039	3034	2962	2926
	2978	2994	3041	3038	2963	2928
	2979	2995	3042	3044	2964	2929
	2980	2997	3043	3046	2965	2930
	2981	3008	3047	3048	2966	2931
	2982	3009	3049	3049	2967	2944
	2983	3010	3051	3050	2968	2947
	2984	3011	3056	3051	2969	2956
	2985	3012	3060	3052	2970	2957
	2986	3013	3061	3053	2971	2980
	2987	3014	3063	3054	2972	2989
	2988	3015	3068	3055	2973	3004
	2989	3016	3069	3056	2974	3005
	2991	3017	3070	3057	2975	3009
	2992	3018	3073	3058	2976	3010

USC
UNIVERSIDADE
DE SANTIAGO
DE COMPOSTELA

	2993	3019	3074	3059	2977	3012
	2994	3020	3077	3060	2978	3020
	3002	3021	3078	3061	2979	3022
	3005	3022	3080	3062	2980	3025
	3007	3023	3083	3063	2981	3028
	3008	3024	3084	3064	2982	3032
	3009	3026	3085	3065	2983	3034
	3010	3027	3086	3066	2984	3036
	3011	3029	3087	3067	2985	3037
	3012	3035	3091	3068	2986	3038
	3013	3041	3092	3069	2987	3043
	3014	3043	3093	3070	2988	3048
	3015	3046	3094	3071	2989	3054
	3016	3049	3096	3072	2990	3055
	3017	3050	3097	3073	2991	3056
	3018	3051	3098	3074	2992	3058
	3019	3052		3075	2993	3061
	3020	3053		3076	2994	3065
	3021	3054		3077	2995	3069
	3022	3055		3079	2996	3071
	3023	3056		3080	2997	3072
	3025	3057		3082	3000	3073
	3026	3058		3086	3002	3074
	3031	3059		3089	3005	3075
	3032	3060		3090	3006	3076
	3033	3061			3007	3079
	3035	3062			3008	3080
	3043	3063			3009	3082
	3044	3064			3010	3083
	3049	3065			3011	3085
	3050	3066			3012	3086
	3061	3067			3013	3088
	3063	3068			3014	3089
	3064	3069			3015	3090
	3065	3070			3016	3091
	3067	3071			3017	3093
	3073	3074			3018	3095
	3074	3077			3019	3098
	3075	3079			3020	3099
	3077	3081			3021	
	3078	3085			3022	
	3079	3090			3023	
	3081	3094			3024	
	3083	3096			3025	
	3084	3097			3026	
	3085				3027	
	3086				3028	
	3088				3029	
	3092				3031	
	3093				3033	
	3094				3039	
	3097				3040	
	3098				3042	
	3099				3045	

USC UNIVERSIDADE DE SANTIAGO DE COMPOSTELA

	3100				3046 3048 3050 3051 3053 3054 3055 3056 3057 3058 3059 3060 3061 3062 3063 3064 3065 3066 3067 3068 3069 3070 3071 3072 3073 3074 3075 3076 3077 3079 3081 3084 3085 3090 3091 3092 3096 3098	

USC
UNIVERSIDADE DE SANTIAGO DE COMPOSTELA





Atrial fibrillation (AF) is the most common arrhythmia in clinical practice. This arrhythmia has a great number of associated
risk factors, such as obesity. The local adipose depot most associated with AF is epicardial adipose tissue (EAT). The results of this work elucidate the role of the cholinergic system in the secretory and inflammatory activity of EAT and a possible mechanism associated with postoperative AF. In addition, chronic cholinergic
imbalance in long-term persistent AF could explain the greater accumulation of fatty acids. Consequently, FABP4
increases in the epicardial stroma, with an effect on paracrine activity in the structure and physiology of atrial cardiomyocytes. Besides, during the pandemic period, we studied the relationship of EAT with the SARS-CoV-2 receptor.